UNIVERSITEIT VAN PRETORIA
UNIVERSITY OF PRETORIA
YUNIBESITHI YA PRETORIA

The anti-tumour properties of novel gold compounds

Margo Judith Nell

Student nr: 80279784

Submitted in the partial fulfillment of the requirements for the degree of

MSc: Pharmacology

June 2007

The Faculty of Health Sciences

Department Pharmacology

University of Pretoria

Pretoria

1. Met dank aan my Hemelse Vader vir krag en deursettings vermoë en Sy onwankelbare Genade.

2. My dank aan prof Connie Medlen vir die geleentheid, geduld en leiding.

3. Dankie aan Gisela Joone vir al die ondersteuning, hulp en moed inpraat.

4. Dankie aan Chrisna du Randt vir haar geduld en hulp met die vloeisitometer.

5. Dankie aan Duncan Cromarty vir sy hulp en leiding.

6. Dankie aan my familie sonder wie se ondersteuning en liefde ek nie hierdie studie sou kon onderneem het nie.

Table of contents

Chapter 3: Cytotoxicity and tumour specificity

Chapter 4: Determination of the mitochondrial membrane potential

Chapter 5: Determination of plasma membrane potential

Chapter 6: Apoptosis

Chapter 7: Cell cycle

Chapter 8: *In vitro* radio labeled drug uptake

Summary

Since the introduction of Auranofin in 1985 there has been no new clinically approved gold containing drugs introduced. Although promising results were achieved with a gold(I) phosphine complex $[Au(dppe)_2]Cl$ (Hoke *et al*., 1991; Mckeage *et al*., 2002), this compound was never entered into clinical trials due to its toxicity to normal tissue such as the liver and heart (Smith *et al*.,1989).

Six novel derivatives of $[Au(dppe)_2]Cl$ were developed and synthesized to identify possible new candidates with improved tumour specificity compared to $[Au(dppe)_2]Cl$ and cisplatin. Human cervical carcinoma cells (HeLa) were used for an initial toxicity screening. IC_{50}'s obtained for $[Au(dppe)_2]Cl$ and cisplatin were 0.661 and 0.710 µM respectively. Three mixed novel derivatives (MM4, MM5 and MM6) displayed IC_{50}'s ranging between 0.026 and 0.103 µM. These compounds were then selected to be tested further for selectivity and cytotoxicity on various malignant and normal cell lines. MM4 showed selectivity for ovarian, prostate, cervical and breast cancer cells, while MM5 was the most effective against ovarian, colon, prostate, cervical and breast cancer cells. MM6 was most active against ovarian, colon, prostate, cervical and breast cancer cells. The experimental compounds had much higher IC_{50}'s when tested on the normal cells, which indicates selectivity for cancer cells.

The octanol/water partition coefficient (lipophilicity) of all the experimental compounds was measured to determine the lipophilicity of the compounds. $[Au(dppe)_2]Cl$ was found to be strongly lipophilic; while the novel compounds had varying degrees of lipo- and hydrophilicity. The octanol/water partition coefficient (lipophilicity) was also used to establish whether there is a correlation between the lipophilicity, IC_{50} and tumour specificity. In this study no correlation was found between these parameters.

$[Au(dppe)_2]Cl$ is known to have an effect on the mitochondrial membrane potential of cells. MM4, MM5, MM6 and cisplatin were compared to $[Au(dppe)_2]Cl$ for effects on

mitochondrial membrane potential. PHA stimulated human lymphocytes and a human undifferentiated leukemia T-cell line (Jurkat cells) were used in these experiments. $[Au(dppe)_2]Cl$, MM4, MM5 and MM6 depolarized the mitochondrial membranes of PHA stimulated lymphocytes significantly, while only $[Au(dppe)_2]Cl$ depolarized the mitochondrial membranes of the Jurkat cells significantly, indicating that a different mechanism of action might be operational.

MM4, MM5, MM6 and cisplatin were compared to $[Au(dppe)_2]Cl$ for effects on plasma membrane potential. PHA stimulated human lymphocytes and Jurkat cells were used in these experiments. $[Au(dppe)_2]Cl$ and MM6 depolarized the plasma membranes of both PHA stimulated lymphocytes and the Jurkat cells significantly.

In order to determine whether the depolarization of mitochondrial and plasma membranes was a precursor for apoptosis, experiments were done to determine whether MM4, MM5 and MM6 induce apoptosis in Jurkat cells. $[Au(dppe)_2]Cl$ and cisplatin were added for comparison. $[Au(dppe)_2]Cl$, cisplatin, MM4 and MM6 did induce apoptosis in Jurkat cells, but MM5 did not.

The effect of $[Au(dppe)_2]Cl$, cisplatin, MM4, MM5 and MM6 on the cell cycle of Jurkat cells was determined to establish whether the experimental compounds altered this process. $[Au(dppe)_2]Cl$, MM4, MM5 and MM6 arrested the cell cycle in the G_1 phase and cisplatin did so in the S phase.

In order to determine whether the inhibition of cell growth and partition coefficient of the experimental compounds is related to the uptake of the drug, radio labeled drug uptake experiments were carried out with ^{198}Au labeled $[Au(dppe)_2]Cl$, MM5 and MM6. Two different types of ovarian cancer cells were used for these studies. One cell line was sensitive to cisplatin (A2780) and the other was resistant to cisplatin (A2780 cis). Results obtained from these experiments showed that the uptake of these experimental compounds was dependent on their octanol/water partition coefficient. However, the

inhibition of cell growth did not correlate with the uptake of these compounds by the cells that were tested.

To confirm the octanol/water partition coefficient and drug uptake results, ^{198}Au labeled $[Au(dppe)_2]Cl$, MM5 and MM6 were tested *in vivo* for bio distribution in rats. $[Au(dppe)_2]Cl$ (lipophilic) had higher bio distribution compared to MM5 and MM6 (hydrophilic).

Conclusion

The experimental compounds show low IC_{50}'s combined with increased tumour specificity. This indicates that these compounds have great potential to target tumour cells selectively and should be investigated further as anti-cancer agents.

Opsomming

Sedert die bekendstelling van Auranofin in 1985 is daar geen nuwe klinies goedgekeurde goudbevattende geneesmiddels bekend gestel nie. Daar is wel belowende resultate verkry met ‘n goud (I) fosfien kompleks $[Au(dppe)_2]Cl$ (Hoke *et al*., 1991; Mckeage *et al*., 2002). Hierdie verbinding is nie verder in kliniese proewe gebruik nie omdat dit baie toksies was vir normale weefsels, byvoorbeeld die lewer en die hart (Smith *et al*., 1989).

Ses nuwe derivate van $[Au(dppe)_2]Cl$ is ontwikkel en gesintetiseer as moontlike kandidate met beter tumor spesifisiteit as $[Au(dppe)_2]Cl$ en cisplatin. Menslike servikale karsinoom selle (HeLa) is gebruik vir die eerste toksisiteit bepaling. Die IC_{50} waardes wat verkry is vir $[Au(dppe)_2]Cl$ en cisplatin was 0.661 en 0.710 µM onderskeidelik. Drie nuwe derivate (MM4, MM5 en MM6) het IC_{50} waardes gehad tussen 0.026 en 0.103 µM. Hierdie drie verbindings is verder getoets vir selektiwiteit en sitotoksisiteit op ‘n verskeidenheid kanker en normale sellyne. MM4 was selektief vir ovariese, prostaat, servikale en bors kankerselle, terwyl MM5 die effektiefste was op ovariese, kolon, prostaat, servikale en bors kankerselle. MM6 was die aktiefste op ovariese, kolon, prostaat, servikale en bors kankerselle. Die eksperimentele verbindings het hoër IC_{50} waardes getoon by die normale selle wat daarop dui dat hulle meer selektief is vir kankerselle.

Die oktanol/water partisie koëffisiënt (lipopfilisiteit) van al die eksperimentele verbindings is bepaal om die lipofilisiteit van die verbindings te bepaal. $[Au(dppe)_2]Cl$ was sterk lipofilies, terwyl die nuwe derivate varieërende grade van lipo- en hidrofilisiteit getoon het. Die oktanol/water partisie koëffisiënt is ook gebruik om te bepaal of daar ‘n korrelasie bestaan tussen lipofilisiteit , IC_{50} en tumor spesifisiteit. In hierdie studie is geen korrelasie gevind tussen hierdie parameters nie.

Dit is ‘n bekende feit dat $[Au(dppe)_2]Cl$ die mitochondriale membraan potensiaal van selle beïnvloed. MM4, MM5, MM6 en cisplatin is ook getoets om te sien of hulle

dieselfde effek op die mitochondriale membraan potensiaal van selle het as $[Au(dppe)_2]Cl$. PHA gestimuleerde menslike limfosiete en ‘n menslike, ongedifferensieërde leukemie T-sellyn (Jurkat selle) is in hierdie eksperimente gebruik. $[Au(dppe)_2]Cl$, MM4, MM5 en MM6 het die mitochondriale membrane van PHA gestimuleerde menslike limfosiete betekenisvol gedepolariseer, terwyl net $[Au(dppe)_2]Cl$ die mitochondriale membrane van die Jurkat selle betekenisvol kon depolariseer. Hierdie resultate mag daarop dui dat die eksperimentele verbindings ‘n ander werkmeganisme het as $[Au(dppe)_2]Cl$.

MM4, MM5, MM6 en cisplatin is tesame met $[Au(dppe)_2]Cl$ getoets vir effek op die plasmamembraan potensiaal van selle. PHA gestimuleerde menslike limfosiete en ‘n menslike, ongedifferensieërde leukemie T-sellyn (Jurkat selle) is in hierdie eksperimente gebruik. $[Au(dppe)_2]Cl$ en MM6 het die plasmamembrane van beide PHA gestimuleerde menslike limfosiete en Jurkat selle betekenisvol gedepolariseer.

Die depolarisasie van mitochondriale- en plasmamembrane is dikwels ‘n voorloper tot apoptose. Eksperimente is op Jurkat selle gedoen om te bepaal of MM4, MM5 en MM6 wel apoptose geïnisieer het. $[Au(dppe)_2]Cl$ en cisplatin is bygevoeg as kontroles. $[Au(dppe)_2]Cl$, cisplatin, MM4 en MM6 het apoptose in Jurkat selle teweeg gebring, terwyl MM5 nie apoptose veroorsaak het nie.

Die invloed van $[Au(dppe)_2]Cl$, cisplatin, MM4, MM5 en MM6 op die selsiklus van Jurkat selle is bepaal om te sien of hierdie verbindings enige veranderinge in hierdie proses teweeg bring. $[Au(dppe)_2]Cl$, MM4, MM5 en MM6 het die selsiklus in die G_1 fase tot stilstand gebring, terwyl cisplatin dit in die S fase gedoen het.

´n Radioaktiewe opname studie is gebruik om te bepaal of die inhibisie van selgroei en die partisie koëffisiënt van die eksperimentele verbindings die opname daarvan in selle beïnvloed. Die radioaktiewe opname studie is gedoen deur gebruik te maak van ^{198}Au gemerkte $[Au(dppe)_2]Cl$, MM5 en MM6. Twee tipes ovariese kankerselle is in hierdie eksperimente gebruik, een sensitief vir cisplatin (A2780) en een wat weerstandig is teen

cisplatin (A2780 cis). Die resultate wat tydens hierdie studie verkry is, dui daarop dat die opname van die eksperimentele verbindings afhanklik is van hulle oktanol/water partisie koëffisiënt. Die inhibisie in selgroei korrelleer egter nie met die opname van die eksperimentele verbindings in die selle wat getoets is nie.

^{198}Au gemerkte [Au(dppe)$_2$]Cl, MM5 en MM6 is in ´n *in vivo* biodistribusie eksperiment op rotte gebruik om die resultate wat in die opname studie verkry is te bevestig. [Au(dppe)$_2$]Cl (lipofilies) het ´n hoër biodistribusie getoon in vergelyking met MM5 en MM6 (hidrofilies).

Gevolgtrekking

Die eksperimentele verbindings vertoon lae IC_{50} waardes gekombineer met verhoogde tumor spesifisiteit. Dit dui daarop dat hierdie verbindings groot potensiaal het om kankerselle selektief te teiken en moet verder ondersoek word as teen-kanker middels.

List of abbreviations

A

([Au(dppe)$_2$]Cl	bis[1,2-bis(diphenylphosphino)ethane]gold(I) chloride
AMP	Adenosine mono-phosphate
ADP	Adenosine di-phosphate
ATP	Adenosine tri-phosphate
ATCC	American Type Culture Collection
AUCC	Animal Use and Care Committee
Au	Gold
Ar	Argon

B

Bq	Becquerel
BC	Before Christ

C

CAM	Chorio-allantoic membrane
CO_2	Carbon dioxide
ºC	Degree Celsius
Ca^{2+}	Calsium
cm	Centimeter

D

DNA	Deoxyribonucleic acid
DMEM	Dulbecco's Minimum Essential Medium
DMSO	Dimetyl sulfoxide
Da	Dalton
DIBAC$_4$(3)	bis (1,3-dibarbituric acid) trimethine

E

EMEM	Eagle's Minimum Essential Medium
ECACC	European Collection of Cell Cultures
EtOH	Ethanol

F

FAD	Flavin adenine dinucleotide
FCS	Fetal calf serum

G

G1	Gap 1
G2	Gap 2
G	Centrifugal force

I

IV	Intravenous
IC_{50}	Inhibitory concentration that results in 50% cell death

J

JC-1	5,5',6,6'-tetrachloro-1,1',3,3' tetraethylbenzimidazolcarbocyanine iodide

M

µl	Microlitre
µm	Micrometer
mM	Millimolar
mg	Milligram
µg	Microgram
µg/ml	Microgram per litre
mg/ml	Milligram per millilitre

ml	Millilitre
µM	Micro molar
M-phase	Mitosis phase
MTT	[3-(4, 5-dimethylthiazol-2-yl)-2, 5-diphenyl tetrazolium bromide]
Mg^{+}	Magnesium
mtDNA	Mitochondrial deoxyribonucleic acid
mCi	Milli Curie
µCi	Micro Curie
µCi/ml	Micro Curie per millilitre
µCi/µl	Micro Curie per microlitre

N

nm	nanometer
nM	nanomolar
ng	nanogram
ng/ml	nanogram per millilitre
NAD^{+}	nicotinamide dinucleotide
NADH	Nicotinamide adenine dinucleotide
NADPH	Nicotinamide adenine dinucleotide phosphate
N	Normal
NRBM	National Repository for Biological materials
NECSA	Nuclear Energy Corporation of South Africa

P

PHA	Phyto-haemagglutenin
PBS	Phosphate Buffered Saline
pH	Percentage hydrogen

R

RA	Rheumatoid Arthritis
Rh 123	Rhodamine 123
RNA	Ribonucleic acid
RPMI 1640	Rosswell Park Memorial Institute
rpm	Revolutions per minute
RNAse	Ribonuclease A

S

Sn	Tin
Sn-O	Tin-oxygen
S-phase	Synthesis phase
SEM	Standard Error of the Mean

U

UPBRC	University of Pretoria Biomedical Research Centre
UV	Ultra Violet

V

V	Vial

Chapter 1: Introduction

1.1 Literature review

The use of gold in medicine dates back to antiquity with both Arabic and Chinese physicians using gold preparations to treat a variety of ailments (Tiekink, 2002). The Chinese used gold, probably as dust or flakes as a medicinal agent as early as 2500 BC. Monovalent gold salts have been used therapeutically since 500 BC to treat leprosy. Over time, monovalent organogold drugs have been used to treat pemphigus, lupus erythematosus, ulcerative colitis, Crohn's disease, various types of arthritis, bronchial asthma, bullous skin conditions, discoid lupus, ankylosing spondylitis, tuberculosis and malaria with mixed results (Eisler, 2003).

The earliest reports on the use of metals or metal-containing compounds in cancer and leukemia date from the sixteenth and nineteenth centuries. They were forgotten until the 1960's when the anti-tumour activity of the inorganic complex *cis*-diammine-chloroplatinum(II) (cisplatin) was discovered. This led to the development of other types of non-organic cytostatic drugs. Numerous other metal compounds containing platinum, other platinum metals and even non-platinum metals were effective against tumours in man and experimental tumours in animals (Köpf-Maier, 1994).

In current medical practice, chrysotherapy – the treatment of rheumatoid arthritis (RA) with gold-based drugs - is well established. Chrysotherapy derives its name from Chryseis, a golden-haired daughter of a priest of Apollo in Greek mythology. Six monovalent organogold complexes are now widely used throughout the world in the treatment of rheumatoid arthritis. Auranofin, the newest drug, was licensed in the mid-1980's. This drug has the advantage of being orally absorbed but it is considered less effective than the injectable gold thiolates (Eisler, 2003). Auranofin is a monomeric linear Au(I) complex stabilized by triethyl phosphine and tetracetylthioglucose ligands.

Within the body, auranofin is known to undergo ligand dissociation reactions to generate various different Au-based metabolites (McKeage *et al*., 2002).

New approaches are needed to overcome the two main problems in cancer chemotherapy – the common occurrence of drug-resistant tumour cells and the lack of selectivity of cancer drugs in differentiating between tumour cells and normal tissues. Most of the existing clinical drugs are non-selective, depending on the more rapid proliferation of cancer cells and act by targeting the DNA of tumour cells (by inhibiting biosynthesis or direct damage) and are susceptible to similar resistance mechanisms (Berners-Price *et al*., 1999).

The mitochondria of cells

Mitochondria are the major source of energy in most eukaryotic cells. These organelles are approximately 1 μm in diameter and of variable length. They are comprised of up to 15% of total cellular protein, varying in accordance with energetic demands of the cell they supply. They are surrounded by a highly permeable outer membrane, an inter membrane space and a relatively impermeable inner membrane that is responsible for inhibiting passage of polar molecules lacking specific transporters. The inner mitochondrial membrane is folded into numerous cristae that increase surface area to accommodate thousands of copies of the enzyme complexes required for the generation of adenosine triphosphate (ATP). Enclosed by the inner mitochondrial membrane is the mitochondrial matrix, containing mitochondrial DNA (mtDNA), ribosomes and enzymes used for the citric acid cycle and fatty acid oxidation (Preston *et al*., 2001).

Figure 1: Simplified structure of a typical mitochondrion. (http://en.wikipedia.org/wiki/mitochondria)

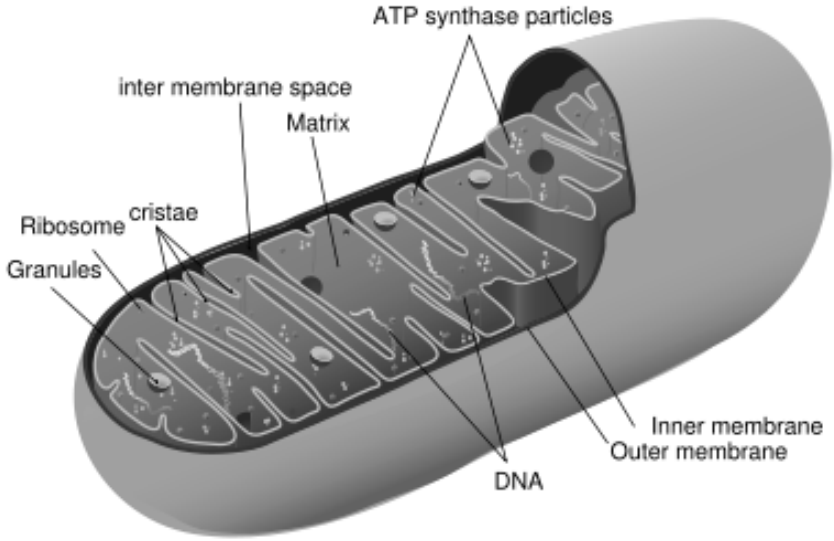

The mitochondria are the primary location for the production of energy-carrying molecules in most cells. Metabolism begins in the cytoplasm with glycolysis, where glucose is metabolized to the primary product pyruvate. The pyruvate enters the mitochondria through shuttles, where it is processed by the citric acid cycle. The co-enzymes nicotinamide adenine dinucleotide (NAD^+) and flavin adenine dinucleotide (FAD) are reduced during the citric acid cycle, yielding NADH and FAD_2 (some NADH is also generated during glycolysis). These electron carriers are used by the electron transport chain, which supplies the energy to establish a proton gradient across the inner membrane of the mitochondria. The gradient is used to power the last stage of metabolism, oxidative phosphorylation. Protons flow down this gradient through the ATP synthase complex to provide energy to phosphorylate adenosine di-phosphate (ADP) to adenosine tri-phosphate (ATP) (Bertram *et al*., 2006). Mitochondria produce ATP for cellular processes and have an integral role in the global cellular regulation of calcium fluxes and the redox state. Mitochondria are also the focal point for a variety of

pro- and anti-apoptotic stimuli, such as the BCl-2 family of proteins. There is an increasing interest in exploiting the pro-apoptotic function of mitochondria to trigger the death of diseased cells, in particular, cancerous cells (Don and Hogg, 2004).

Mitochondrial membrane permeabilization, regulated by the mitochondrial permeability transition pore (a voltage dependant, cyclosporin A sensitive, high conductance inner membrane channel), is widely accepted as being central to the process of mitochondrial induced apoptosis (Barnard, *et al*., 2004). The mitochondrial permeability transition is a reversible phenomenon whereby the mitochondrial inner membrane becomes freely permeable to solutes of less than 1500 Da. At the onset of the mitochondrial permeability transition, mitochondria depolarize, uncouple and undergo large amplitude swelling (Rodriguez-Enriquez *et al*., 2004). This causes dissipation of mitochondrial membrane potential, loss of mitochondrion homeostasis, impairment of ATP synthesis and diffusion of solutes down their concentration gradient. *In vitro*, this is followed by an osmotically obligatory water flux across the inner membrane with passive swelling, outer membrane rupture, and cytochrome *c* release (Basso *et al*., 2005). It remains unclear exactly how mitochondrial outer-membrane permeabilization occurs, but it is apparent that it is a rapid event, coordinated within individual cells but it occurs asynchronously in a population of cells. The permeabilization event leaves the mitochondrial inner membrane in tact and the mitochondria can maintain some, if not all of their essential functions, at least in the short term (Waterhouse *et al*., 2002). It will be a challenge to develop drugs with a strong mitochondrion-permeabilizing potential that selectively target tumour cells. Mitochondrion-targeted reagents might become a valuable tool for destroying cancer cells that have become resistant to the cytotoxic effects of conventional cancer therapies (Debatin, *et al*., 2002).

The specific targeting of mitochondria has the potential to overcome the two overriding problems in cancer chemotherapy – the common occurrence of drug-resistant tumour cells and the lack of selectivity of cancer drugs in differentiating between tumour cells and normal tissues (Barnard *et al*., 2003). Significantly, carcinoma cells have an elevated mitochondrial membrane potential relative to normal cells (Chen, 1988), leading to more

rapid accumulation of lipophilic cations, which are concentrated within mitochondria in response to the negative mitochondrial membrane potential. There is, therefore, potential for selectively targeting tumour cells by compounds having optimal lipophilic-hydrophilic character (Modica-Napolitano *et al*., 2001).

Lipophilic cations

Lipophilic cations are an interesting new class of anti-tumour drugs with the potential to selectively target the mitochondria in tumour cells. These compounds concentrate in the mitochondria due to their lipophilic-cationic character and exhibit preferential cytotoxicity to carcinoma cells with hyperpolarized membranes (Berners-Price *et al*., 1999). The use of lipophilic cations as anti-cancer agents has shown promise, but there is no real understanding of the biochemical basis for increased mitochondrial membrane potential in carcinoma cells. Consequently, the choice for the design or selection of potentially therapeutic lipophilic cations has been based almost solely on physical properties (i.e., lipid solubility and delocalization of positive charge) and the preliminary screening for the selective cytotoxicity of these compounds is very important (Modica-Napolitano *et al*., 2001).

Elevated mitochondrial membrane potential is found in a variety of cancerous cells, relative to normal cells and this may allow the selective targeting of mitochondria in cancerous cells. Relative differences in the abilities of mitochondria from normal and cancerous cells to accumulate lipophilic cationic dyes such as Rhodamine 123 have been reported (Hoke *et al*., 1988). Other cationic lipophilic cations that have demonstrated anti-tumour activity include $[Au(dppe)_2]Cl$, dequalinium, bis-quaternary ammonium heterocycles and triarylalkyl phosphonium salts; as well as MKT-077. MKT-077 has entered phase 1 clinical trials (Berners-Price *et al*., 1999).

The fluorescent dye Rhodamine 123 (Rh 123) is a small cationic molecule which is selectively toxic towards carcinoma cells compared with normal epithelial cells, and inhibits the growth of carcinomas in mice. Carcinomas are the most common solid

tumours in humans and cause the most deaths. It was subsequently shown that the mitochondria of carcinoma cells derived from kidney, ovary, pancreas, lung, adrenal cortex, skin , breast, prostate, cervix, vulva, colon, liver and testis accumulated RH 123 to a greater extent and with a longer retention than did normal epithelial cells. The increased uptake has been attributed to the higher mitochondrial membrane potential in the carcinoma cells. Although it is apparent that small lipophilic cations are mitochondrial toxins, the exact bases for their toxicity is difficult to pinpoint. The hydrophobic nature of the cation appears to dictate the mitochondrial target, with more hydrophobic compounds (Rh 123) affecting electron transport and ATP synthesis and more hydrophilic compounds perturbing matrix proteins and functions (Chen, 1988). If the high mitochondrial membrane potential of carcinoma cells is responsible for their susceptibility to lipophilic cations, these compounds might also carry the risk of harming other cells that have high mitochondrial membrane potentials such as cardiac muscle cells. Conversely, myelotoxicity is less of a problem with these compounds than conventional chemotherapeutics. Although bone marrow cells proliferate very rapidly, their mitochondrial membrane potentials are low and very little of the cations are accumulated (Koya *et al*., 1996).

Au(I) phosphines

Gold derivatives are well known for their clinical use in the treatment of rheumatoid arthritis, but they have also shown promise as anti-tumour agents. Among the many gold complexes that have been investigated for potential anti-tumour properties, gold(I) phosphine derivatives have shown the most reproducible and significant activity in murine tumour models *in vivo*. Auranofin was found to be effective at increasing the life span of mice inoculated with P388 lymphocytic leukemia (McKeage *et al*., 2002).

Over the last two decades evidence has shown that gold complexes exhibit significant cytotoxic effects on cancer cell lines and also display anti-tumour activity in some transplantable *in vivo* tumour models. The exact mode of action of gold(I)- diphosphine derivatives is still largely unknown, but several possible mechanisms responsible for the

cytotoxic activity have been proposed. In one of the proposed mechanisms, gold seems to function as a carrier for the diphosphine ligand which can be released. Therefore, gold can protect the diphosphine ligand from oxidation reactions, enabling it to be delivered to cells and display its anti-proliferative activity. However, a more direct involvement of gold in anti-tumour activity is also possible (Caruso *et al*., 2007).

The anti-tumour activity of the Au(I) phosphine complex, bis[1,2-bis(diphenylphosphino)ethane]gold(I) chloride ([Au(dppe)$_2$]Cl) was first discovered in the mid 1980's. The lipophilic-cationic nature of the complex seems important and early studies provided evidence for an anti-mitochondrial mode of action (Hoke, *et al*., 1991). *In vitro* studies of [Au(dppe)$_2$]Cl showed that the compound is cytotoxic to tumour cell lines and is only minimally inhibited by serum. It produces DNA protein cross-links and DNA strand breaks in cells; it also inhibits macromolecular synthesis with a preferential inhibitory effect on protein synthesis relative to DNA and RNA synthesis (Berners-Price *et al*., 1986).

Promising results were obtained with [Au(dppe)$_2$]Cl as an anti-cancer agent, but in pre-clinical toxicity studies with Beagle dogs, [Au(dppe)$_2$]Cl, was shown to produce cardiac, hepatic and vascular toxicities. *In vitro*, [Au(dppe)$_2$]Cl was also very cytotoxic to isolated dog and rat hepatocytes (Hoke *et al*., 1988; Smith *et al*., 1989). Rat hepatocytes exposed to [Au(dppe)$_2$]Cl underwent pronounced changes in their ultra-structural morphology, the earliest change being mitochondrial swelling. [Au(dppe)$_2$]Cl caused a rapid initial increase in cellular respiration and a decrease in total cellular ATP. These results confirm the theory that mitochondria are target organelles for [Au(dppe)$_2$]Cl. In subsequent experiments it was found that [Au(dppe)$_2$]Cl stimulated state 4 respiration in isolated rat liver mitochondria which indicates that it may uncouple oxidative phosphorylation (Hoke *et al*., 1988).

Pre-clinical development of [Au(dppe)$_2$]Cl was abandoned because of the severe hepatotoxicity in dogs. The hepatotoxicity was attributed to alterations in mitochondrial function. [Au(dppe)$_2$]Cl is very lipophilic and consequently targets mitochondria in all

cells. Studies were done in order to vary the hydrophilic character in $[Au(dppe)_2]Cl$ derivatives to achieve greater selectivity for tumour cells versus normal cells (Berners-Price *et al*., 1999).

Tin and tin compounds

Human beings have used tin since the Bronze Age. For thousands of years, tin and tin alloys were used for production of consumer products such as tin dishes or drinking mugs. Starting with the Industrial Revolution, inorganic tin compounds were produced for various purposes. Around 1940 the industrial production of organotin compounds started. Organotin compounds are technically and economically important, for example, as biocides and plastic stabilizers and they are of high toxicological relevance. Tin exists mainly in the oxidation states Sn(0), Sn(II) and Sn(IV) (Rüdel, 2003).

Inorganic tin salts are poorly absorbed and rapidly excreted in the faeces; as a result they have a low toxicity. Only about 5% is absorbed from the gastrointestinal tract, widely distributed in the body and then excreted by the kidney. Some tin is deposited in lung and bone and some tin salts can cause renal necrosis after parenteral doses. Long-term animal carcinogenic studies have shown fewer malignant tumours in animals exposed to tin than in controls (Winship, 1988).

A number of organotin compounds have been shown to be active against the P388 murine leukemia. This tumour screening model was shown to be very sensitive to tin compounds. These compounds were not active in solid tumour models and their anti-tumour potential was not fully realized until screening of metal-based anti-tumour drugs began against human tumour-derived cell lines. A number of organotin complexes were found to be cytotoxic to human tumour cells in these screening systems (Bonire and Fricker, 2001).

Organotin compounds are involved in cancer treatment via different mechanisms at the molecular level. The binding ability of organotin compounds towards DNA depends on

the coordination number and nature of groups bonded to the central tin atom. Recent studies have shown that low doses of organotin compounds exhibit anti-tumour activity and have suggested an action mode via gene-mediated pathway in the cancer cells, opening a new research sub-area on organotin compounds. Organotin(IV) compounds can induce apoptosis and are therefore important in cancer chemotherapy (Tabassum and Pettinari, 2006).

1.2 General outline of this study

1.2.1 Experimental Compounds

Berners-Price *et al*., (1999) found that by varying the balance between lipophilicity and hydrophilicity of $[Au(dppe)_2]Cl$ derivatives, the selectivity for cancer cells could be improved with a consequent decrease in toxicity to normal tissues.

The $[Au(dppe)_2]Cl$ derivatives in this study have varying degrees of lipophilicity and hydrophilicity. Different combinations of these parameters will be looked at in this study ,in order to find more selectivity towards cancer cells than normal cells. Tin and ruthenium were used in combination with gold for the experimental compounds.

Combination therapy involving concurrent administration of two or more compounds is a strategy to try and enhance the anti-cancer efficacy of lipophilic cations (Modica-Napolitano *et al*., 2001).

$[Au(dppe)_2]Cl$, plus six experimental derivatives of $[Au(dppe)_2]Cl$ were synthesized by Messai Mamo under supervision of Prof Marcus Layh of the School of Chemistry, University of the Witwatersrand. NMR studies were done to verify the structures of these compounds. Cisplatin was obtained from Sigma.

The six experimental compounds are Bu_2SnRu **(MM1)**, 2RuAudpmaa **(MM2)**, 1RuAudpmma **(MM3)**, $Bu_2Sndpmaa$ **(MM4)**, $(Bu_2Sn)_2Audpmaa$ **(MM5)** and $Bu_2SnAudpmaa$ **(MM6)**. The structures of these compounds can be seen in **Figure 1.**

Five (MM1, MM2, MM3, MM5 and MM6) of the six novel derivatives of $[Au(dppe)_2]Cl$ are chloride salts and have $Au(dppe)_2^+$ at the center of the molecule. MM1 has $Au(dppe)_2^+$ combined with one tin and one ruthenium molecule. Two butyl molecules were added to the tin side of the compound. MM2 has $Au(dppe)_2^+$ combined with two ruthenium molecules, while MM3 has $Au(dppe)_2^+$ and only one ruthenium molecule. MM4 lacks the $Au(dppe)_2^+$ and has only one tin molecule in the compound and two butyl groups. MM5 also features the $Au(dppe)_2^+$ combined with two tin molecules while MM6 has the $Au(dppe)_2^+$ combined with one tin molecule. MM5 has four butyl groups, while MM6 has only two.

Figure 1: Structures of the experimental compounds

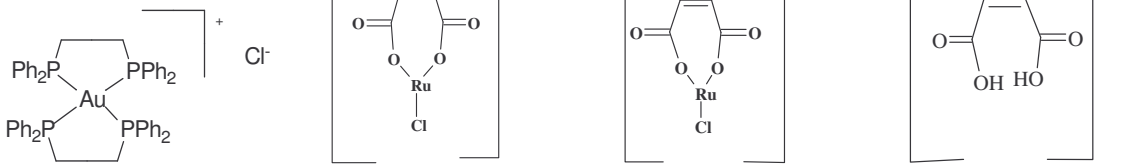

[Au(dppe)$_2$]Cl **Bu$_2$SnRu (MM1)** **2RuAudpmaa (MM2)** **1RuAudpmaa (MM3)**

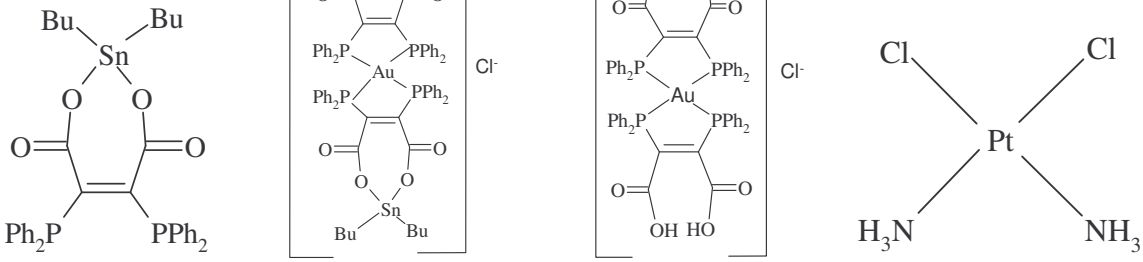

Bu$_2$Sndpmaa (MM4) **(Bu$_2$Sn)$_2$Audpmaa (MM5)** **Bu$_2$SnAudpmaa (MM6)** **Cisplatin**

1.2.2 Hypothesis

The selected novel metal compounds have higher selectivity for cancer cells, are less toxic towards normal cells and have improved bio distribution compared to $[Au(dppe)_2]Cl$.

1.2.3 Aim of the study

The aim of the study was to determine the tumour specificity, mechanism of action and bio distribution of the selected novel experimental complexes.

1.2.4 Study objectives

1.2.4.1 Stage one (refer chapters 2 and 3)

1. To screen six organometallic compounds for activity against HeLa cells (human cervical carcinoma).

2. To identify three compounds based on lipophilicity and cytotoxicity for stage two and three studies.

1.2.4.2 Stage two (refer chapters 3, 4, 5, 6 and 7)

1. To test the selected compounds together with $[Au(dppe)_2]Cl$ and cisplatin on a range of normal and cancer cell cultures to determine toxicity and tumour specificity.

2. To determine the effect of the selected compounds on mitochondrial and plasma membrane potentials of:
    a. Primary PHA stimulated human lymphocyte cultures

b. Jurkat cells (human undifferentiated leukemia T-cell line).

3. To determine whether the selected compounds induce apoptosis in Jurkat cells.

4. To determine whether the selected compounds have an effect on the cell cycle of Jurkat cells.

1.2.4.3 Stage three (refer chapters 8 and 9)

1. To compare drug uptake of MM5 and MM6 labeled with ^{198}Au *in vitro* with [^{198}Au(dppe)$_2$]Cl, using a cisplatin sensitive ovarian cancer cell line (A2780) and its cisplatin resistant subline (A2780 cis).

2. To determine drug distribution *in vivo* using ^{198}Au labeled MM5, MM6 and [Au(dppe)$_2$]Cl in rats.

Stage 1.

Chapter 2: Determination of the octanol/water partition coefficient

2.1 Introduction

The ability of a drug to dissolve in a lipid phase when an aqueous phase is also present (often referred to as lipophilicity) can be best characterized by a partition coefficient defined as the equilibrium constant of drug concentrations in the two phases.

$$P = [Drug]_{lipid} / [Drug]_{water}$$

Since partition coefficients are difficult to measure in living systems, they are usually determined *in vitro* using 1-octanol as the lipid phase and a phosphate buffer of pH 7.4 or water as the aqueous phase. This permits standardized measurements of partition coefficients. Because it is a ratio, P is dimensionless, and its logarithm (log P) is used as the measure of lipophilicity (Partitioning and Complexation, PHA 5110).

Partitioning coefficients thoroughly influence drug transport characteristics – the way drugs reach the site of action from the site of application (e.g., injection site, gastrointestinal tract). Since drugs are distributed by the blood, they must penetrate and traverse many cells to reach the site of action. Hence, the partition coefficient will determine what tissues a given compound can reach. Extremely water soluble drugs may be unable to cross lipid barriers and gain access to organs rich in lipids, such as the brain and other neuronal tissues. The partition coefficient is one of several physicochemical parameters influencing drug transport and distribution, which in itself is only one aspect of drug activity. The contribution of individual functional groups and their structural

arrangement help determine the polarity and therefore the lipophilic or hydrophilic character of the molecule (Partitioning and Complexation, PHA 5110).

Since the lipophilicity is one of the most important parameters for quantitative structure activity and property relationships, the design of drugs significantly depends on the accuracy of lipophilicity determinations (Scholz *et al*., 2003). Lipophilicity is the single most informative and successful physiochemical property in medicinal chemistry. Not only has lipophilicity found innumerable applications in quantitative structure-activity relationships and quantitative structure-pharmacokinetic relationships, but its study has revealed a wealth of information on intermolecular forces, intra molecular interactions, and molecular structure in the broadest sense ([2]Liu *et al*., 2005).

Even if the importance of drug-membrane interactions in drug design received far less attention than drug-protein interactions, the molecular lipophilicity of small drug molecules has a prominent role in various physico-chemical models, e.g. absorption, distribution, permeability and protein binding. Drug penetration through various biological membranes is a very limitative phenomenon on drug efficiency and has a direct impact on its bioavailability (Darrouzain *et al*., 2006).

Lipophilicity is therefore one of the most important parameters to decide the status achievable by a new molecule in the pharmacological development process. This property plays an important role in the mechanism of pharmacokinetic action and in the pharmaco-dynamics as well, estimation of the lipophilic character of a new drug candidate has proved to be one of the first parameters to be determined (Hallgas *et al*., 2005).

2.2 Aim

The aim of this study was to determine the octanol/water partition coefficient (lipophilicity) of $[Au(dppe)_2]Cl$, Cisplatin and the six novel $[Au(dppe)_2]Cl$ derivatives (MM1, MM2, MM3, MM4, MM5 and MM6).

2.3 Materials and methods

2.3.1 Experimental compounds

Preparation of experimental compounds

i. $[Au(dppe)_2]Cl$

Molecular weight: 1028 g/mol

A 60 µM stock solution was prepared with an end volume of 10 ml. 0.617 mg of the compound was weighed out on a micro-balance using spheres of weighing paper. 100 µl DMSO was used to rinse the compound off the weighing paper and make it more soluble in the octanol. 10 ml of water saturated octanol was added. From this concentration a 20 µM dilution was prepared with a final volume of 5 ml. 10 ml plastic tubes were used. The Anthelie Advanced spectrophotometer was used to determine the absorbance maxima (λ_{max}). λ_{max} = 286 nm.

ii. Cisplatin

Molecular weight: 300 g/mol

A 60 µM stock solution was prepared with an end volume of 10 ml. 0.18 mg of the compound was weighed out on a micro-balance using spheres of weighing paper. 100 µl DMSO was used to rinse the compound off the weighing paper and make it more soluble in the octanol. 10 ml of water saturated octanol was added. From this concentration a 20 µM dilution was prepared with a final volume of 5 ml. 10 ml plastic tubes were used. The Anthelie Advanced spectrophotometer was used to determine the absorbance maxima (λ_{max}). λ_{max} = 231 nm.

iii.Bu_2SnRu (MM1)

Molecular weight: 1464.72 g/mol

A 60 µM stock solution was prepared with an end volume of 10 ml. 0.879 mg of the compound was weighed out on a micro-balance using spheres of weighing paper. 100 µl DMSO was used to rinse the compound off the weighing paper and make it more soluble

in the octanol. 10 ml of water saturated octanol was added. From this concentration a 20 µM dilution was prepared with a final volume of 5 ml. 10 ml plastic tubes were used. The Anthelie Advanced spectrophotometer was used to determine the absorbance maxima (λ_{max}). λ_{max} = 275 nm.

iv. 2RuAudpmaa (MM2)

Molecular weight: 147.45 g/mol

A 60 µM stock solution was prepared with an end volume of 10 ml. 0.89 mg of the compound was weighed out on a micro-balance using spheres of weighing paper. 100 µl DMSO was used to rinse the compound off the weighing paper and make it more soluble in the octanol. 10 ml of water saturated octanol was added. From this concentration a 20 µM dilution was prepared with a final volume of 5 ml. 10 ml plastic tubes were used. The Anthelie Advanced spectrophotometer was used to determine the absorbance maxima (λ_{max}). λ_{max} = 355 nm.

v. 1RuAudpmaa (MM3)

Molecular weight: 1335.84 g/mol

A 60 µM stock solution was prepared with an end volume of 10 ml. 0.80 mg of the compound was weighed out on a micro-balance using spheres of weighing paper. 100 µl DMSO was used to rinse the compound off the weighing paper and make it more soluble in the octanol. 10 ml of water saturated octanol was added. From this concentration a 20 µM dilution was prepared with a final volume of 5 ml. 10 ml plastic tubes were used. The Anthelie Advanced spectrophotometer was used to determine the absorbance maxima (λ_{max}). λ_{max} = 278 nm.

vi. Bu_2Sndpmaa (MM4)

Molecular weight: 715.35 g/mol

A 60 µM stock solution was prepared with an end volume of 10 ml. 0.43 mg of the compound was weighed out on a micro-balance using spheres of weighing paper. 100 µl DMSO was used to rinse the compound off the weighing paper and make it more soluble in the octanol. 10 ml of water saturated octanol was added. From this concentration a 20

µM dilution was prepared with a final volume of 5 ml. 10 ml plastic tubes were used. The Anthelie Advanced spectrophotometer was used to determine the absorbance maxima (λ_{max}). λ_{max} = 233 nm.

vii. $(Bu_2Sn)_2$Audpmaa (MM5)

Molecular weight: 1661.85 g/mol

A 60 µM stock solution was prepared with an end volume of 10 ml. 0.997 mg of the compound was weighed out on a micro-balance using spheres of weighing paper. 100 µl DMSO was used to rinse the compound off the weighing paper and make it more soluble in the octanol. 10 ml of water saturated octanol was added. From this concentration a 20 µM dilution was prepared with a final volume of 5 ml. 10 ml plastic tubes were used. The Anthelie Advanced spectrophotometer was used to determine the absorbance maxima (λ_{max}). λ_{max} = 335 nm.

viii. Bu_2SnAudpmaa (MM6)

Molecular weight: 1432.2 g/mol

A 60 µM stock solution was prepared with an end volume of 10 ml. 0.86 mg of the compound was weighed out on a micro-balance using spheres of weighing paper. 100 µl DMSO was used to rinse the compound off the weighing paper and make it more soluble in the octanol. 10 ml of water saturated octanol was added. From this concentration a 20 µM dilution was prepared with a final volume of 5 ml. 10 ml plastic tubes were used. The Anthelie Advanced spectrophotometer was used to determine the absorbance maxima (λ_{max}). λ_{max} = 271 nm.

2.3.2 Reagents

i. Octan-1-ol (octanol)

Octan-1-ol, cat no 01540, was supplied by Radchem (Brackendowns, RSA) and was used undiluted.

2.3.3 Method

Partition coefficients (PC) between water and octanol were determined using standard methods. Concentrations in each phase were calculated from U.V-visible absorption data using extinction coefficients determined in water-saturated octanol and in octanol-saturated water (Bowen, 1999).

The octanol/water partition coefficient values were calculated according to the following formula:

PC = Co/Cw

Where PC is the octanol/water partition coefficient, Co is the concentration in the octanol phase and Cw is the concentration in the aqueous phase.

A volume of water-saturated octanol and octanol-saturated water was prepared by shaking equal volumes of octanol and de-ionized water for 15 minutes. The layers were allowed to separate overnight in a separation funnel. The two fractions were collected separately being careful not to allow cross contamination of one solvent layer into another. Hereafter, octanol will refer to de-ionized water-saturated octanol and water will refer to octanol-saturated water.

Octanol = de-ionized water-saturated octanol.
Water = octanol-saturated de-ionized water.

5 ml of 20 µM solutions were made up in octanol for each drug. Each of these solutions was added to a 1 ml quartz cuvette and analyzed separately by UV-visible spectroscopy to give absorbance maxima at a wavelength between 340 nm and 220 nm. This absorbance corresponds to a Ci value (initial concentration) for each solution. 5 ml of octanol-saturated de-ionized water was added to each of these solutions so that the final volumes were 10 ml and shaken vigorously for 15 minutes. The two phases were

allowed to settle over a period of 30 minutes and was centrifuged at 150G for 8 minutes. The aqueous extract was carefully removed with a Pasteur pipette to ensure that no contamination from the octanol occurred. This was added to a 1 ml quartz cuvette for analysis by UV-visible spectroscopy to give an absorbance maximum at the wavelength identified from Ci determination. This absorbance corresponded to a Cw value for each solution. The concentration of each complex remaining in the octanol layer, Co, was determined by Ci – Cw.
Partition Coefficient (PC) will be given by Co/Cw.

2.4 Results

The final octanol/water partition coefficient values were the average of five independent experiments.

Results are expressed as the mean log values (log P) ± SEM of the final octanol/water partition coefficient value.

Table 2.1 represent the octanol/water partition coefficient values for the concentration of 20 µM for each compound.

The mean octanol/water partition coefficient values ± SEM and the mean log octanol/water coefficient values ± SEM are summarized in **Table 2.1.** Each value represents the mean of 5 independent experiments.

Table 2.1: The mean octanol/water partition coefficient values ± SEM and the mean log octanol/water partition coefficient values ± SEM of $[Au(dppe)_2]Cl$, cisplatin and six novel $[Au(dppe)_2]Cl$ derivatives (MM1, MM2, MM3, MM4, MM5 and MM6). Each value represents the mean of 5 independent experiments.

Octanol/water partition coefficient and mean log octanol/water partition coefficient ± SEM

Experimental compounds	Mean octanol/water partition coefficient ± SEM	Mean log octanol/water partition coefficient ± SEM
$[Au(dppe)_2]Cl$	13.718 ± 0.841	1.136 ± 0.027
Cisplatin	1.269 ± 0.154	0.094 ± 0.055
MM1	0.341 ± 0.057	-0.474 ± 0.073
MM2	1.067 ± 0.130	0.021 ± 0.055
MM3	0.420 ± 0.181	-0.455 ± 0.18
MM4	1.845 ± 0.220	0.266 ± 0.057
MM5	0.169 ± 0.143	-1.045 ± 0.540
MM6	0.043 ± 0.027	-1.209 ±0.255

2.5 Discussion

The lipophilicity of lipophilic cationic compounds such as $[Au(dppe)_2]Cl$ determines the degree of protein binding and cellular uptake of these compounds, hence a correlation between the lipophilicity of the compound and the degree of selectivity and cytotoxic potency of these compounds has been established. This implies that higher selectivity of a compound can be achieved with an increase in the hydrophilicity of the compound. With an increase in lipophilicity, an increase in the cytotoxicity of the compound can be achieved (Berners-Price *et al*., 1999).

The octanol/water partition coefficient of the experimental compounds was determined to establish whether there is a correlation between the lipophilicity, the IC_{50} and the tumour specificity. Results obtained in this study showed that $[Au(dppe)_2]Cl$ had a log P value of 1.136 ± 0.027 which makes it a strong lipophilic compound. Cisplatin had a log P value of 0.094 ± 0.055 which gives it limited lipophilic character. MM2 and MM4 also show limited lipophilic characteristics with log P values of 0.021 ± 0.055 and 0.266 ± 0.057 respectively. MM3 had a log P value of -0.455 ± 0.180 which make this compound weakly hydrophilic, MM5 and MM6, on the other hand have log P values of -1.045 ± 0.540 and -1.209 ± 0.255 respectively, which makes them strongly hydrophilic.

[1]Hollósy *et al*., (2002) also found in their study that the higher the lipophilicity values, the higher the anti-tumour and apoptotic activity (programmed cell death) in their compounds.

Alteration of lipophilicity of aromatic cationic anti-tumour drugs greatly affects the cellular uptake and binding to plasma proteins. Changes in lipophilicity also affect host toxicity and optimal lipophilicity may be a critical factor in the design of analogues with high anti-tumour activity (McKeage *et al*., 2000).

Berners-Price *et al.*, (1999) established that there is a correlation between the degree of selectivity and the cytotoxic potency of the compound and the octanol/water partition

coefficient. Compounds with intermediate lipophilicity display significant tumour activity with less dose limiting toxicity (McKeage *et al*., 2002).

$[Au(dppe)_2]Cl$ induced a rapid dissipation of the inner mitochondrial membrane potential, efflux of calcium, increased mitochondrial respiration, mitochondrial swelling and increased permeability of the inner membrane to cations and protons in isolated rat mitochondria. Structure/activity relationship comparisons suggested that these mitochondrial effects were determined by the uptake of $[Au(dppe)_2]Cl$ into mitochondria, which in turn was related to the cationic-lipophilic nature of the molecule (McKeage *et al*., 2002).

In **Chapter 3**, it will become apparent whether the experimental compounds exhibit more selectivity and less toxicity than $[Au(dppe)_2]Cl$, and whether there is a correlation between the lipophilicity, the IC_{50} and the tumour specificity.

Stage 1 and 2

Chapter 3: Cytotoxicity and tumour specificity

3.1 Introduction

Since the discovery in the 1950's that some human tumour cells could be propagated indefinitely in culture in the presence of the appropriate nutrients and growth factors, human tumour cell lines have played an important part in the discovery and characterization of new chemotherapeutic drugs. A potential weakness of such cell lines is that they may have lost important properties originally possessed *in vivo*, including potential targets for chemotherapy (Baguley, 2004).

Drug discovery and toxicological testing share the need for dependable *in vitro* cellular toxicity tests. Ideally these tests should be objective, quantitative and reproducible (Cree and Andreotti, 1997). Cytotoxicity has been defined as the adverse effects resulting from interference of agents with structures and processes essential for cell survival, proliferation and function (Tuschl and Schwab, 2004). Early toxicity prediction is becoming a very important issue in pharmaceutical development. *In vitro* methods for toxicity assessment are the experimental models of choice because of their simplicity and their reduced requirement for test material, and are therefore an absolute necessity in drug development (Paillard *et al*., 1999). In drug design and drug development adequate model systems have to be introduced at an early stage to avoid loss of promising compounds at an advanced stage due to insufficient absorption into, and distribution throughout the body. Besides toxicity, the pharmacokinetic characteristics were a major reason for failures of compounds in clinical studies in the past (Braun *et al*., 2000).

Many biological assays require the measurement of surviving and or proliferating mammalian cells. This can be achieved by several methods, one of which is counting cells that include or exclude a dye (Mossman, 1983).

Cytotoxicity assays were performed to establish the sensitivity of cancer cell lines and normal cell cultures to the experimental compounds. A known concentration of cells was exposed to different concentrations of the experimental drug in a 96 well tissue culture plate and incubated for a period of time. The incubation period ranged from three to seven days. The results obtained in this experiment enabled the researcher to calculate the concentration of the experimental compound that inhibits 50% of growth (IC_{50}). The viable cells in each well of the tissue culture plate will be determined with the MTT method originally described by Mossman (1983) and adapted by Van Rensburg *et al*., (1997). MTT [3-(4, 5-dimethylthiazol-2-yl)-2, 5-diphenyl tetrazolium bromide] is a pale yellow substance that is metabolized to dark blue formazan crystals by metabolically active cells.

The MTT method will be used for cancer cells and primary cultures.

The HeLa cell line is widely used for the evaluation of drugs (Caldwell *et al*., 1999; Schoonen *et al*., 2005) and was therefore used in this study for initial drug evaluation.

Chen (1988) showed that the mitochondria of carcinoma cells derived from ovary, breast, prostate, cervix, colon, and liver accumulated lipophilic cations to a greater extent and with a longer retention than did normal epithelial cells. The increased uptake has been attributed to the higher mitochondrial membrane potential in these carcinoma cells. Based on these findings a colon cancer cell culture (CoLo 320 DM), a breast carcinoma (MCF 7), a non-cancerous breast cell culture (MCF 12A), a prostate cancer cell culture (Du 145), an ovarian cancer cell culture, sensitive to cisplatin (A2780) and its cisplatin resistant subline (A2780 cis) were selected for this study.

Jurkat T leukemia cells are a well known model system for apoptosis, since they are vulnerable to diverse stimuli, such as death receptor ligands and conventional chemotherapeutic drugs like Cisplatin (Wang *et al*., 2006). Jurkat cells were therefore included in this study.

[Au(dppe)$_2$]Cl has shown reproducible and significant *in vivo* anti-tumour activity in a range of murine models including P388 leukemia and B16 melanoma, mammary adenocarcinoma 16/C, intra-peritoneal transplanted tumours and subcutaneous transplanted tumours. [Au(dppe)$_2$]Cl also inhibited the formation of tumour colonies from B16 melanoma and P388 leukemia cells *in vitro*. This activity was not associated with acute loss of cell viability (McKeage *et al*., 2002). Therefore the B16 mouse melanoma cell line was included in this study.

[Au(dppe)$_2$]Cl was very hepatotoxic in *in vivo* dog studies (Smith *et al*., 1989) and for this reason the toxicity of the novel derivatives will also be evaluated in primary cultures of porcine hepatocytes, chicken fibroblasts and human lymphocytes.

3.2 Aim

The aim of this study was:

i. To screen six novel compounds for activity against HeLa cells (human cervical carcinoma).

ii. To determine if there is a correlation between the octanol/water partition coefficient (lipophilicity), cytotoxicity and tumour specificity of the novel compounds.

iii. To identify the three most effective compounds based on cytotoxicity studies done on cancer and normal primary cultures.

3.3 Materials and methods

3.3.1 Experimental Compounds

Bu_2SnRu **(MM1)**, 2RuAudpmaa **(MM2)**, 1RuAudpmma **(MM3)**, Bu_2Sndpmaa **(MM4),** $(Bu_2Sn)_2$Audpmaa **(MM5)** and Bu_2SnAudpmaa **(MM6)** were used. The structures of these compounds can be seen in **Figure 1** on page 11. $[Au(dppe)_2]Cl$ and cisplatin were included for comparison.

Preparation of experimental compounds

i. $[Au(dppe)_2]Cl$

Molecular weight: 1028 g/mol

A 10 mM stock solution was prepared by dissolving 10.28 mg of the compound in 1 ml DMSO. The stock solution was frozen in 50 µl aliquots at - 20ºC and relevant dilutions were done in the appropriate tissue culture medium (see page 36) which was supplemented with 10 % bovine FCS just before use on the day of the experiment.

ii. Cisplatin

Molecular weight: 300 g/mol

A 20 mM stock solution was prepared by dissolving 6 mg of the compound in 1 ml DMSO. The stock solution was frozen in 50 µl aliquots at - 20ºC and relevant dilutions were done in the appropriate tissue culture medium (see page 36) which was supplemented with 10 % bovine FCS just before use on the day of the experiment.

iii.Bu_2SnRu (MM1)

Molecular weight: 1464.72 g/mol

A 10 mM stock solution was prepared by dissolving 10.28 mg of the compound in 1 ml DMSO. The stock solution was frozen in 50 µl aliquots at - 20ºC and relevant dilutions were done in the appropriate tissue culture medium (see page 36) which was supplemented with 10 % bovine FCS just before use on the day of the experiment.

iv. 2RuAudpmaa (MM2)

Molecular weight: 147.45 g/mol

A 10 mM stock solution was prepared by dissolving 10.28 mg of the compound in 1 ml DMSO. The stock solution was frozen in 50 µl aliquots at - 20ºC and relevant dilutions were done in the appropriate tissue culture medium (see page 36) which was supplemented with 10 % bovine FCS just before use on the day of the experiment.

v. 1RuAudpmaa (MM3)

Molecular weight: 1335.84 g/mol

A 10 mM stock solution was prepared by dissolving 10.28 mg of the compound in 1 ml DMSO. The stock solution was frozen in 50 µl aliquots at - 20ºC and relevant dilutions were done in the appropriate tissue culture medium (see page 36) which was supplemented with 10 % bovine FCS just before use on the day of the experiment.

vi. Bu_2Sndpmaa (MM4)

Molecular weight: 715.35 g/mol

A 10 mM stock solution was prepared by dissolving 10.28 mg of the compound in 1 ml DMSO. The stock solution was frozen in 50 µl aliquots at - 20ºC and relevant dilutions were done in the appropriate tissue culture medium (see page 36) which was supplemented with 10 % bovine FCS just before use on the day of the experiment.

vii. $(Bu_2Sn)_2$Audpmaa (MM5)

A 10 mM stock solution was prepared by dissolving 10.28 mg of the compound in 1 ml DMSO. The stock solution was frozen in 50 µl aliquots at - 20ºC and relevant dilutions were done in the appropriate tissue culture medium (see page 36) which was supplemented with 10 % bovine FCS just before use on the day of the experiment.

.

viii. Bu_2SnAudpmaa (MM6)

Molecular weight: 1432.2 g/mol

A 10 mM stock solution was prepared by dissolving 10.28 mg of the compound in 1 ml DMSO. The stock solution was frozen in 50 µl aliquots at - 20ºC and relevant dilutions

were done in the appropriate tissue culture medium (see page 36) which was supplemented with 10 % bovine FCS just before use on the day of the experiment.

3.3.2 Reagents

i. Trypsin/Versene solution

A trypsin/versene solution (cat no CN 3175) containing the following: 0.25% Trypsin, 0.1% Versene EDTA in Ca^{++} and Mg^{++} free phosphate buffered saline, was supplied by Highveld Biologicals (Sandringham, RSA).

ii. White blood cell counting fluid

One ml of 0.1% Crystal violet (Cat no 90132, Sigma, St Louis, USA) was added to 2 ml acetic acid (Sigma, Darmstadt, Germany) and made up to 100 ml with de-ionized water.

iii. Phosphate buffered saline (PBS)

Phosphate buffered saline, cat no 211248, was supplied by The Scientific Group (Johannesburg, RSA). 9.23 g was dissolved in 1 liter de-ionized water and stored at 4 ºC.

iv. MTT

MTT [3-(4, 5-dimethylthiazol-2-yl)-2, 5-diphenyl tetrazolium bromide], cat no M2128-5G, was supplied by Sigma (St Louis, USA). 250 mg was dissolved in 50 ml PBS (5 mg/ml) and filter sterilized through a 0.22 µm pore size syringe filter (Sartorius). The solution was stored in the dark at 4ºC.

v. Dimetylsulfoxide (DMSO)

DMSO manufactured by Acros Organics (New Jersey USA), cat no 167850010, was supplied by Sigma (Johannesburg, RSA) and used undiluted.

vi. Penicillin/streptomycin

Penicillin/streptomycin solution cat no 17-602E, was supplied from The Scientific Group (Johannesburg, RSA). 1% was added to tissue culture media.

vii. Bovine fetal calf serum (FCS)

FCS manufactured by Delta bio-products, cat no 14-501BI was supplied by The Scientific Group (Johannesburg, RSA). FCS was heat inactivated for 45 minutes at 56ºC. 10% was added to tissue culture media.

viii. Phyto-haemagglutenin (PHA)

Phyto-haemagglutenin, cat no 30852701 HA 15, was supplied by Bioweb (Edenglen, RSA). The contents of each bottle was dissolved in 5 ml of sterile saline and dispensed in 0.4 ml aliquots. Aliquots were stored at -20ºC. 1.6 ml RPMI supplemented with 10% bovine FCS was used to dilute these aliquots prior to use.

ix. Histopaque

Histopaque, cat no 10771 was supplied by Sigma (St Louis, USA) and was used to separate the lymphocytes from the whole blood.

x. Ammoniumchloride

All reagents were supplied by Sigma (Johannesburg, RSA)

8.3 g NH_4Cl,

1 g $NaHCO_3$,

74 mg EDTA

Reagents were added in sequence and made up to 1 liter with distilled water.

xi. Tissue culture media

RPMI (RPMI-1640)

RPMI, cat no R6504, was supplied by Sigma (St Louis, USA).
52 g RPMI-1640 was dissolved in 5 liters of autoclaved ultra pure, pyrogen-free, de-ionized water. De-ionized water was produced by an Elga PureLab Ultra water unit in the department. 10 g $NaHCO_3$ (Sigma S5761) was added just before filtration to adjust the pH. The pH was adjusted further, if necessary, by adding small quantities of 1N HCl or 1N NaOH until an end pH of 7.4 was obtained. Medium was filtrated under vacuum using a Sartorius vacuum flask filter system with a Sartorius glass-fiber pre-filter and a 0.2 µm Sartorius cellulose acetate filter. The medium was filtrated a second time using two Sartorius glass-fiber pre-filters which preceded the sterile Sartolab P pressure filtration unit (0.2 µm). A Heidolph peristaltic pump was used to force the medium through the filters. Medium was dispensed into sterile 500 ml flasks containing 1% penicillin/streptomycin. Medium was stored at 4ºC until needed. Just before use the medium was supplemented with 10% bovine FCS.

EMEM (Earl's Minimum Essential Medium)

EMEM, cat no M0643, was supplied by Sigma (St Louis, USA).
48 g EMEM was dissolved in 5 liters of autoclaved ultra pure, pyrogen-free de-ionized water. De-ionized water was produced by an Elga PureLab Ultra water unit in the department. 11 g $NaHCO_3$ (Sigma S5761) was added just before filtration to adjust the pH. The pH was adjusted further, if necessary, by adding small quantities of 1N HCl or 1N NaOH until an end pH of 7.4 was obtained. Medium was filtrated under vacuum using a Sartorius vacuum flask filter system with a Sartorius glass-fiber pre-filter and a 0.2 µm Sartorius cellulose acetate filter. The medium was filtrated a second time using two Sartorius glass-fiber pre-filters which preceded the sterile Sartolab P pressure filtration unit (0.2 µm). A Heidolph peristaltic pump was used to force the medium through the filters. Medium was dispensed into sterile 500 ml flasks containing 1%

penicillin/streptomycin. Medium was stored at 4ºC until needed. Just before use the medium was supplemented with 10% bovine FCS.

DMEM (Dulbecco's Minimum Essential Medium)

DMEM, cat no D 7777, was supplied by Sigma (St Louis, USA)..
67.35 g DMEM was dissolved in 5 liters of autoclaved ultra pure, pyrogen-free, de-ionized water. De-ionized water was produced by an Elga PureLab Ultra water unit in the department. 18.5 g $NaHCO_3$ (Sigma S5761) was added just before filtration to adjust the pH. The pH was adjusted further, if necessary, by adding small quantities of 1N HCl or 1N NaOH until an end pH of 7.4 was obtained. Medium was filtrated under vacuum using a Sartorius vacuum flask filter system with a Sartorius glass-fiber pre-filter and a 0.2 µm Sartorius cellulose acetate filter. The medium was filtrated a second time using two Sartorius glass-fiber pre-filters which preceded the sterile Sartolab P pressure filtration unit (0.2 µm). A Heidolph peristaltic pump was used to force the medium through the filters. Medium was dispensed into sterile 500 ml flasks containing 1% penicillin/streptomycin. Medium was stored at 4ºC until needed. Just before use the medium was supplemented with 10% bovine FCS.

DMEM/Ham's F12 mixture for MCF 12Acells

DMEM, cat no D6046 was supplied by Sigma (St Louis, USA).
Ham's F12 nutrient mixture, cat no N3520 was supplied by Sigma (St Louis, USA). 11.1 g was dissolved in 1 liter of autoclaved ultra pure, pyrogen-free, de-ionized water. De-ionized water was produced by an Elga PureLab Ultra water unit in the department. 2.5 g $NaHCO_3$ (Sigma S5761) was added just before filtration to adjust the pH. The pH was adjusted further, if necessary, by adding small quantities of 1N HCl or 1N NaOH until an end pH of 7.4 was obtained. Medium was filtrated under vacuum using a Sartorius vacuum flask filter system with a Sartorius glass-fiber pre-filter and a 0.2 µm Sartorius cellulose acetate filter. The medium was filtrated a second time using two Sartorius glass-fiber pre-filters which preceded the sterile Sartolab P pressure filtration unit (0.2

µm). A Heidolph peristaltic pump was used to force the medium through the filters. Medium was dispensed into sterile 500 ml flasks containing 1% penicillin/streptomycin. Medium was stored at 4ºC until needed.

A 1:1 mixture of DMEM and Ham's F12 medium was made containing 20 ng/ml epidermal growth factor (Sigma E-9644), 100 ng/ml cholera toxin (Sigma C8052), 0.01 mg/ml insulin (Sigma I5500) and 500 ng/ml hydrocortisone (Sigma H0396) according to ATCC requirements.
Just before use the medium was supplemented with 10% bovine FCS.

Table 3.1: Cell cultures used in this study.

Cancer cell lines			
Name	**Species of Origin**	**Tissue type of origin**	**Used in this study to determine the following:**
A 2780 (cisplatin sensitive)	Human	Ovarian	**i.** Tumour specificity(Stage 2) (MTT assay) **ii.** *In vitro* drug uptake(Stage 3) (Uptake of radio-isotope)
A 2780 cis (cisplatin resistant)	Human	Ovarian	**i.** Tumour specificity(Stage 2) (MTT assay) **ii.** I*n vitro* drug uptake (Stage 3) (Uptake of radio-isotope)
B16	Mouse		Tumour specificity (Stage 2) (MTT assay)
CoLo	Human	Colon	Tumour specificity (Stage 2) (MTT assay)
DU 145	Human	Prostate	Tumour specificity (Stage 2) (MTT assay)
HeLa	Human	Cervical	Initial evaluation of compound effectiveness (Stage 1) (MTT assay)
Jurkat	Human	T-lym-phocyte	**i.** Tumour specificity (Stage 2) (MTT assay) **ii.** Mitochondrial and plasma membrane potentials (Stage 2) (Flow cytometry) **iii.** Cell death: apoptosis or necrosis (Stage 2) (Flow cytometry) **iv.** Effects on cell cycle (Stage 2) (Flow cytometry)
MCF 7	Human	Breast	Tumour specificity (Stage 2) (MTT assay)

Normal cell lines

Name	Species of Origin	Tissue type of origin	Used in this study to determine the following:
MCF 12A	Human	Breast	Tumour specificity (Stage 2) (MTT assay)

Primary Cultures

Name	Species of origin	Tissue type of origin	Used in this study to determine the following:
Chicken embryo fibroblasts	Chicken	Fibroblasts	Tumour specificity (Stage 2) (MTT assay)
Porcine hepatocytes	Porcine	Hepatocytes	Tumour specificity (Stage 2) (MTT assay)
Resting lymphocytes	Human	Lymphocytes	Determination of tumour specificity (Stage 2) (MTT assay)
PHA stimulated lymphocytes	Human	Lymphocytes	**i.** Tumour specificity (Stage 2) (MTT assay) **ii.** Mitochondrial and plasma membrane potentials (Stage 2) (Flow cytometry)

3.3.3 Cell lines and media required

3.3.3.1 Carcinoma cell lines

i. A2780 (Human ovarian carcinoma, cisplatin sensitive) (ECACC no 93112519)
A2780 cells are adherent epithelial cells, maintained in RPMI 1640 medium supplemented with 10 % bovine FCS.

ii. A2780 cis (Human ovarian carcinoma, cisplatin resistant) (ECACC no 93112517)
A2780 cis cells are adherent epithelial cells, maintained in RPMI 1640 medium supplemented with 10 % bovine FCS supplemented with 3µg/ml cisplatin to maintain cisplatin resistance.

iii. B16 (Mouse melanoma) (ECACC no 92101203)
B16 cells are adherent epithelial cells, maintained in RPMI 1640 medium supplemented with 10 % bovine FCS.

iv. CoLo 320 DM (Human colon cancer) (ATCC no CCL-220)
CoLo cells grow loosely attached and in suspension and are rounded and refractile. Cultures are maintained in RPMI 1640 medium supplemented with 10 % bovine FCS.

v. Du 145 (Human prostate cancer) (ATCC no HTB-81)
DU 145 cells are adherent epithelial cells, maintained in RPMI 1640 medium supplemented with 10 % bovine FCS.

vi. HeLa (Human cervical carcinoma) (ATCC no CCL 2)
HeLa cells are adherent epithelial cells, maintained in Eagles minimum essential medium (EMEM) supplemented with 2 mM L-glutamine, 0.1mM non-essential amino acids, 1.0 mM sodium pyruvate and 10 % bovine FCS.

vii. Jurkat cells (human undifferentiated leukemia T-cell line) (NRBM no 0062)
Jurkat cells grow loosely attached and in suspension and are rounded and refractile. Cultures were maintained in RPMI 1640 medium supplemented with 10 % bovine FCS.

viii. MCF 7 (Human breast carcinoma) (ATCC no HTB 22)
MCF 7 cells are adherent epithelial cells, maintained in Dulbecco's minimum essential (DMEM) medium supplemented with 2 mM L-glutamine, 0.1mM non-essential amino acids, 1.0 mM sodium pyruvate and 10 % bovine FCS.

ix. MCF 12A (Human non-tumourogenic breast cell line) (ATCC no CRL 10782)
MCF 12A cells are adherent epithelial cells, maintained in a 1:1 mixture of DMEM and Ham's F12 medium supplemented with 20 ng/ml epidermal growth factor, 100 ng/ml cholera toxin, 0.01 mg/ml insulin, 500 ng/ml hydrocortisone and 10 % bovine FCS.

All the cell cultures were maintained in the required tissue culture medium supplemented with 10% bovine FCS and 1% penicillin/streptomycin solution at 37 ºC and in an atmosphere containing 5% CO_2. Cell cultures were cultured in 75 cm^3 culture flasks and sub-cultured as needed.

3.3.3.2 Normal cell lines

i. Chicken embryo fibroblasts
This is a primary cell culture isolated from chicken embryos. Chicken embryos are easily accessible and larger to work with than mouse embryos (Freshney, 2000).

Ethical approval by the Animal Use and Care Committee of the University of Pretoria was obtained.

ii. Human lymphocytes

To determine tumour specificity of the new compounds it was necessary to measure its effects on the proliferation of lymphocytes obtained from normal healthy individuals. Lymphocytes were prepared as previously described by Anderson *et al*., (1993).

This method measures inhibition of cell growth and is limited to actively growing cells.

Preservative free heparinized peripheral blood was used.

iii. Primary porcine hepatocytes

Freshly prepared primary porcine hepatocytes were provided by the Bio Liver Research Unit, Dept of Internal Medicine, University of Pretoria. These cells were prepared according to standard procedures as described by Frühauf, *et al*., 2004 and Nieuwoudt *et al.*, 2005. Porcine hepatocytes were maintained in a 1:1 mixture of DMEM and Ham's F12 medium supplemented with 20 ng/ml epidermal growth factor, 100 ng/ml cholera toxin, 0.01 mg/ml insulin, 500 ng/ml hydrocortisone and 10 % bovine FCS.

3.3.4 Methods

i. Preparation of chicken embryo fibroblasts:

Eggs were incubated at 38.5ºC in a humid atmosphere for 6 days. Eggs were kept in an egg incubator which turned them over once in 24 hours. All procedures were carried out under sterile conditions. Eggs were swabbed with 70% alcohol and placed with its blunt end facing up in a small beaker. The top of the shell was cracked and the shell covering the air sac was removed completely. Sterile forceps were used for this purpose. The forceps were re-sterilized and used to peel off the white shell membrane to reveal the chorio-allantoic membrane (CAM) below, with its blood vessels. The CAM was pierced with sterile curved forceps and the embryo lifted out by grasping it gently under the head. Embryos were transferred to a sterile petri dish and decapitated to kill them instantly. Fat and necrotic material was removed from the embryos and they were transferred to a clean sterile petri dish. Embryos were cut with crossed scalpels into very small pieces and transferred to a sterile 50 ml centrifuge tube and washed three times with RPMI medium supplemented with 10% bovine FCS. Tissue was allowed to settle each time before the

medium was discarded. Tissue was transferred to a sterile 100 ml glass bottle with a screw cap (Schott bottle) –most of the residual fluid was removed with a Pasteur pipette. 45 ml phosphate buffered saline (PBS) (filter sterilized) and 5 ml 2.5% trypsin/versene were added to the tissue mixture together with a magnetic stirrer bar and the flask closed. Tissue and trypsin/versene mixture was stirred on a magnetic stirrer at 100 rpm for 30 minutes at room temperature. Pieces were allowed to settle, and the supernatant was poured (with disaggregated cells in suspension) into a sterile 50 ml centrifuge tube and placed on ice. These steps were repeated until the disaggregation was complete (3-4 hours). The disaggregated cell suspension that was stored on ice was decanted into new sterile tubes (leave debris behind) and then centrifuged at 200G for 5 minutes. The supernatant was discarded and cell pellet re-suspended in medium supplemented with 10% bovine FCS. The cell suspension was transferred to 75 cm^3 cell culture flasks and incubated at 37°C and in an atmosphere containing 5% CO_2. Cultures were maintained in RPMI 1640 medium supplemented with 10 % bovine FCS. The medium was changed at regular intervals (2-4 days) as pH decreased (growth medium turns yellow).

ii. Lymphocyte preparation:

30 ml of heparinized blood was loaded carefully onto 15 ml Histopaque with a Pasteur pipette, and centrifuged for 25 minutes at 650G at room temperature. The top plasma layer was removed with a Pasteur pipette and discarded. The lymphocyte/monocyte layer (± 12 ml) was transferred to a sterile 50 ml centrifuge tube with a Pasteur pipette. The tube was filled with sterile RPMI medium without bovine FCS and centrifuged for 15 minutes at 200G at room temperature (to get rid of contaminating platelets). Supernatant was discarded and the cell pellet re-suspended in 50 ml of sterile RPMI medium without bovine FCS. This cell suspension was again centrifuged for 10 minutes at 200G at room temperature. The supernatant was discarded and the cell pellet was re-suspended in 50 ml sterile, ice cold ammonium chloride. The cell suspension was left on ice for ± 10 minutes (to lyse contaminating red cells) and centrifuged for 10 minutes at 200G at room temperature. The supernatant was discarded and the cell pellet was re-suspended in 50 ml sterile RPMI medium without bovine FCS. The cell suspension was centrifuged for 10 minutes at 200G at room temperature and the supernatant discarded.

The cell pellet was re-suspended in 1 ml sterile RPMI medium supplemented with 10% bovine FCS and cells were counted. Cells were diluted in sterile RPMI medium supplemented with 10% bovine FCS to 2 x 10^6 cells per ml, the concentration needed for the proliferation experiments. Resting and PHA – stimulated lymphocytes were used in cytotoxicity tests.

iii. Preparation of cells for proliferation experiments

Cell cultures were prepared in the prescribed ATCC tissue culture medium (specified for each cell line) supplemented with 10% FCS in 75 cm^3 culture flasks and sub-cultured 3 times a week. Tissue culture medium was discarded from the tissue culture flask containing the cells that were to be used and ± 5 ml trypsin/versene was added. Care was taken to coat all interior surfaces with the solution, before it was discarded. A small amount of trypsin/versene (2-5 ml) was added, enough to cover the adherent cells on the bottom of the flask. The culture flask with trypsin/versene cell mixture was incubated at 37º for a few minutes until the cells detached from the flask. The trypsin/versene cell mixture was transferred to a 15 ml centrifuge tube. Tissue culture media supplemented with 10% bovine FCS was used to rinse the culture flask and this was added to the mixture in the centrifuge tube, thus neutralizing the action of the trypsin/versene. Cell cultures which grow in suspension were decanted directly into 15 ml centrifuge tubes. The cell suspension was centrifuged for 6 minutes at 200G. The supernatant was discarded and the cell pellet was re-suspended in 1 ml of the tissue culture medium specified for that specific cell line, supplemented with 10% bovine FCS. The cell suspension was mixed repeatedly by pippetting repeatedly with an automatic pipette to make sure that the cells were separated from each other and that a uniform suspension was formed.

iv. Counting of cells

50 µl of the cell suspension which was prepared as described above was added to 450 µl of white cell counting fluid and mixed well. A small volume of this suspension was put onto a Haemocytometer and the cells were counted using a Reichert Jung Micro Star microscope. Dilutions were then made with the tissue culture medium specified for the

specific cell line used, supplemented with 10% bovine FCS to achieve the required cell concentration for the cell proliferation assay.

v. Cell proliferation assay

Tissue culture plates were divided into different sections for controls (untreated cells) and experimental compounds (treated cells). 80 µl of the tissue culture medium (specified for the specific cell line used) supplemented with 10% bovine FCS (60 µl in the case of the lymphocytes earmarked to be stimulated) was dispensed into each well of a 96 well tissue culture plate. 100 µl cell suspension was added to each well. Cultures were incubated at 37ºC in an atmosphere of 5% CO_2 for an hour. 20 µl of dilutions of the drugs to be tested (different concentrations) was added to the wells. Untreated control wells received 20 µl of culture medium. A control with DMSO was also done to make sure that there was no DMSO effect. Lymphocytes earmarked to be stimulated received 20 µl PHA 5 minutes after the addition of the drug. Cultures were incubated at 37ºC in an atmosphere of 5% CO_2 for 7 days with the exception of the lymphocytes, which were incubated for 3 days before the MTT was added.

All the cell cultures were incubated before the MTT was added.

A 2780, A2780 cis, B16, Du 145, and HeLa cells were used with a final concentration of 500 cells per well. CoLo, MCF 7 and MCF 12A were used with a final concentration of 400 cells per well and Jurkat cells had an end concentration of 600 cells per well. Primary porcine hepatocytes and chicken fibroblasts were used with a final concentration of 50 000 cells per well while the human lymphocytes had an end concentration of 200 000 cells per well.

vi. MTT assay

After the incubation period (3 or 7 days) of the tissue culture plates, 20 µl MTT (5 mg/ml) was added to each well. Cultures were incubated for 4 hours (The chicken fibroblasts were incubated for 24 hours) at 37ºC in an atmosphere of 5% CO_2 and then centrifuged for 10 minutes at 800G. Supernatant was removed from each well without

disturbing the pellet with a Pasteur pipette and cells were washed by addition of 150 µl PBS and centrifuged 10 minutes at 800G. Supernatant was removed from each well without disturbing the pellet with a Pasteur pipette and plates were left an hour to dry off at 37ºC. 100 µl DMSO was added to each well to solubulize the formazan crystals. Culture plates containing the DMSO/formazan solution were put on a shaker for about 1-2 hours and absorbance was measured on a Universal Microplate Reader (ELx800 uv, Bio-tek Instruments) using a wavelength of 570 nm and a reference wavelength of 630 nm.

Percentage of control of cell growth in drug treated wells was calculated by dividing the mean absorbance of the treated cells by the mean absorbance of the untreated controls x 100 and these values were used to determine the IC_{50} value. IC_{50} = the concentration (µM) of the experimental compound inducing a 50% decrease in cell growth. IC_{50} value was calculated with the Graphpad program.

Cytotoxicity assays were conducted to determine the level of sensitivity of cancer and normal cells to the experimental compounds. The three best compounds were selected to do further testing, to determine the sensitivity of cancer and normal cells to these substances, as well as the selectivity (tumour specificity). MM4, MM5 and MM6 were selected for further testing.

Tumour specificity was calculated by dividing the mean IC_{50} values of the primary cultures by the mean IC_{50} values of the cancer cells. MCF 12A results were not included in this calculation. Tumour specificity is an indicator of the selectiveness of the compound towards cancer cells.

The octanol/water partition coefficient of each of the compounds, the mean IC_{50} values and the tumour specificity on the cancer cells and normal cultures was correlated using the Pearson correlation at a 95% confidence interval to determine if the inhibition of cell growth is related to the octanol/water partition coefficient of the compounds.

3.4 Results

Results are expressed as mean IC_{50} ± SEM in drug-treated wells. Each value represents the mean of 7 independent experiments. The Student's t-test for paired values was used for the statistical analysis of the data.

Tumour specificity was calculated as the average of the IC_{50} values for primary cultures divided by the average of the IC_{50} values for the cancer cells. MCF 12A results were not included in this calculation. Tumour specificity was calculated for $[Au(dppe)_2]Cl$, MM4, MM5 and MM6.

The Pearson test at a 95% confidence interval was used to determine whether there was a correlation between cytotoxicity and the octanol/water partition coefficient.

Table 3.2 represents the results of the initial screening of the experimental compounds on HeLa cells.

The table shows that MM1, MM4, MM5 and MM6 the most promising agents with IC_{50}'s of 0.130 ± 0.054, 0.030 ± 0.004, 0.026 ± 0.006, and 0.103 ± 0.029 µM respectively. MM4, MM5 and MM6 were selected for further testing.

Figures 3.1 - 3.13 represent the percentage of control ± SEM of cell growth of the cell lines treated with $[Au(dppe)_2]Cl$.

These figures show that all the malignant cell cultures were sensitive to this compound at the concentrations tested. The non-malignant cell cultures were slightly less sensitive to this compound.

Figures 3.14 - 3.26: represent the percentage of control ± SEM of cell growth of the cell lines treated with cisplatin.

These figures show that all the malignant cell cultures were sensitive to this compound at the concentrations tested. The non-malignant cell cultures were a lot less sensitive to this compound.

Figures 3.27 - 3.39: represent the percentage of control ± SEM of cell growth of the cell lines treated with MM4.

These figures show that all the malignant cell cultures were sensitive to this compound at the concentrations tested. The non-malignant cell cultures were slightly less sensitive to this compound.

Figures 3.40 - 3.52: represent the percentage of control ± SEM of cell growth of the cell lines treated with MM5.

These figures show that all the malignant cell cultures were sensitive to this compound at the concentrations tested. The non-malignant cell cultures were less sensitive to this compound.

Figures 3.53 - 3.65: represent the percentage of control ± SEM of cell growth of the cell lines treated with MM6.

These figures show that all the malignant cell cultures were sensitive to this compound at the concentrations tested. The non-malignant cell cultures were less sensitive to this compound.

The IC_{50} values of the compounds on the cancer cell lines are summarized in **Table 3.3** and those on the normal cells in **Table 3.4**

These tables show that the IC_{50} values obtained with the normal cell cultures are higher than those obtained with the cancer cell lines.

Table 3.5 represents the results of tumour specificity.

The table shows that MM5 and MM6 had higher tumour selectivity than $[Au(dppe)_2]Cl$.

Table 3.6 represents the results of the Pearson correlation.

The table shows that the relationship between the octanol/water partition coefficient of the experimental compounds, the IC_{50} values and the tumour specificity of the compounds on the cancer and normal cell cultures is non-significant.

Table 3.2: Mean IC_{50} ± SEM for HeLa cells treated with different concentrations of [Au(dppe)2]Cl, cisplatin and the six novel gold derivatives (MM1, MM2, MM3, MM4, MM5 and MM6 for 7 days.

Calculated IC_{50} (1) (µM) obtained for 8 different drugs tested on HeLa cells

Drug	IC_{50} (2)
[Au(dppe)$_2$]Cl	0.661 ± 0.150
Cisplatin	0.710 ± 0.061
MM1	0.130 ± 0.054
MM2	32.804 ±11.540
MM3	21.990 ± 11.776
MM4	0.030 ± 0.004
MM5	0.026 ± 0.006
MM6	0.103 ± 0.029

(1) Average of 3 independent experiments

(2) IC_{50} = the concentration (µM) of the experimental compound inducing a 50% decrease in cell growth.

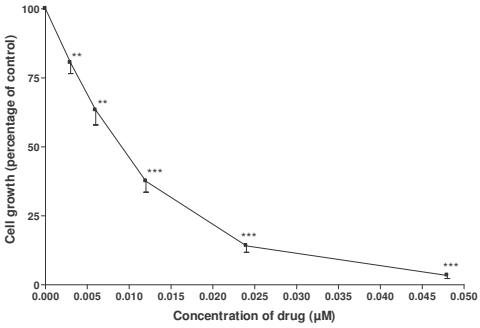

Figure 3.1: Mean growth inhibition of $[Au(dppe)_2]Cl$ on A2780 cells ±SEM

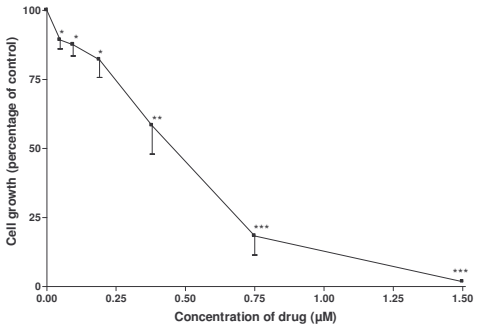

Figure 3.2: Mean growth inhibition of $[Au(dppe)_2]Cl$ on A2780 cis cells ± SEM

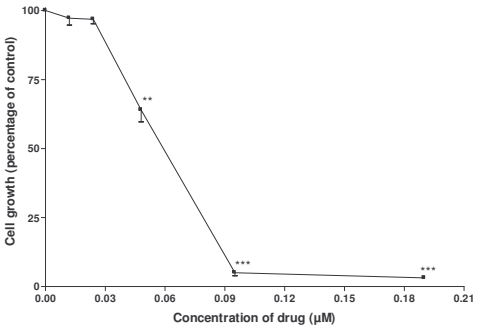

Figure 3.3: Mean growth inhibition of $[Au(dppe)_2]Cl$ on B16 cells ± SEM

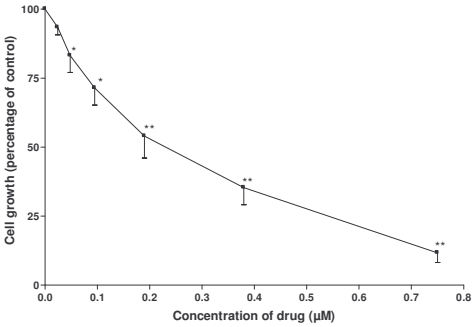

Figure 3.4: Mean growth inhibition of $[Au(dppe)_2]Cl$ on CoLo 320 DM cells ± SEM

Each value represents the mean of seven independant experiments ± SEM. Significance was determined with the Student's t-test for paired values.

* $p < 0.01$; ** $p < 0.001$; *** $p < 0.0001$ compared to the untreated control

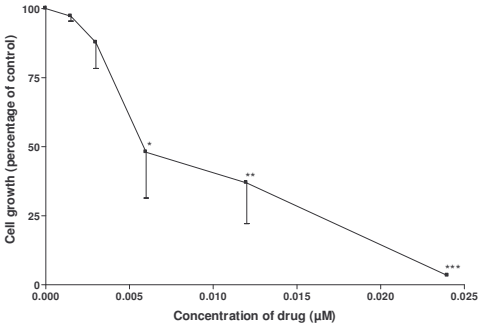

Figure 3.5: Mean growth inhibition of $[Au(dppe)_2]Cl$ on DU 145 cells ± SEM

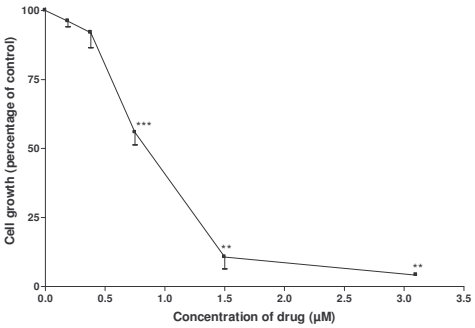

Figure 3.6: Mean growth inhibition of $[Au(dppe)_2]Cl$ on HeLa cells ± SEM

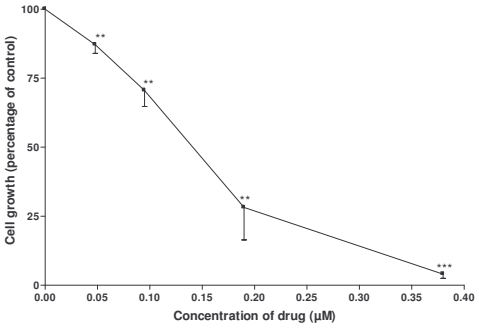

Figure 3.7: Mean growth inhibition of $[Au(dppe)_2]Cl$ on Jurkat cells ± SEM

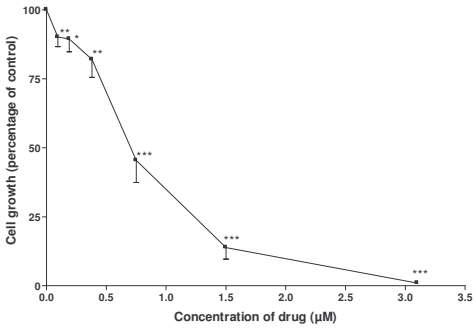

Figure 3.8: Mean growth inhibition of $[Au(dppe)_2]Cl$ on MCF 7 cells ± SEM

Each value represents the mean of seven independant experiments ± SEM. Significance was determined with the Student's t-test for paired values.

* $p < 0.01$; ** $p < 0.001$; *** $p < 0.0001$ compared to the untreated control

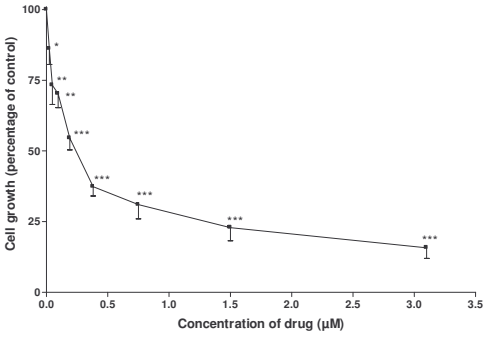

Figure 3.9: Mean growth inhibition of $[Au(dppe)_2]Cl$ on chicken fibroblasts ± SEM

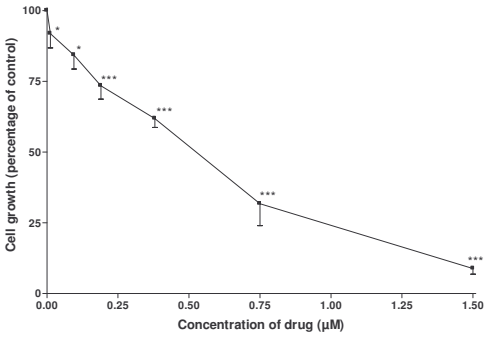

Figure 3.10: Mean growth inhibition of $[Au(dppe)_2]Cl$ on porcine hepatocytes ± SEM

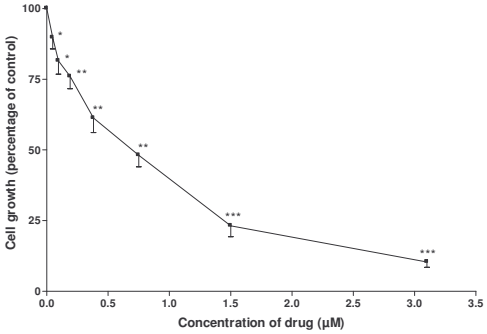

Figure 3.11: Mean growth inhibition of $[Au(dppe)_2]Cl$ on resting human lymphocytes ± SEM

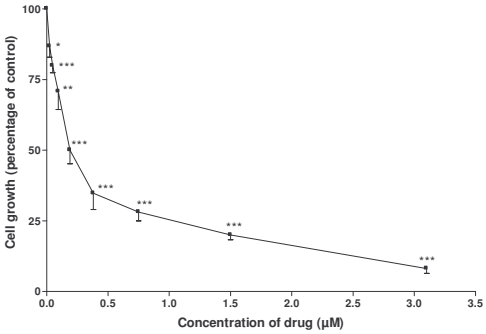

Figure 3.12: Mean growth inhibition of $[Au(dppe)_2]Cl$ on PHA stimulated human lymphocytes ± SEM

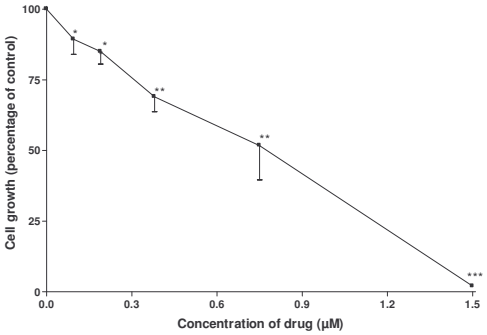

Figure 3.13: Mean growth inhibition of $[Au(dppe)_2]Cl$ on MCF 12A cells ± SEM

Each value represents the mean of seven independant experiments ± SEM. Significance was determined with the Student's t-test for paired values.

* $p < 0.01$; ** $p < 0.001$; *** $p < 0.0001$ compared to the untreated control

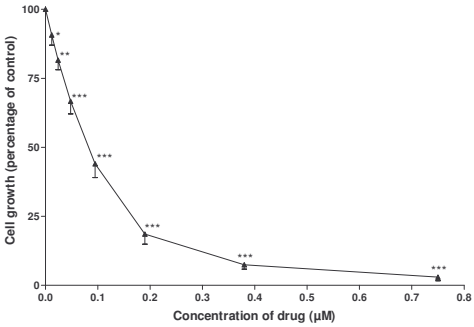

Figure 3.14: Mean growth inhibition of Cisplatin on A2780 cells ± SEM

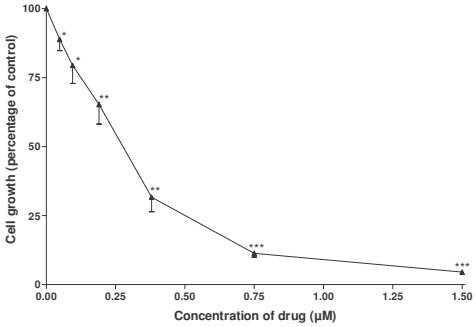

Figure 3.15: Mean growth inhibition of Cisplatin on A2780 cis cells ± SEM

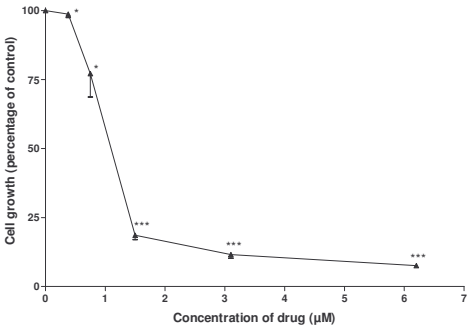

Figure 3.16: Mean growth inhibition of Cisplatin on B16 cells ± SEM

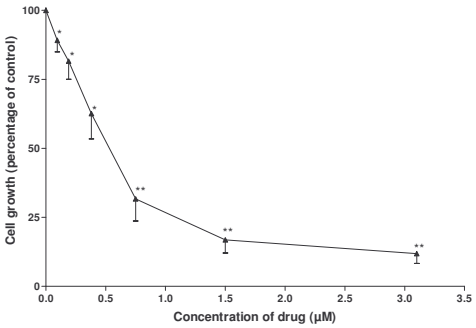

Figure 3.17: Mean growth inhibition of Cisplatin on CoLo 320 DM cells ± SEM

Each value represents the mean of seven independant experiments ± SEM. Significance was determined with the Student's t-test for paired values.

* $p < 0.01$; ** $p < 0.001$; *** $p < 0.0001$ compared to the untreated control

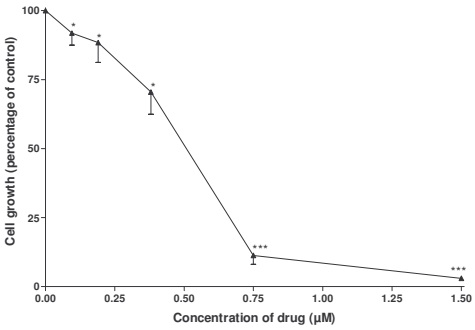

Figure 3.18: Mean growth inhibition of Cisplatin on DU 145 cells ± SEM

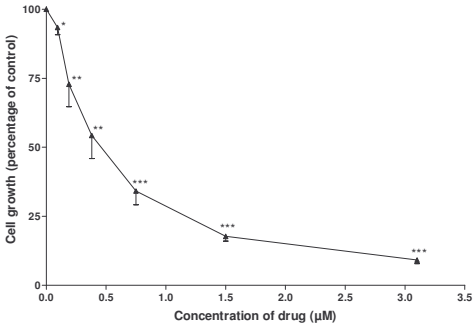

Figure 3.19: Mean growth inhibition of Cisplatin on HeLa cells ± SEM

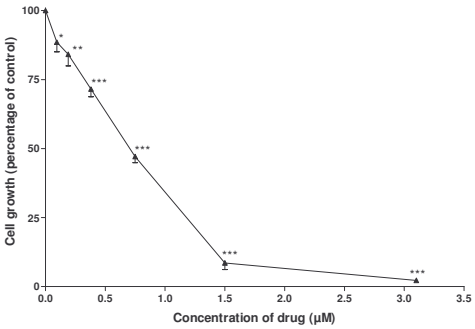

Figure 3.20: Mean growth inhibition of Cisplatin on Jurkat cells ± SEM

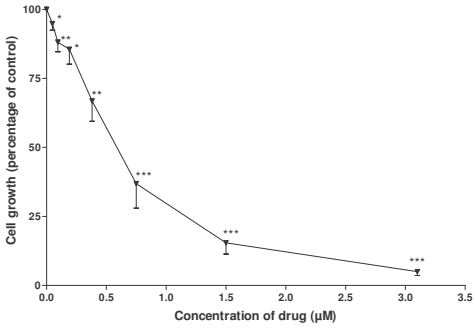

Figure 3.21: Mean growth inhibition of Cisplatin on MCF 7 cells ± SEM

Each value represents the mean of seven independant experiments ± SEM. Significance was determined with the Student's t-test for paired values.

* $p < 0.01$; ** $p < 0.001$; *** $p < 0.0001$ compared to the untreated control

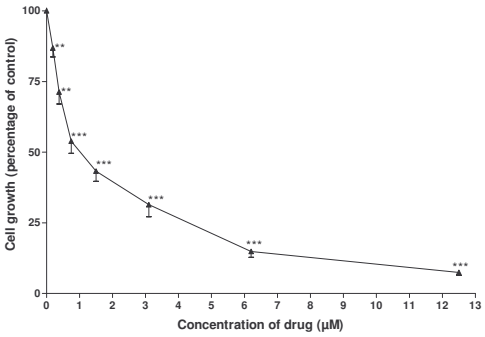

Figure 3.22: Mean growth inhibition of Cisplatin on chicken fibroblasts ± SEM

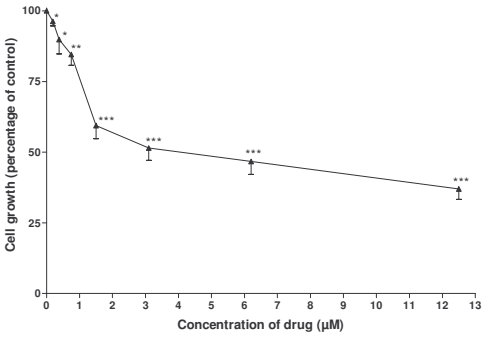

Figure 3.23: Mean growth inhibition of Cisplatin on porcine hepatocytes ± SEM

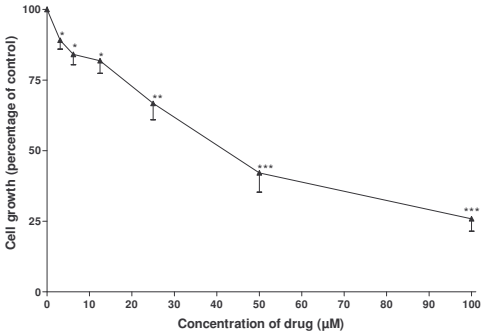

Figure 3.24: Mean growth inhibition of Cisplatin on resting human lymphocytes ± SEM

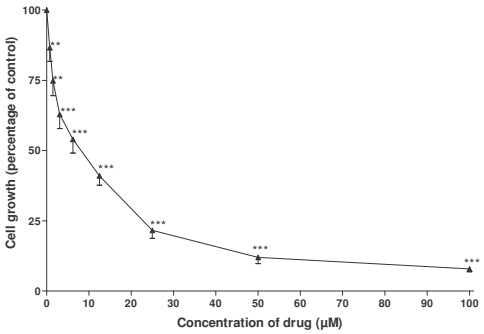

Figure 3.25: Mean growth inhibition of Cisplatin on PHA stimulated human lymphocytes ± SEM

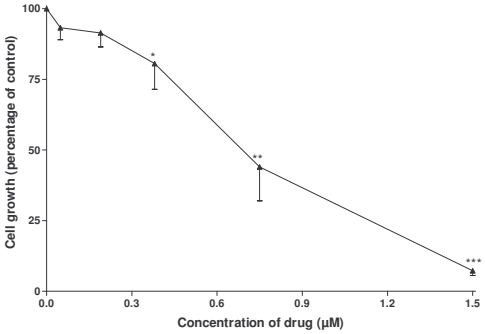

Figure 3.26: Mean growth inhibition of Cisplatin on MCF 12A cells ± SEM

Each value represents the mean of seven independant experiments ± SEM. Significance was determined with the Student's t-test for paired values.

* $p < 0.01$; ** $p < 0.001$; *** $p < 0.0001$ conpared to the untreated control

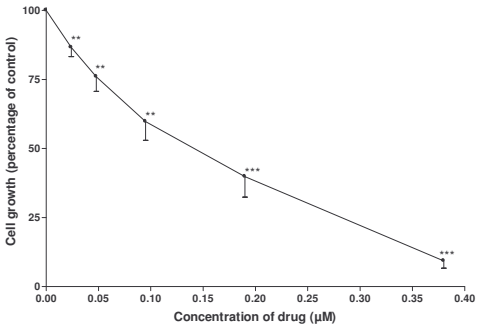

Figure 3.27: Mean growth inhibition of MM4 on A2780 cells ± SEM

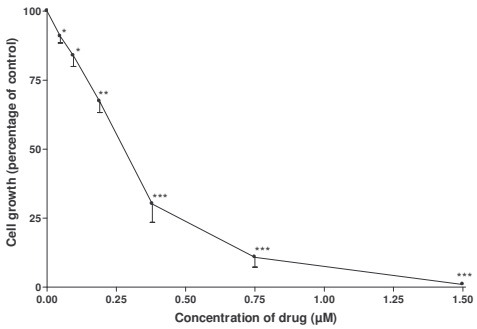

Figure 3.28: Mean growth inhibition of MM4 on A2780 cis cells ± SEM

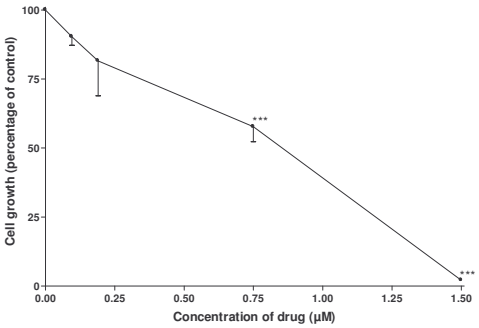

Figure 3.29: Mean growth inhibition of MM4 on B16 cells ± SEM

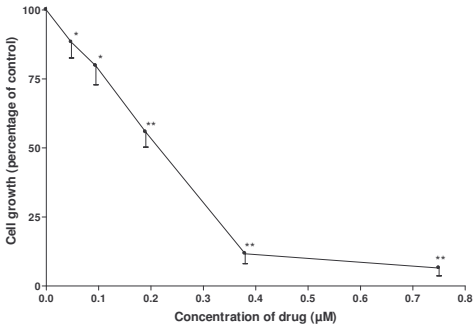

Figure 3.30: Mean growth inhibition of MM4 on CoLo 320 DM cells ± SEM

Each value represents the mean of seven independant experiments ± SEM. Significance was determined with the Student's t-test for paired values.

* $p < 0.01$; ** $p < 0.001$; *** $p < 0.0001$ compared to the untreated control

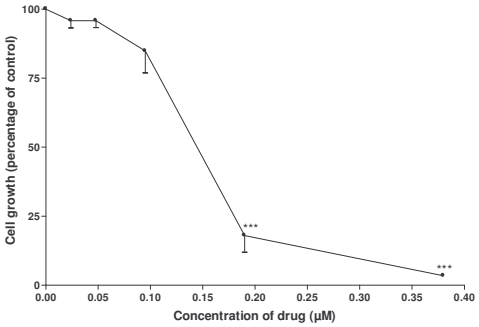

Figure 3.31: Mean growth inhibition of MM4 on Du 145 cells ± SEM

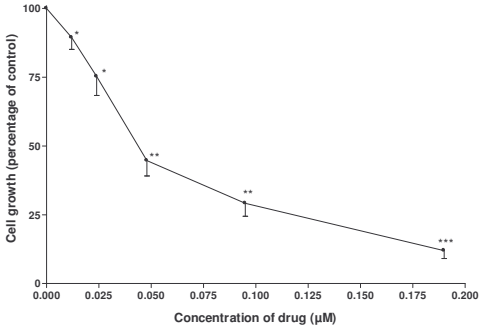

Figure: 3.32: Mean growth inhibition of MM4 on HeLa cells ± SEM

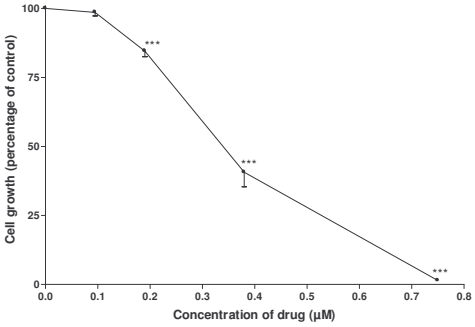

Figure 3.33: Mean growth inhibition of MM4 on Jurkat cells ± SEM

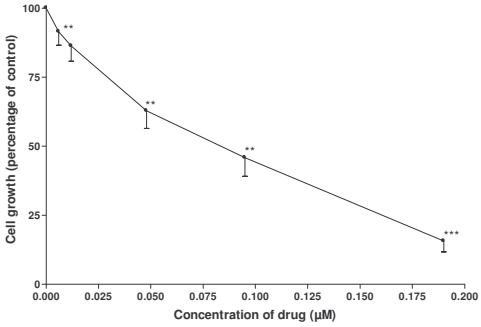

Figure 3.34: Mean growth inhibition of MM4 on MCF 7 cells ± SEM

Each value represents the mean of seven independant experiments ± SEM. Significance was determined with the Student's t-test for paired values.

* $p < 0.01$; ** $p < 0.001$; *** $p < 0.0001$ compared to the untreated control

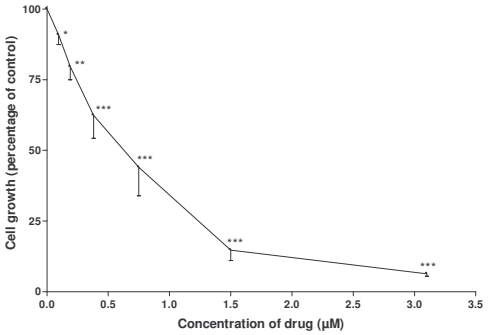

Figure 3.35: Mean growth inhibition of MM4 on chicken fibroblasts ± SEM

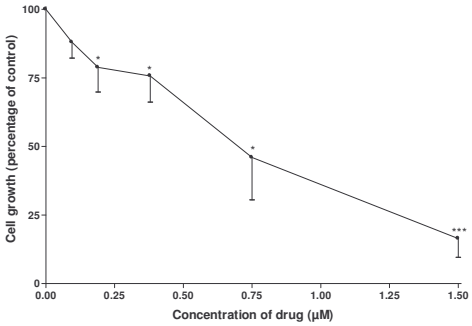

Figure 3.36: Mean growth inhibition of MM4 on porcine hepatocytes ± SEM

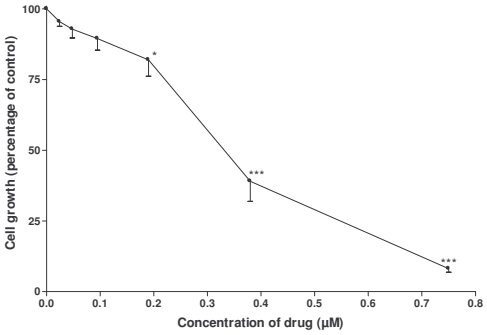

Figure 3.37: Mean growth inhibition of MM4 on resting human lymphocytes ± SEM

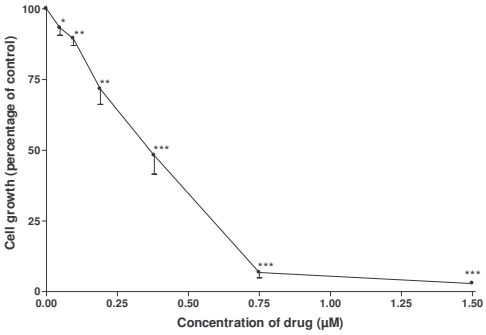

Figure 3.38: Mean growth inhibition of MM4 on PHA stimulated human lymphocytes ± SEM

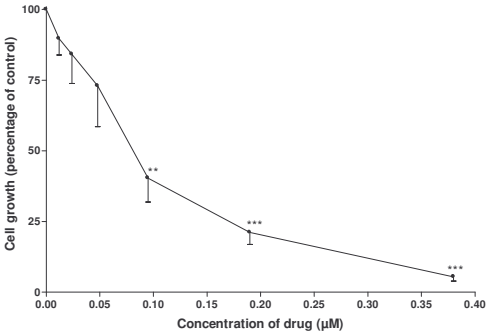

Figure 3.39: Mean growth inhibition of MM4 on MCF 12A cells ± SEM

Each value represents the mean of seven independant experiments ± SEM. Significance was determined with the Student's t-test for paired values.

* $p < 0.01$; ** $p < 0.001$; *** $p < 0.0001$ compared to the untreated control

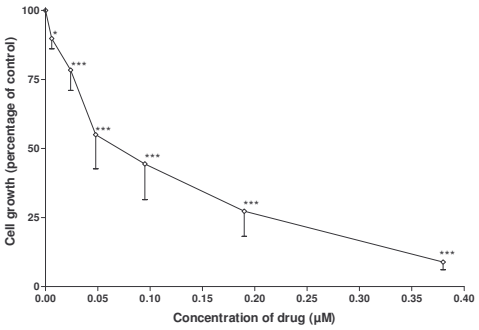

Figure 3.40: Mean growth inhibition of MM5 on A2780 cells ± SEM

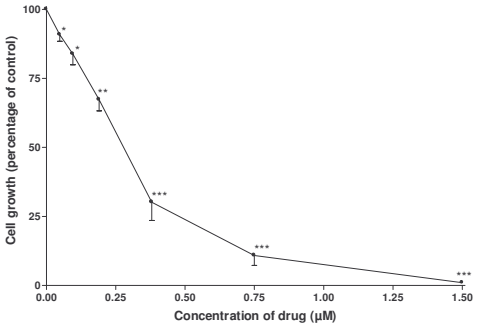

Figure 3.41: Mean growth inhibition of MM5 on A2780 cis cells ± SEM

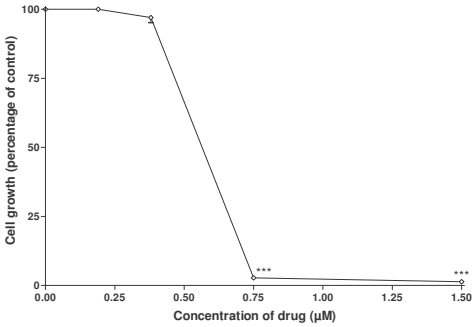

Figure 3.42: Mean growth inhibition of MM5 on B16 cells ± SEM

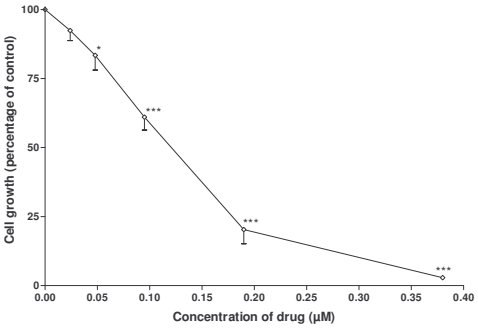

Figure 3.43: Mean growth inhibition of MM5 on CoLo 320 DM cells ± SEM

Each value represents the mean of seven independant experiments ± SEM. Significance was determined with the Student's t-test for paired values.

* $p < 0.01$; ** $p < 0.001$; *** $p < 0.0001$ compared to the untreated control

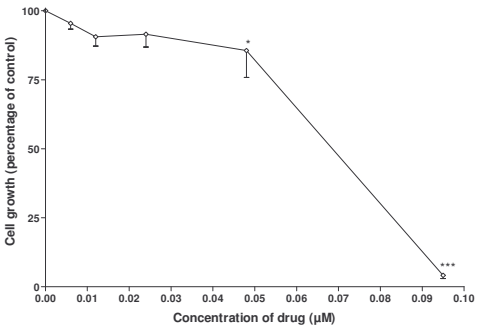

Figure 3.44: Mean growth inhibition of MM5 on DU 145 cells ± SEM

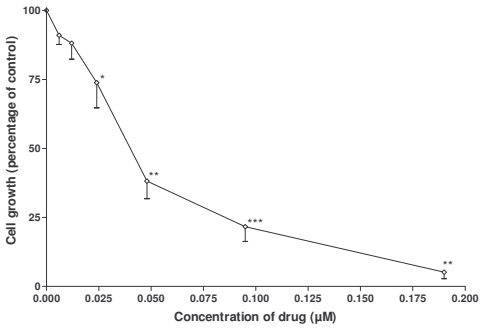

Figure 3.45: Mean growth inhibition of MM5 on HeLa cells ± SEM

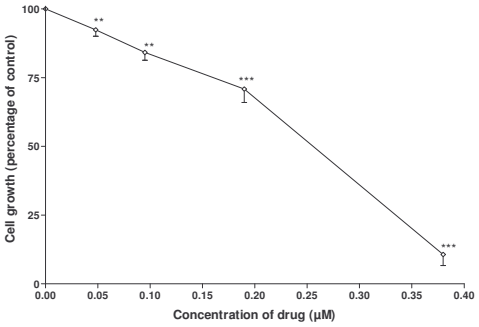

Figure 3.46: Mean growth inhibition of MM5 on Jurkat cells ± SEM

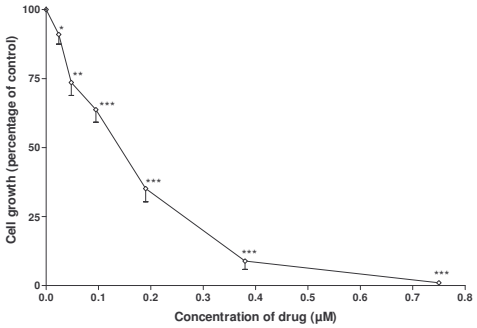

Figure 3.47: Mean growth inhibition of MM5 on MCF 7 cells ± SEM

Each value represents the mean of seven independant experiments ± SEM. Significance was determined with the Student's t-test for paired values.

* $p < 0.01$; ** $p < 0.001$; *** $p < 0.0001$ compared to the untreated control

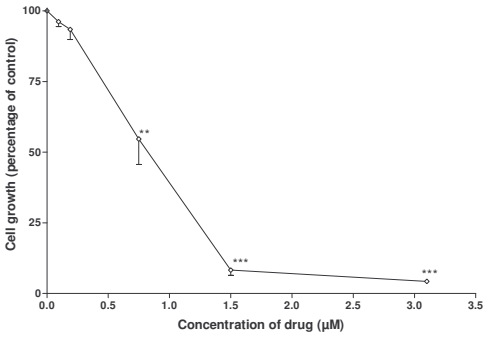

Figure 3.48: Mean growth inhibition of MM5 on chicken fibroblasts ± SEM

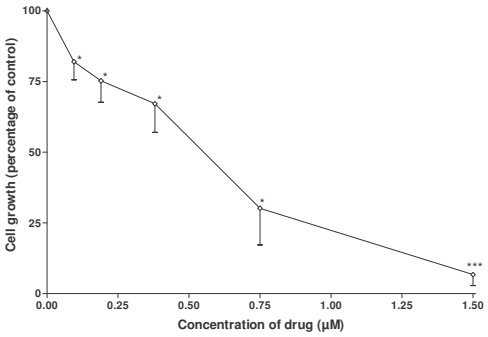

Figure 3.49: Mean growth inhibition of MM5 on porcine hepatocytes ± SEM

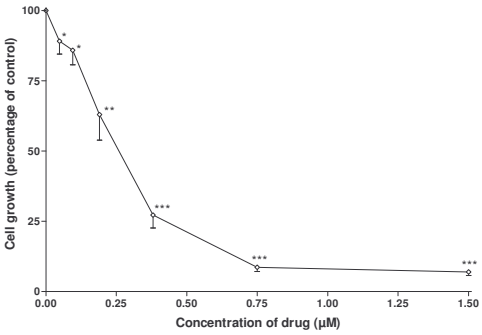

Figure 3.50: Mean growth inhibition of MM5 on resting human lymphocytes ± SEM

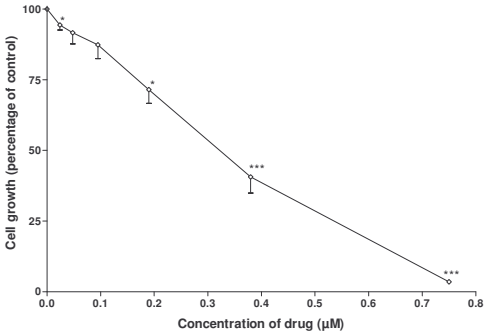

Figure 3.51: Mean growth inhibition of MM5 on PHA stimulated human lymphocytes ± SEM

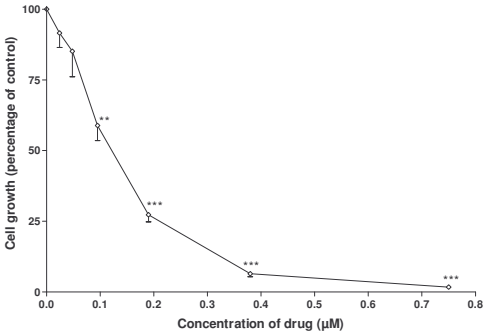

Figure 3.52: Mean growth inhibition of MM5 on MCF 12A cells ± SEM

Each value represents the mean of seven independant experiments ± SEM. Significance was determined with the Student's t-test for paired values.

* $p < 0.01$; ** $p < 0.001$; *** $p < 0.0001$ compared to the untreated control

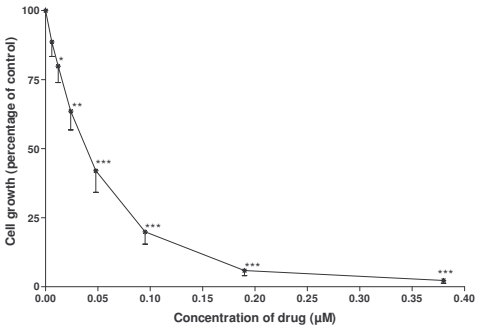

Figure 3.53: Mean growth inhibition of MM6 on A2780 cells ± SEM

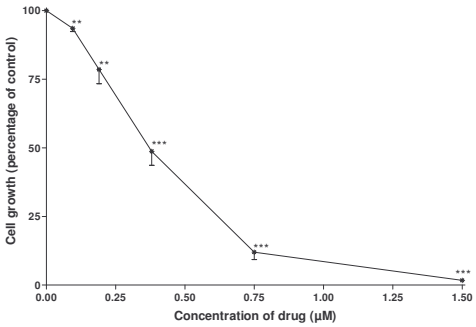

Figure 3.54: Mean growth inhibition of MM6 on A2780 cis cells ± SEM

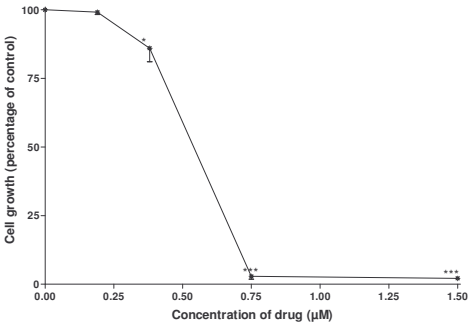

Figure 3.55: Mean growth inhibition of MM6 on B16 cells ± SEM

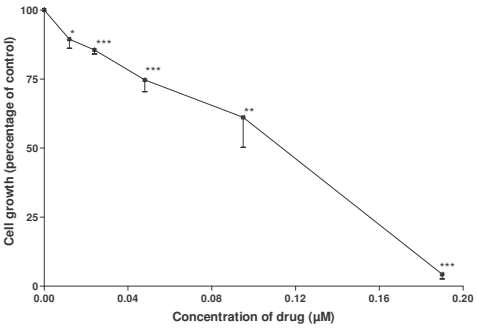

Figure 3.56: Mean growth inhibition of MM6 on CoLo 320 DM cells ± SEM

Each value represents the mean of seven independant experiments ± SEM. Significance was determined with the Student's t-test for paired values.

* $p < 0.01$; ** $p < 0.001$; *** $p < 0.0001$ compared to the untreated control

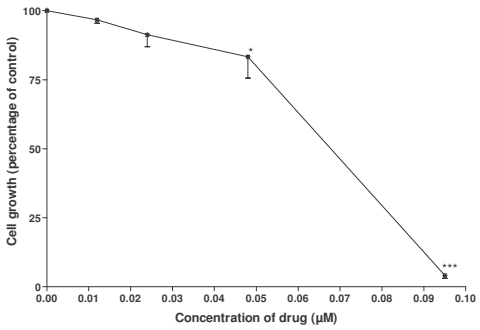

Figure 3.57: Mean growth inhibition of MM6 on Du 145 cells ± SEM

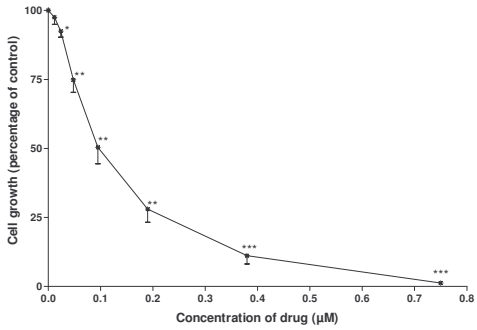

Figure 3.58: Mean growth inhibition of MM6 on HeLa cells ± SEM

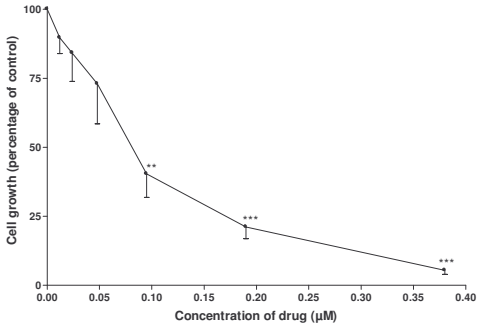

Figure 3.59: Mean growth inhibition of MM6 on Jurkat cells ± SEM

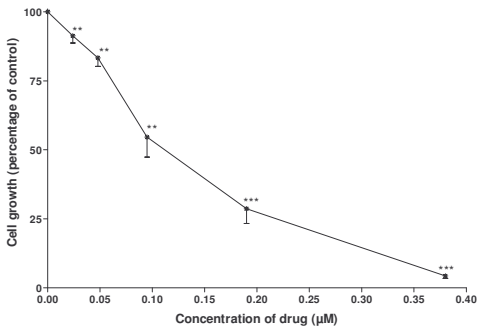

Figure 3.60: Mean growth inhibition of MM6 on MCF 7 cells ± SEM

Each value represents the mean of seven independant experiments ± SEM. Significance was determined with the Student's t-test for paired values.

* $p < 0.01$; ** $p < 0.001$; *** $p < 0.0001$ compared to the untreated control

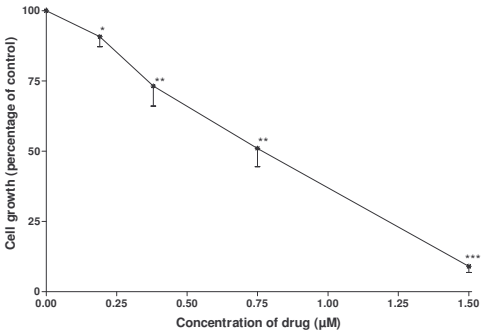

Figure 3.61: Mean growth inhibition of MM6 on Chicken fibroblasts ± SEM

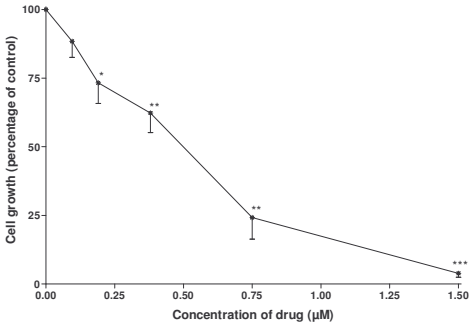

Figure 3.62: Mean growth inhibition of MM6 on porcine hepatocytes ± SEM

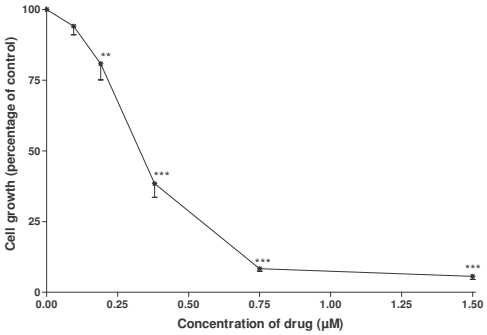

Figure 3.63: Mean growth inhibition of MM6 on resting human lymphocytes ± SEM

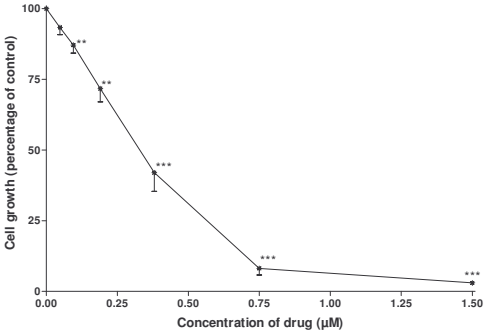

Figure 3.64: Mean growth inhibition of MM6 on PHA stimulated human lymphocytes ± SEM

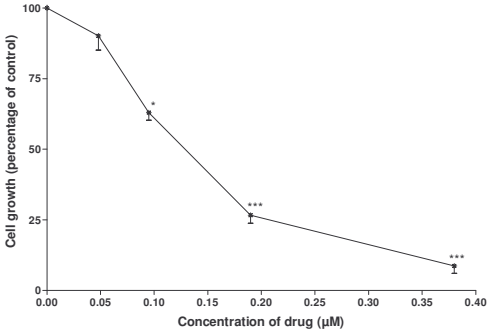

Figure 3.65: Mean growth inhibition of MM6 on MCF 12A cells ± SEM

Each value represents the mean of seven independant experiments ± SEM. Significance was determined with the Student's t-test for paired values.

* $p < 0.01$; ** $p < 0.001$; *** $p < 0.0001$ compared to the untreated control

Table 3.3: Mean IC_{50} ± SEM for cancer cell cultures treated with different concentrations of [Au(dppe)2]Cl, cisplatin, MM4, MM5 and MM6 for 7 days.

Calculated IC_{50}[(1)] (µM) for 5 different drugs on cancer cell lines[(2)]								
Drug	**A 2780**	**A 2780 cis**	**B16**	**CoLo**	**Du 145**	**HeLa**	**Jurkat**	**MCF 7**
$[Au(dppe)_2]Cl$	0.0084 ±0.001	0.437 ±0.066	0.051 ±0.004	0.291 ±0.06	0.009 ±0.002	0.778 ±0.07	0.157 ±0.023	0.568 ±0.065
Cisplatin	0.078 ±0.085	0.322 ±0.078	1.023 ±0.078	0.641 ±0.145	0.434 ±0.048	0.468 ±0.098	0.707 ±0.030	0.631 ±0.123
MM4	0.1363 ±0.025	0.330 ±0.034	0.830 ±0.045	0.203 ±0.026	0.146 ±0.011	0.0460 ±0.009	0.337 ±0.020	0.092 ±0.015
MM5	0.041 ±0.008	0.295 ±0.025	0.576 ±0.004	0.121 ±0.011	0.056 ±0.009	0.039 ±0.007	0.261 ±0.017	0.145 ±0.019
MM6	0.040 ±0.009	0.347 ±0.037	0.514 ±0.033	0.112 ±0.013	0.0631 ±0.007	0.105 ±0.018	0.369 ±0.044	0.150 ±0.027

(1) Average of 7 independent experiments

(2) IC_{50} = the concentration (µM) of the experimental compound inducing a 50% decrease in cell growth.

Table 3.4: Mean IC_{50} ± SEM for normal cell cultures treated with different concentrations of [Au(dppe)2]Cl, cisplatin, MM4, MM5 and MM6 for 3 or 7 days.

Calculated IC_{50}[(1)] (µM) for 5 different drugs on normal cell cultures[(2)]					
Drug	**Chicken embryo fibroblasts**	**Porcine hepatocytes**	**Lymphocytes (PHA stimulated)**	**Lymphocytes (resting)**	**MCF12 A**
$[Au(dppe)_2]Cl$	0.226 ±0.059	0.560 ±0.100	0.254 ±0.076	1.095 ±0.234	0.758 ±0.131
Cisplatin	1.268 ±0.393	5.017 ±1.657	8.798 ±1.721	40.357 ±5.466	0.695 ±0.113
MM4	0.722 ±0.123	0.744 ±0.175	0.288 ±0.044	0.364 ±0.028	0.085 0.018
MM5	0.787 ±0.083	0.659 ±0.140	0.340 ±0.047	0.268 ±0.032	0.107 ±0.013
MM6	0.804 ±0.094	0.615 ±0.140	0.397 ±0.038	0.354 ±0.043	0.125 ±0.008

(1) Average of 7 independent experiments

(2) IC_{50} = the concentration (µM) of the experimental compound inducing a 50% decrease in cell growth.

Table 3.5: Tumour specificity of $[Au(dppe)_2]Cl$, MM4, MM5 and MM6 was calculated by dividing the mean IC_{50} values of primary cultures by the mean IC_{50} values of the cancer cells. MCF 12A results were not included in this calculation.

Calculated tumour specificity of 4 drugs tested on cancer and normal cell cultures

$[Au(dppe)_2]Cl$	1.857
MM4	1.998
MM5	2.678
MM6	2.553

Table 3.6: Pearson correlation at a 95% confidence interval of the octanol/water partition coefficient of the experimental compounds with the tumour specificity and the IC_{50} values of the experimental compounds on cancer and normal cell cultures.

Pearson correlation at a 95% confidence interval of the octanol/water partition coefficient with tumour specificity and IC_{50} values of cancer and normal cell cultures

	Tumour specificity	IC_{50} cancer cells	IC_{50} normal cells
Pearson r	0.8832	-0.8792	0.5617
95% confidence interval	-0.5155 to 0.9975	-0.9975 to 0.5278	-0.8681 to 0.9889
P value	0.1168	0.1208	0.4383
R squared	0.7801	0.7730	0.3155

3.5 Discussion

The HeLa cell line is widely used for the evaluation of drugs (Caldwell *et al*., 1999; Schoonen *et al*., 2005) and was therefore used in this study for the initial drug evaluation.

During the screening of these compounds on HeLa cells, $[Au(dppe)_2]Cl$ had an IC_{50} of 0.661 ± 0.150 µM. The IC_{50} obtained for cisplatin was 0.710 ± 0.061 µM. MM2 and MM3 were the least active of all the compounds with IC_{50}'s of 32.804 ± 11.540 and 21.990 ± 11.776 µM respectively. MM1, MM4, MM5 and MM6 were identified as the most promising agents with IC_{50}'s of 0.130 ± 0.054, 0.030 ± 0.004, 0.026 ± 0.006, and 0.103 ± 0.029 µM respectively. MM4, MM5 and MM6 were selected for further testing.

$[Au(dppe)_2]Cl$ was found to be the most active against A2780, B16, Du 145 and Jurkat cells. MM4 showed selectivity for A2780, Du 145, HeLa and MCF7 cells. MM5 was most effective against A2780, CoLo, Du 145, HeLa and MCF 7 cells, while MM6 was very active against A2780, CoLo, Du 145, HeLa and MCF 7. IC_{50}'s obtained from the three novel derivatives were considerably lower than those of $[Au(dppe)_2]Cl$ and Cisplatin. Cisplatin did not show much selectivity for any of the cells used, except A2780.

Tumour specificity of MM4 is almost the same as that of $[Au(dppe)_2]Cl$. Despite the low IC_{50} values for MM4 it lacks selectivity for cancer cells. MM5 and MM6 both had higher specificity for cancer cells than normal cells when compared to $[Au(dppe)_2]Cl$ with tumour specificities of 2.677 and 2.553 respectively. MM5 and MM6 have strong hydrophilic characteristics which support the theory that more hydrophilic, less lipophilic = more selective with less toxicity.

In this study no correlation between the lipophilicity, the IC_{50} and the tumour specificity was found with the Pearson test.

Stage 2

Chapter 4: Determination of mitochondrial membrane potential

4.1 Introduction

Electrical potential differences are present across the cytoplasmic membranes of living prokaryotic and eukaryotic cells and also between the cytosol and the interior of organelles such as mitochondria. Mitochondrial membrane potential is generated and maintained by concentrations of ions such as sodium, potassium, chloride and hydrogen. Mitochondrial membrane potential is reduced when energy metabolism is disrupted. Estimation of mitochondrial membrane potential in individual eukaryotic cells by flow cytometry, using any of a large number of fluorescent probes has been practiced for over 20 years (Shapiro, 2000). The most popular dyes for monitoring mitochondrial membrane potential are rhodamine 123, tetramethylrhodamine methylester (TMRM), tetramethylrhodamine ethyl ester (TMRE), $DiOC_6(3)$ and JC-1 (5,5',6,6'-tetrachloro-1,1',3,3'-tetraethylbenzimidazolcarbocyanine iodide). JC-1 appears to be the most suitable dye for probing mitochondria in living cells. It has an absorption maximum of 510 nm and a fluorescence maximum of 520 nm for monomers and an absorption maximum of 585 nm and a fluorescence maximum of 585 nm for the J-aggregates (Smiley *et al*., 1991). Cationic redistribution dyes tend to accumulate within mitochondria. Thus the intensity of probe fluorescence can be used as a measure of mitochondrial membrane potential (Plášek *et al*., 2005).

To stain mitochondria, the probe has to enter into the cell in order to reach the organelles. It's cytoplasmic accumulation is a crucial event, because a critical intracellular concentration is required to obtain an adequate fluorescence signal. For lipophilic, cationic molecules, such accumulation mainly depends on plasma membrane potential.

Due to the necessity of an adequate intracellular concentration of fluorescent dyes, changes in plasma membrane potential influence mitochondrial stain ability, and can mimic changes in mitochondrial membrane potential. JC-1 staining is unaffected by agents that depolarize the plasma membrane, while it is strongly affected by drugs that dissipate the mitochondrial membrane potential. This confirms that JC-1 is a reliable probe for analyzing changes in mitochondrial membrane potentials (Salvioli *et al*., 1997)

The loss of mitochondrial membrane potential is a hallmark for apoptosis or programmed cell death. In non-apoptotic cells JC-1 exists as a monomer in the cytosol (green) and also accumulates as J-aggregates in the mitochondria which stains red. In apoptotic and necrotic cells, JC-1 exists in a monomeric form and stains the cytosol green. JC-1 uses a cationic dye to signal the loss of the mitochondrial membrane potential. In healthy cells, the dye stains the mitochondria bright red. The negative charge established by the intact mitochondrial membrane potential allows the lipophilic dye, bearing a delocalized positive charge, to enter the mitochondrial matrix where it accumulates. When the critical concentration is exceeded, JC-1 aggregates are formed which become fluorescent red. In apoptotic cells, the mitochondrial membrane potential collapses and JC-1 cannot accumulate in the mitochondria. In these cells JC-1 remains in the cytoplasm in the green fluorescent monomeric form. Apoptotic cells, showing primarily green fluorescence, are easily differentiated from healthy cells, which show red and green fluorescence (Smiley *et al*., 1991).

Mitochondrial membrane potential, *in situ*, is an important indicator of mitochondrial function and dysfunction (Rottenberg and Wu, 1998). Smiley *et al.,* (1991) established that the formation of J-aggregates by JC-1 is dependant on the mitochondrial membrane potential.

In a study it was found that the mitochondrial membranes of Jurkat cells are sensitive to agents that achieve a loss of membrane integrity such as anti-human Fas IgM, A23187 and thapsigargin (Bortner and Cidlowski, 1999). Therefore, this system is an ideal choice for the comparison of the usefulness of lipophilic cationic dyes to monitor the

mitochondrial function in lymphoid cells under various experimental conditions (Jayaraman, 2005). Chen (1988) found that resting human lymphocytes have low mitochondrial membrane potentials while PHA stimulated lymphocytes have an elevated mitochondrial membrane potential. The Jurkat cell line and normal PHA stimulated human lymphocytes were used to study the effects of the selected drugs on mitochondrial and plasma membrane potential based on these findings.

4.2 Aim

The aim of this study was to determine the effect of $[Au(dppe)_2]Cl$, cisplatin, MM4, MM5 and MM6 on mitochondrial membrane potential of:

i. Primary PHA stimulated human lymphocyte cultures
ii. Jurkat cells

4.3 Materials and methods

4.3.1 Reagents

i. JC-1 (5,5',6,6'-tetrachloro-1,1',3,3'-tetraethylbenzimidazolcarbocyanine iodide)

JC-1, cat no T 4069, was supplied by Sigma (St Louis, USA). 5 mg was dissolved in 5.140 ml DMSO. Stock solution was dispensed in 50 µl aliquots in 1.8 ml eppendorf tubes and stored in the dark at -70ºC. This is the stock solution with a concentration of 1.5 mM. 50 µl of the stock solution was diluted with 1950 µl PBS immediately before use. Care was taken to keep the solution in the dark at all times.

ii. Valinomycin

Valinomycin, cat no V0627, was supplied by Sigma (St Louis, USA). 2.2 mg was dissolved in 2 ml of HPLC grade MeOH (Sigma) to make a stock solution of 1 mM. Stock solution was dispensed in 50 µl aliquots in 1.8 ml eppendorf tubes and stored in the dark at -70ºC. 0.1 and 10 µM dilutions were made just before use with RPMI supplemented with 10% bovine FCS.

iii. PHA

Phyto-haemagglutenin, cat no 30852701 HA 15, was supplied by Bioweb (Edenglen, RSA). The contents of each bottle was dissolved in 5 ml of sterile saline and dispensed in 0.4 ml aliquots. Aliquots were stored at -20ºC. 1.6 ml RPMI supplemented with 10% bovine FCS was used to dilute these aliquots prior to use.

iv. PBS

Phosphate buffered saline, cat no 211248, was supplied by The Scientific Group (Johannesburg, RSA). 9.23 g was dissolved in 1 liter de-ionized water and stored at 4 ºC.

4.3.2 Method

A standard flow cytometric method with the mitochondrial membrane stain, JC-1 was used for this study. By using JC-1 it is possible to detect single cell variations in mitochondrial membrane potential. JC-1 is able to enter selectively into mitochondria and this is dependant on mitochondrial membrane potential. The color of the dye changes reversibly from green to red as the mitochondrial membrane becomes more polarized (Cossarizza *et al*., 1993).

The three selected experimental compounds (MM4, MM5 and MM6) were tested on Jurkat cells and normal PHA stimulated lymphocytes for effects on mitochondrial membrane potential together with $[Au(dppe)_2]Cl$ and cisplatin.

Concentrations equal to the IC_{50} value and double the IC_{50} value of the experimental compounds were used.

An untreated control and a positive control were included. Valinomycin was used as the positive control at concentrations of 0.1 and 10 µM (Cossarizza *et al*., 1993; Caruso *et al*., 2007).

Cell concentrations that were used:

PHA stimulated lymphocytes: 2×10^6 cells per ml

Jurkat: 3×10^5 cells per ml

Experiments were set up in flow cytometer tubes with loose fitting caps.

PHA stimulated human lymphocytes:

Lymphocytes were isolated as described in **Chapter 3** and made up to 2×10^6 cells per ml with RPMI supplemented with 10% FCS.

i. Untreated cell suspensions (untreated control)

1.8 ml cell suspension

0.220 ml RPMI supplemented with 10% bovine FCS.

0.200 ml PHA

ii. Cell suspensions treated with Valinomycin (positive control)

1.8 ml cell suspension

0.200 ml PHA

iii. Cell suspensions treated with experimental compounds

1.8 ml cell suspension

0.220 ml experimental compound (diluted to the concentrations described in **Table 4.1** in RPMI supplemented with 10% bovine FCS).

0.200 ml PHA

Jurkat cells

Jurkat cells were made up to 3 x 10^5 cells per ml in RPMI supplemented with 10% FCS.

i. Untreated cell suspensions (untreated control)

1.8 ml cell suspension

0.200 ml RPMI supplemented with 10% bovine FCS

ii. Cell suspensions treated with Valinomycin (positive control)

1.8 ml cell suspension

iii. Cell suspensions treated with experimental compounds

1.8 ml cell suspension

0.200 ml experimental compound (diluted to the concentrations described in **Table 4.2** in RPMI supplemented with 10% bovine FCS).

Cell suspensions were incubated for 1 hour at 37ºC and in an atmosphere containing 5% CO_2 before the experimental compounds were added. Controls received no treatment except in the case of Valinomycin, where 0.200 ml and 0.220 ml was added to Jurkat and lymphocytes respectively, 10 minutes before the experiment was terminated. Cells or experimental cells were incubated with the experimental compounds for 24 hours at 37ºC and in an atmosphere containing 5% CO_2. After 24 hours Valinomycin of 0.1 and 10 µM concentrations was added and the cell suspensions were incubated for a further 10 minutes at 37ºC and in an atmosphere containing 5% CO_2. All cell suspensions were centrifuged at 500G for 5 minutes and the supernatant discarded. Cell pellets were re-suspended in 900 µl RPMI supplemented with 10% bovine FCS and 100 µl JC-1 (1.5 mM) was added to each tube. Cells were incubated at room temperature in the dark for 20 minutes and centrifuged at 500G for 5 minutes. Supernatant was discarded and the cell pellets were washed twice with 2 ml PBS and centrifuged at 500G for 5 minutes. The cell pellets were re-suspended in 1 ml PBS containing 1% bovine FCS. Cells were analyzed immediately using the Beckman Coulter EPICS XL flow cytometer.

4.4 Results

Results are expressed as the mean ratio between red and green fluorescence ± SEM. The Student's t-test for paired values was used for the statistical analysis of data.

Table 4.1 represents the mean ratio between green and red fluorescence of JC-1 ± SEM in Jurkat cells treated for 24 hours with different concentrations of 5 selected drugs, treated and untreated controls. Each value represents the mean of 13 independent experiments.

The table shows that $[Au(dppe)_2]Cl$ depolarized the mitochondrial membranes of Jurkat cells significantly, while cisplatin hyperpolarized the mitochondrial membranes of Jurkat cells significantly. MM4 and MM5 depolarized the mitochondrial membranes as well, although not significantly, while MM6 depolarized at the lower concentration of 0.369 µM and hyperpolarized the mitochondrial membranes at the higher concentration of 0.738 µM. The differences in the mean ratio of red to green fluorescence for MM6 were not statistically significant.

Table 4.2 represents the mean ratio between green and red fluorescence of JC-1 ± SEM in PHA stimulated human lymphocytes treated for 24 hours with different concentrations of 5 selected drugs, treated and untreated controls. Each value represents the mean of 8 independent experiments.

The table shows that the mitochondrial membranes of the PHA stimulated human lymphocytes were significantly depolarized by $[Au(dppe)_2]Cl$. Cisplatin had the same effect on the PHA stimulated lymphocytes than on the Jurkat cells, and hyperpolarized the mitochondrial membranes of the lymphocytes. Significance was only found at the lower concentration of 8.798 µM. MM4, MM5 and MM6 depolarized the mitochondrial membranes of PHA stimulated human lymphocytes significantly with the exception of MM4 at the lower concentration of 0.288 µM, which showed no significance.

Table 4.1: The mean ratio between green and red fluorescence of JC-1 ± SEM in Jurkat cells treated for 24 hours with different concentrations of 5 selected drugs, treated and untreated controls.

Mean ratio[1] between green and red fluorescence of JC-1 ± SEM in Jurkat cells treated for 24 hours with different concentrations of 5 selected drugs, treated and untreated controls

Experimental compound	Concentration (µM)	Mean Ratio
$[Au(dppe)_2]Cl$,	0.157	408.477 ± 9.297 ***[2]
	0.314	406.777 ± 10.116 ***
Cisplatin	0.707	511.031 ± 14.397 *
	1.414	516.800 ± 13.577**
MM4	0.377	472.192 ± 12.428
	0.674	493.054 ± 19.403
MM5	0.261	476.092 ± 12.460
	0.522	453.785 ± 13.271
MM6	0.369	468.677 ± 10.839
	0.738	520.215 ± 21.642
Valinomycin	0.1	422.262 ± 11.476 ***
Valinomycin	10	424.659 ± 8.113 ***
Untreated control	0	482.231 ± 14.313

(1) Mean of 13 independent experiments.

(2) Significance was determined by the Student's t-test for paired values. * $p < 0.01$; ** $p < 0.001$ and *** $p < 0.0001$ compared to the untreated control.

Table 4.2: The mean ratio between green and red fluorescence of JC-1 ± SEM in PHA stimulated human lymphocytes treated for 24 hours with different concentrations of 5 selected drugs, treated and untreated controls.

Mean ratio(1) between green and red fluorescence of JC-1 ± SEM in PHA stimulated lymphocytes treated for 24 hours with different concentrations of 5 selected drugs, treated and untreated controls

Experimental compound	Concentration (μM)	Mean Ratio
$[Au(dppe)_2]Cl$	0.254	447.450 ± 14.579 ***(2)
	0.508	415.150 ± 15.685 ***
Cisplatin	8.798	570.337 ± 25.082 *
	17.596	563.975 ± 27.190
MM4	0.288	510.025± 21.728
	0.576	459.975 ± 16.063 *
MM5	0.340	478.388 ± 22.285 **
	0.680	445.413 ± 9.757 **
MM6	0.397	467.713 ± 14.791*
	0.794	441.213 ±15.658 **
Valinomycin	0.1	396.500 ± 10.244 ***
Valinomycin	10	373.450 ± 10.662 ***
Untreated control	0	542.125 ± 26.217

(1) Mean of 8 independent experiments.

(2) Significance was determined by the Student's t-test for paired values. * $p < 0.01$; ** $p < 0.001$ and *** $p < 0.0001$ compared to the untreated control.

4.5 Discussion

In this study, Valinomycin depolarized the mitochondrial membranes of both Jurkat cells and PHA stimulated human lymphocytes very significantly.

$[Au(dppe)_2]Cl$ depolarized the mitochondrial membranes of Jurkat cells significantly, while cisplatin hyperpolarized the mitochondrial membranes of Jurkat cells significantly. MM4, MM5 and MM6 had no significant effect on the mitochondrial membranes of Jurkat cells.

The mitochondrial membranes of the PHA stimulated human lymphocytes were significantly depolarized by $[Au(dppe)_2]Cl$. Cisplatin hyperpolarized the mitochondrial membranes of the lymphocytes. MM4, MM5 and MM6 depolarized the mitochondrial membranes of PHA stimulated human lymphocytes significantly with the exception of MM4 at the lower concentration of 0.288 μM, which showed no significance.

The study of mitochondria and the changes in the mitochondrial membrane potential have become a focus of apoptosis regulation. A loss of mitochondrial membrane potential initiates the opening of the mitochondrial permeability transition pores, located on the inner mitochondrial membrane. Activation of these mitochondrial permeability transition pores permits the redistribution of molecules across the inner mitochondrial membrane, thus disrupting the membrane potential of this organelle. Induction of mitochondrial permeability transition, results in the release of several apoptotic factors (Bortner and Cidlowski, 1999).

The results obtained in this study suggest that the novel compounds MM4, MM5 and MM6 have similar effects to $[Au(dppe)_2]Cl$ on the mitochondrial membrane potentials of the cells tested, but to a lesser extent. Since depolarization of mitochondrial membrane potential is indicative of the start of apoptosis, this could be an indication of the mechanism of action of these compounds. Cisplatin did not depolarize the mitochondrial membranes in either the Jurkat cells or the PHA stimulated human lymphocytes in this

study. The incubation time of these experiments was 24 hours, and it is possible that this was not long enough for the cisplatin to take full effect. Giovaninni *et al*., (2002) found that hyper polarization of mitochondria (described in lymphocytes), seems to represent a pre-requisite for rapid mitochondrial-mediated apoptotic cell death that eventually leads to the loss of mitochondrial membrane potential. This could also be applicable to MM6 which hyperpolarized the mitochondrial membranes of Jurkat cells at a concentration of 0.738 μM. These hyper polarization effects can result from different actions, such as increased mitochondrial mass and number per cell or an increase in matrix volume, the latter leading to swelling and rupture of the outer membrane, followed by a decrease in mitochondrial membrane potential ([1]Liu *et al*., 2005). Mitochondrial or cellular receptor activation and increased respiration are also reported to induce mitochondrial hyper polarization in cells (Carlson and Ehrich, 1999).

Maintenance of a significant electrical potential difference across biological membranes is crucial for a variety of cellular functions including development, signaling, movement, energy balance and apoptosis. Intracellular organelles such as mitochondria possess function-related membrane potentials far exceeding that of the plasma membrane. The dissipation of the inner mitochondrial transmembrane potential marks the point-of-no-return during the apoptotic program and occurs prior to DNA fragmentation. Mitochondrial depolarization is associated with outer mitochondrial membrane permeability which is induced by many physiological effectors including reactive oxygen species and the blockade of the respiratory chain. Thus, evaluation of the mitochondrial membrane potential is of critical importance for the assessment of apoptosis (Jayaraman, 2005).

Stage 2

Chapter 5: Determination of plasma membrane potential

5.1 Introduction

The cell membrane, also called the plasma membrane or plasma lemma, is a semi-permeable lipid bi-layer common to all living cells. It contains a variety of biological molecules, primarily proteins and lipids, which are involved in a vast array of cellular processes (Alberts *et al*., 1994). Membrane proteins and other components, mainly glyco- and phospholipids, are involved in receptor- binding and further transport of bound components into the cell. Plasma membranes are also involved in cell-cell and cell-matrix interactions, in the organization of the cytoskeleton, and they determine the immunological identity of the cell (Clifton *et al*., 2006). Cells in solid tissues are usually polarized, i.e. their plasma membrane is divided into two discrete regions – the apical and the basolateral domains – displaying distinct lipid and protein compositions required by their biological function (Vámosi *et al*., 2006).

Figure 5.1: Diagram of a plasma membrane (http://en.wikipedia.org/wiki/Pasma_membrane)

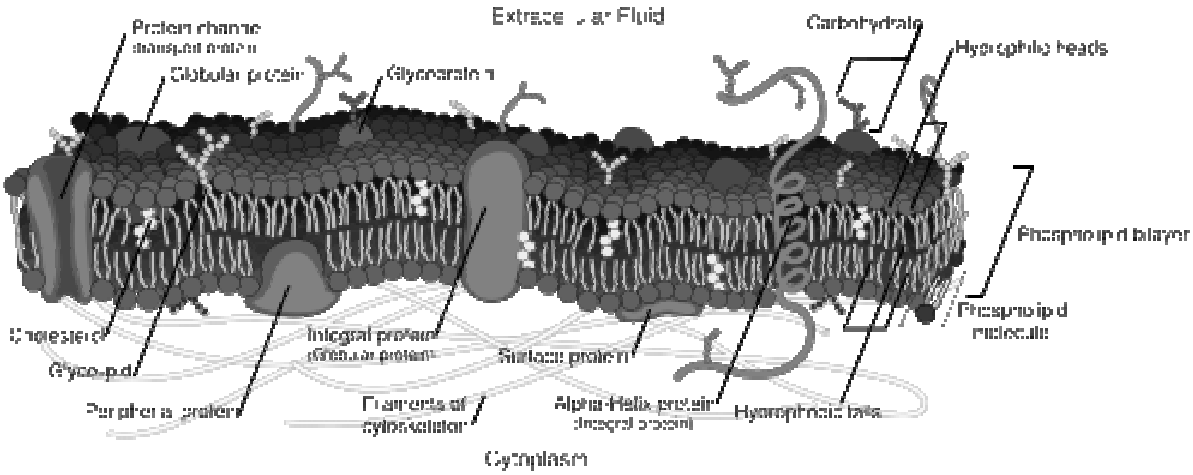

A primary function of the plasma membrane is the maintenance of a potential difference by its ability to barricade the free passage of ions across the membrane. Normally, most cells maintain an electrical potential across the plasma membrane of minus 60 to minus 70 mV that renders the inside of the membrane more negative than the outside. This is due to the asymmetrical distribution of ions across the plasma membrane. Until recently the role of plasma membrane potential in apoptosis has been largely ignored; however, recent studies have suggested that the plasma membrane potential may be compromised during apoptosis of lymphocytes (Mann and Cidlowski, 2001).

Mitochondrial uptake of a lipophilic cation such as Rhodamine 123 (Rh 123) is driven by both the plasma and the mitochondrial membrane potentials. The plasma membrane potential pre-concentrates Rh 123 into the cytoplasm relative to the extra-cellular medium and the mitochondrial membrane potential, in turn, concentrates the cation within the mitochondria. Therefore, any lipophilic cationic molecule that can pass through the plasma and mitochondrial membranes should be accumulated by the mitochondria (Davis *et al*., 1985).

This assay will determine whether selected cells will undergo changes in plasma membrane potential when treated with the experimental compounds.

5.2 Aim

The aim of this study was to determine the effect of $[Au(dppe)_2]Cl$, cisplatin, MM4, MM5 and MM6 on plasma membrane potentials of:

i. Primary PHA stimulated human lymphocyte cultures
ii. Jurkat cells.

5.3 Materials and methods

5.3.1 Reagents

i. bis (1,3-dibarbituric acid) trimethine ($DIBAC_4(3)$)

$DIBAC_4(3)$, cat no D-8189, was supplied by Sigma (St Louis, USA). 3.12 mg was dissolved in 4 ml 100% ethanol to make a stock solution of 1.5 mM. Stock solution was dispensed in 50 µl aliquots in 1.8 ml eppendorf tubes and stored in the dark at -70ºC. 1.5 µM dilutions were made before use with RPMI supplemented with 10% bovine FCS.

ii. Dexamethasone

Dexamethasone, cat no D-4902, was supplied by Sigma (St Louis, USA). 1.572 mg was dissolved in 4 ml 100% ethanol to make a stock solution of 1 mM. Stock solution was dispensed in 50 µl aliquots in 1.8 ml eppendorf tubes and stored in the dark at -70ºC. 0.250 and 0.500 µM dilutions were made just before use with RPMI supplemented with 10% bovine FCS.

iii. PHA

Phyto-haemagglutenin, cat no 30852701 HA 15, was supplied by Bioweb (Edenglen, RSA). The contents of each bottle was dissolved in 5 ml of sterile saline and dispensed

in 0.4 ml aliquots. Aliquots were stored at -20ºC. 1.6 ml RPMI supplemented with 10% bovine FCS was used to dilute these aliquots prior to use.

iv. PBS

Phosphate buffered saline, cat no 211248, was supplied by The Scientific Group (Johannesburg, RSA). 9.23 g was dissolved in 1 liter de-ionized water and stored at 4 ºC.

5.3.2 Method

A standard flow cytometric method with bis (1,3-dibarbituric acid) trimethine ($DIBAC_4(3)$) was used. (Mann and Cidlowski, 2001, Radošević *et al*., 1993). Bis (1,3-dibarbituric acid) trimethine ($DIBAC_4(3)$), is an anionic probe whose distribution across the cell membrane depends on plasma membrane potential. When the membrane depolarizes, the inside of the cell becomes more positively charged, more dye enters the cell resulting in an increase in cellular fluorescence. With hyper polarization, the dye is extruded from the cell resulting in a decrease in fluorescence (Radošević *et al*., 1993). Previous studies have established that $DIBAC_4(3)$ serves as an indicator for the plasma membrane potential in lymphoid cells and it is the most sensitive to manipulations of plasma membrane potential (Mann and Cidlowski, 2001, Radošević *et al*., 1993).

The three selected experimental compounds (MM4, MM5 and MM6) were tested on Jurkat cells and normal PHA stimulated human lymphocytes for effects on plasma membrane potential together with $[Au(dppe)_2]Cl$ and cisplatin.

Concentrations equal to the IC_{50} value and double the IC_{50} value of the experimental compounds were used.

An untreated control and a positive control were included. Dexamethasone (Mann and Cidlowski, 2001) was used as the positive control at concentrations of 0.250 and 0.500 µM for Jurkat cells and PHA stimulated human lymphocytes respectively.

Cell concentrations that were used:

PHA stimulated lymphocytes: 2×10^6 cells per ml

Jurkat: 3×10^5 cells per ml

Experiments were set up in flow cytometer tubes with loose fitting caps.

PHA stimulated lymphocytes

Lymphocytes were isolated as described in **Chapter 3** and made up to 2×10^6 cells per ml in RPMI supplemented with 10% FCS.

i. Untreated cell suspensions (untreated control)

1.8 ml cell suspension

0.220 ml RPMI supplemented with 10% bovine FCS.

0.200 ml PHA

ii. Cell suspensions treated with Dexamethasone (positive control)

1.8 ml cell suspension

0.200 ml PHA

iii. Cell suspensions treated with experimental compounds

1.8 ml cell suspension

0.220 ml experimental compound (diluted to the concentrations described in **Table 5.1** in RPMI supplemented with 10% bovine FCS).

0.200 ml PHA

Jurkat cells

Jurkat cells were made up to 3 x 10^5 cells per ml with RPMI supplemented with 10% FCS.

i. Untreated cell suspensions (untreated control)

1.8 ml cell suspension

0.200 ml RPMI supplemented with 10% bovine FCS

ii. Cell suspensions treated with Dexamethasone (positive control)

1.8 ml cell suspension

iii. Cell suspensions treated with experimental compounds

1.8 ml cell suspension

0.200 ml experimental compound (diluted to the concentrations described in **Table 5.2** in RPMI supplemented with 10% bovine FCS).

Cell suspensions were incubated for 1 hour at 37ºC and in an atmosphere containing 5% CO_2 before the experimental compounds were added. Controls received no treatment except in the case of Dexamethasone, where 0.200 ml and 0.220 ml was added to Jurkat cells and lymphocytes respectively, 4-6 hours before the experiment was terminated. Cell suspensions were incubated with the experimental compounds for 24 hours at 37ºC and in an atmosphere containing 5% CO_2. After 18-20 hours Dexamethasone of designated concentrations was added and incubated for 4-6 hours at 37ºC and in an atmosphere containing 5% CO_2. Cell suspensions were centrifuged at 720G for 5 minutes, the supernatant discarded and re-suspended in 900 µl RPMI supplemented with 10% FCS. 100 µl $DIBAC_4(3)$ (1.5 µM) was added to each tube and incubated for 30 minutes at 37ºC and in an atmosphere containing 5% CO_2. 100 µl propidium iodide (100 µg/ml) was added to each tube to exclude non-viable cells (final concentration of 10 µg/ml).

All fluorescence determinations were done on a Cytomics FC 500 series Beckman Coulter flow cytometer.

5.4 Results

Results are expressed as the mean change in the fluorescence of $DIBAC_4$ (3) ± SEM. The Student's t-test for paired values was used for the statistical analysis of data.

Table 5.1 represents the mean change in fluorescence of $DIBAC_4$ (3) ± SEM in Jurkat cells treated for 24 hours with different concentrations of 5 selected drugs, treated and untreated controls. Each value represents the mean of 9 independent experiments.

The table shows that $[Au(dppe)_2]Cl$ and cisplatin depolarized the plasma membranes of Jurkat cells significantly while MM4 and MM5 had only a slight depolarizing effect. MM6 depolarized the plasma membranes of the Jurkat cells significantly.

Table 5.2 represents the mean change in fluorescence of $DIBAC_4$ (3) ± SEM in PHA stimulated lymphocytes treated for 24 hours with different concentrations of 5 selected drugs, treated and untreated controls. Each value represents the mean of 7 independent experiments.

The table shows that $[Au(dppe)_2]Cl$ and cisplatin depolarized the plasma membranes of PHA stimulated human lymphocytes significantly. MM4 depolarized the plasma membrane significantly at 0.576 µM. MM5 depolarized the plasma membranes of PHA stimulated human lymphocytes but only significantly at 0.680 µM, while MM6 depolarized significantly at both the high and the low concentrations.

Table 5.1: The mean change in fluorescence of $DIBAC_4$ (3) ± SEM in Jurkat cells treated for 24 hours with different concentrations of 5 selected drugs, treated and untreated controls.

Mean change in fluorescence of $DIBAC_4(3)^{(1)}$ ± SEM in Jurkat cells treated for 24 hours with different concentrations of 5 selected drugs, treated and untreated controls

Experimental compound	Concentration (µM)	$DIBAC_4(6)$ Fluorescence
$[Au(dppe)_2]Cl$,	0.157	20.289 ± 1.274 *** (2)
	0.314	21.367 ± 2.011 ***
Cisplatin	0.707	10.160 ± 0.930 *
	1.414	10.862 ± 0.950 ***
MM4	0.377	9.607± 0.751
	0.674	9.410 ± 0.974 *
MM5	0.261	9.881 ± 0.831
	0.522	9.866 ± 0.817
MM6	0.369	10.814 ± 0.954 ***
	0.738	11.188 ± 0.904 ***
Dexamethasone	0.250	10.489± 1.284 **
Untreated control	0	9.169 ± 0.882

(1) Mean of 9 independent experiments.

(2) Significance was determined by the Student's t-test for paired values. * $p < 0.01$; ** $p < 0.001$ and *** $p < 0.0001$ compared to the untreated control.

Table 5.2: The mean change in fluorescence of $DIBAC_4(3)$ ± SEM in PHA stimulated human lymphocytes treated for 24 hours with different concentrations of 5 selected drugs, treated and untreated controls.

Mean change in fluorescence of $DIBAC_4(3)$[(1)] ± SEM in PHA stimulated lymphocytes treated for 24 hours with different concentrations of 5 selected drugs, treated and untreated controls

Control

Experimental compound	**Concentration (μM)**	**$DIBAC_4(6)$ Fluorescence**
$[Au(dppe)_2]Cl$	0.254	57.486 ± 7.042 ** [(2)]
	0.508	69.557 ± 9.389 **
Cisplatin	8.798	40.229 ± 4.559 **
	17.596	43.600 ± 5.030 **
MM4	0.288	36.729 ± 4.176
	0.576	43.486 ± 5.407
MM5	0.340	40.071 ± 5.373
	0.680	46.986 ± 6.139 *
MM6	0.397	51.357± 8.077 *
	0.794	60.829 ± 9.358 **
Dexamethasone	0.500	40.200 ± 4.192 **
Untreated control	0	36.986 ± 3.990

(1) Mean of 7 independent experiments.

(2) Significance was determined by the Student's t-test for paired values. * $p < 0.01$; ** $p < 0.001$ and *** $p < 0.0001$ compared to the untreated control.

5.5 Discussion

Dexamethasone depolarized the plasma membranes of both Jurkat cells and PHA stimulated human lymphocytes significantly.

$[Au(dppe)_2]Cl$ and cisplatin depolarized the plasma membranes of Jurkat cells. MM6 depolarized the plasma membranes of the Jurkat cells significantly, but not to the same extent as $[Au(dppe)_2]Cl$.

$[Au(dppe)_2]Cl$, cisplatin and MM6 depolarized the plasma membranes of PHA stimulated human lymphocytes significantly.

As was mentioned in **Chapter 4,** to accumulate within the mitochondria, lipophilic cationic probes must first cross the plasma membrane. A decrease of plasma membrane potential might affect mitochondrial accumulation of the probe (Bernardi *et al*., 2001). From the results obtained in this study it is clear that $[Au(dppe)_2]Cl$, cisplatin, MM4, MM5 and MM6 depolarized the plasma membranes of both the cell types that were tested. The positive control and $[Au(dppe)_2]Cl$, however, depolarized the mitochondrial membranes of both Jurkat cells and PHA stimulated PHA human lymphocytes very significantly. This confirms the theory of Davis *et al* (1985), that any lipophilic cationic molecule that can pass through both the plasma and the mitochondrial membranes should be accumulated by the mitochondria.

The depolarization of the plasma membranes in this study does not appear to influence the accumulation of the mitochondrial probe (JC-1) in the mitochondria, which confirms the fact that JC-1 staining is unaffected by agents that depolarize the plasma membrane, while it is strongly affected by drugs that dissipate the mitochondrial membrane potential (Salvioli *et al*., 1997).

In lymphocyte-apoptosis, actively induced plasma membrane depolarization has been previously investigated, as the maintenance of the plasma membrane potential is of vital

importance for cells. Plasma membrane potential contributes to the driving force of ions like Ca^{2+} across the plasma membrane and is therefore essential for different signal transduction pathways and the regulation of uptake and excretion of metabolites. These processes located at the plasma membrane are of great importance due to their key role in the regulation of apoptotic volume decrease, a feature that distinguishes apoptosis from necrosis. To date, breakdown of plasma membrane potential has been described for a few apoptosis inducing agents like Dexamethasone (Nolte *et al*., 2004).

In **Chapter 6** it will be investigated whether the experimental compounds did induce apoptosis in Jurkat cells.

Stage 2

Chapter 6: Apoptosis

6.1 Introduction

Apoptosis is an essential process for excluding damaged or harmful cells and maintaining homeostasis in biological systems. The disruption of this process is assumed to cause various diseases, including cancer, autoimmune diseases and neurodegenerative diseases. Apoptosis can be induced experimentally by such stimuli as UV irradiation, growth factor withdrawal, death receptor ligands or cytotoxic drugs (Kawai *et al*., 2004).

Programmed cell death or apoptosis plays an important role in the normal development and homeostasis mechanisms of multi cellular organisms (Ludovico *et al*., 2002). Under physiological conditions, the occurrence of apoptosis in tissues is typically a rare event. Thus only a small number of apoptotic cells can be seen at any time point (Saraste and Pulkki, 2000).

Apoptosis can be defined as a cell death process in which activation of catabolic processes and enzymes occurs prior to cytolysis, thereby facilitating the recognition, uptake, and digestion of the apoptotic cell by neighbouring cells (Susin *et al*., 1998). Apoptosis is expressed as an active, intrinsic mechanism based on the concerted action of specific proteases (caspases) and endonucleases. Necrosis is the consequence of irreversible destruction of cell membranes, followed by collapse of cellular metabolism resulting from extrinsic damage to the cell (Somosy, 2000). Necrosis is caused by an external noxious stimulus and involves contiguous portions of tissue. The process is passive and pathologic. Necrosis causes lysis or rupture of cell membranes and the leakage of cytosol into the surroundings. The release of cytosol releases kinins into the tissue and this can incite inflammation (Kuan and Passaro, 1998).

The first sign of apoptotic cell death is a condensation of the nuclear material, with a marked accumulation of densely stained chromatin, typically at the edge of the nucleus. This is accompanied by cell shrinkage. Cytoplasmic blebs appear on the cell surface and the cell detaches from its neighbours. The nuclear outline often becomes highly folded and the nucleus breaks up, with discrete fragments dispersing throughout the cytoplasm. Eventually, the cells themselves fragment, with the formation of a number of membrane bounded apoptotic bodies (Hall, 1999). The formation of cell membrane-bound apoptotic bodies avoids spillage of intracellular contents within the intercellular space, thus effectively preventing inflammatory changes (Woodle and Kulkarni, 1998). The apoptotic bodies are rapidly phagocytosed into neighbouring cells, including macrophages and parenchymal cells. Apoptotic bodies can be recognized inside these cells, but eventually they become degraded (Saraste and Pulkki, 2000).

Many existing treatments (non-steroidal anti-inflammatory and anti-cancer treatments) act through apoptosis. New treatments that are developed are aimed at modifying apoptosis (Renehan, *et al*., 2001). Apoptosis is an innate phenomenon whereby cells commit suicide and it is a desired end point of anti-cancer therapy (Keen *et al*., 2005). The future of cancer therapy appears to be dependent on finding new tools to lower the threshold of cancer cells to molecules that induce apoptosis (Nuutinen *et al*, 2006).

Apoptosis in cancer cells can be triggered by extra-cellular stimuli that mediate at least two apoptotic signaling pathways, so called receptor-mediated extrinsic and mitochondria-mediated intrinsic pathways. Regardless of the entry site of apoptosis, eventually these two pathways cooperatively amplify its apoptotic signaling for cell death (Wang *et al*., 2006).

Figure 6.1: A schematic representation of the continuum of programmed cell death cascades (Ashe and Berry, 2003)

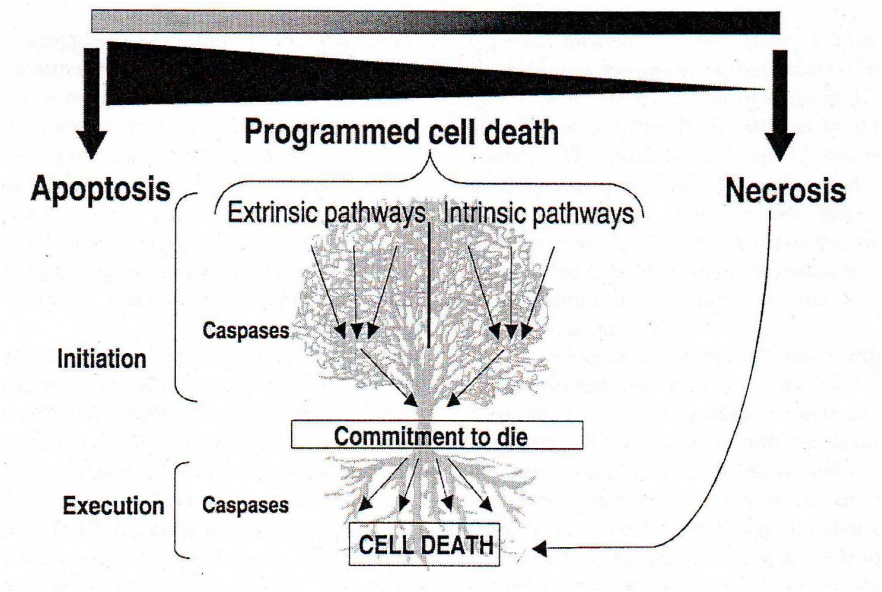

6.2 Aim

The aim of this study was to determine whether apoptosis is induced in Jurkat cells by $[Au(dppe)_2]Cl$, cisplatin, MM4, MM5 and MM6.

6.3 Materials and methods

6.3.1 Reagents

i. Annexin V-FITC

Annexin V-FITC, cat no 556419 BD Pharmingen, was supplied by The Scientific Group (Johannesburg, RSA). Annexin V was used undiluted.

ii. Binding buffer

All chemicals were obtained from Sigma.

238 mg Hepes

876 mg NaCl

37.3 mg KCl

26.5 mg $CaCl_2$

9.5 mg $MgCl_2$

Ingredients were dissolved in sequence and made up to a 100 ml with de-ionized water. pH was adjusted to 7.4. Solution was stored at 4ºC.

iii. PBS

Phosphate buffered saline, cat no 211248, was supplied by The Scientific Group (Johannesburg, RSA). 9.23 g was dissolved in 1 liter de-ionized water and stored at 4 ºC.

iv. Propidium iodide

Propidium iodide, cat no P-4170, was obtained from Sigma (St Louis, USA). 2.5 mg was dissolved in 50 ml PBS. Solution was stored at 4ºC and care was taken to keep it in the dark.

6.3.2 Method

A standard flow cytometer method with propidium iodide (PI) and Annexin V-FITC staining was used. This method measures the decline of viable cells and the appearance of early apoptotic and late apoptotic/necrotic cells in one assay. The method is based upon Annexin V-FITC binding to tag early apoptotic cells and propidium iodide staining to identify late apoptotic/necrotic cells (Michie *et al*., 2003; Tuschl and Schwab, 2004).

$[Au(dppe)_2]Cl$, cisplatin, MM4, MM5 and MM6 were tested to determine whether they induce apoptosis in Jurkat cells.

Concentrations equal to the IC_{50} value and double the IC_{50} value of the experimental compounds were used.

Cell concentration that was used: 1 x 10^5 cells per ml.

Cells were counted and made up to 1 x 10^5 cells per ml in RPMI medium supplemented with 10% FCS, as described in **Chapter 3**.

Experiments were set up in 75 cm^3 tissue culture flasks.

i. Untreated cell suspensions (untreated control)

45 ml cell suspension

5 ml RPMI supplemented with 10% bovine FCS.

ii. Cell suspensions treated with experimental compounds

45 ml cell suspension

5 ml of the experimental compounds diluted to the concentrations described in **Table 6.1** and **Table 6.2** in RPMI supplemented with 10% bovine FCS.

Cell suspensions were incubated at least 1 hour at 37°C and in an atmosphere of 5% CO_2 before the experimental compounds were added.

Cell suspensions were incubated with the experimental compounds for 18, 24 and 48 hours at 37°C and in an atmosphere of 5% CO_2 in tissue culture flasks.

15 ml of the cell suspension was decanted from culture flasks at the set times and centrifuged for 5 minutes at 200G. Cells were washed twice with 3 ml PBS supplemented with 1% bovine FCS. The cell pellet was re-suspended in 1 ml binding buffer. 100 µl of the control cell suspension was transferred to 4 different flow cytometer tubes which were labeled unstained, Annexin V-FITC, PI and stained. The unstained tube did not receive Annexin V-FITC or PI, while the tubes labeled Annexin V-FITC and

PI received only the solution that they were labeled for and the stained tube received Annexin V-FITC and PI These tubes were used to set the protocol on the flow cytometer. 100 µl of the cell suspensions of all the experimental tubes were transferred to labeled flow cytometer tubes and received 5 µl Annexin V-FITC and 10 µl propidium iodide. Cell suspensions were mixed gently and incubated at room temperature (20-25°C) for 15 minutes in the dark. 400 µl binding buffer was added to each tube.

Samples were analyzed by flow cytometery within 1 hour using a Cytomics FC 500 series Beckman Coulter flow cytometer.

6.4 Results

Results are expressed as the mean percentage ± SEM. Each value represents the mean of 7 independent experiments. The Student's t-test for paired values was used for the statistical analysis of the data.

Table 6.1 represents the mean percentage of Jurkat cells still viable, in early apoptosis, late apoptosis and necrosis ± SEM treated with different concentrations of $[Au(dppe)_2]Cl$ and cisplatin for 18, 24 and 48 hours.

Table 6.2 represents the mean percentage of Jurkat cells still viable, in early apoptosis, late apoptosis and necrosis ± SEM treated with different concentrations of MM4, MM5 and MM6 for 18, 24 and 48 hours.

These tables show that the control cells had viability that changed very little over the time span used. At 18 hours 93.18% ± 1.06 cells were viable with 93 18% ± 1.13 at 24 hours and 93.81% ± 0.45 at 48 hours. Early apoptosis was found to be 1.91% ± 0.43 at 18 hours and 2.25% ± 0.55 and 2.69% ± 0.48 for 24 and 48 hours respectively. Percentage of cells in late apoptosis for the control was 2.05% ± 0.27 at 18 hours, 2.33% ± 0.23 at 24 hours and 1.48% ± 0.08 at 48 hours. 1.22% ± 0.36 of cells were necrotic at 18 hours while 1.29% ± 0.33 and 0.99% ± 0.11 were necrotic at 24 and 48 hours respectively.

These results for the control show that there were no major changes in any of the parameters that were looked at, at the given times.

Viability of the cells treated with $[Au(dppe)_2]Cl$ at the lower concentration of 0.157 µM did not show much change at 18 and 24 hours, but dropped to 69.38% ± 11.95 at 48 hours. Percentage early and late apoptosis as well as necrosis increased proportionally at 48 hours. It seems as if $[Au(dppe)_2]Cl$ at this concentration takes at least 24 hours to have a noticeable effect. Viability of the cells treated with $[Au(dppe)_2]Cl$ at the higher concentration of 0.314 µM did not show much change at 18 and 24 hours either, but sharply dropped to 34.49% ± 16.43 at 48 hours. Percentage early apoptosis showed a slight increase at 24 hours, but no further increase at 48 hours. Percentage late apoptosis did not show much difference between 18 and 24 hours, but increased to 15.61% ± 4.16 at 48 hours. A slight increase of necrosis was seen at 24 hours, which drastically increased to 68.06% ± 2.51 at 48 hours. The higher concentration of 3.14 µM of $[Au(dppe)_2]Cl$ had a slight effect at 24 hours but had killed most of the cells at 48 hours. $[Au(dppe)_2]Cl$ induced apoptosis at both the concentrations that were tested, but more so at the higher concentration.

The viability of the cells treated with cisplatin at the lower concentration of 0.707 µM decreased from 93.57% ± 0.073 to 86.24% ± 2.77 at 18 and 48 hours respectively. Percentage early apoptosis increased steadily from 1.99% ± 0.45 at 18 hours to 2.72% ± 0.48 at 24 hours and 6.63 % ± 2.23 at 48 hours. Percentage late apoptosis increased very slightly at 24 hours and showed no further increase at 48 hours. Percentage necrosis showed the same trend of a slight increase at 24 hours and no further increase at 48 hours. The percentage viability of the cells treated with cisplatin at the higher concentration of 1.414 µM decreased slightly from 90.62% ± 1.5 at 18 hours to 88.72% ± 1.62 at 24 hours and then dropped to 70.99% ± 3.1 at 48 hours. Percentage early apoptosis did not show much change after 24 hours but almost doubled at 48 hours. Percentage late apoptosis increased very slightly at 24 hours from 3.26% ± 1.00 at 18 hours to 3.84% ± 0.79 at 24 hours and then increased to12.88% ± 2.65 at 48 hours. Percentage necrosis did not show much increase over the total incubation time of 48 hours which suggests that cisplatin did

not induce apoptosis to the full extent. A longer incubation time might have produced more pronounced results. Jurkat cells have a doubling time of 48 hours (Kainthla et al., 2006), which means that the time available for cisplatin to act was very limited during this study.

MM4 at the lower concentration of 0.337 µM did not induce apoptosis in Jurkat cells. Only very small fluctuations could be seen in the percentage necrotic cells which increased from 1.94% ± 0.32 at 18 hours to 2.49 % ± 0.55 at 24 hours and 3.20% ± 0.71 at 48 hours. Percentage viability was maintained at an average of 90.41 % over the total incubation period of 48 hours. Percentage early and late apoptosis was equally unaffected and their values were only slightly higher than those recorded for the untreated control. Percentage viability of the Jurkat cells treated with MM4 at the higher concentration of 0.674 µM showed a marked decrease at 18 hours of incubation. Only 77.67% ± 3.72 cells were viable at 18 hours, with a further decrease to 69.65% ± 5.67 at 24 hours, and 47.58% ± 10.87 at 48 hours. There were no changes in percentage early apoptosis but late apoptosis showed a steady increase from 10.72% ± 2.03 at 18 hours to15.96 % ± 2.33 at 24 hours and 19.88% ± 3.41 at 48 hours. Percentage necrosis showed the same trend with 7.22% ± 1.57 at 18 hours, 11.15% ± 3.13 at 24 hours and 36.08% ± 9.80 at 48 hours. MM4 at the higher concentration did induce apoptosis in the Jurkat cell line.

MM5 at the low concentration of 0.261 µM had no effect on the viability, late apoptosis or necrosis. Only a small increase was noticed in the percentage of early apoptosis. At 18 hours 2.04% ± 0.40 of the cells were in early apoptosis, which increased to 3.03% ± 0.51 at 24 hours and 3.81% ± 0.77 at 48 hours. At the higher concentration of 0.522 µM viability is already affected at 18 hours with decrease to 87.52% ± 3.28. Viability decreases further at 24 hours to 80.64% ± 8.83 and 75.28% ± 13.74 at 48 hours. Percentage early and late apoptosis did not follow any pattern of increase or decrease. Necrosis showed a steady increase ranging from 2.38% ± 0.59 at 18 hours to 15.37% ± 12.5 at 48 hours. Since there is no real pattern of increase for early and late apoptosis

that fit in with the decrease of viability and the increase of necrosis, it seems that MM5 is killing the cells by necrosis rather than apoptosis.

MM6 at the lower concentration of 0.369 µM had an effect on the viability of the Jurkat cells at 18 hours, with a decrease to 79.53% ± 2.86 which decreased further to 70.69 % ± 2.24 at 48 hours. Percentage early apoptosis did not follow any pattern of increase or decrease, but late apoptosis steadily increased from 7.52% ± 1.03 at 18 hours to 14.92% ± 4.12 at 48 hours. Necrosis also showed a steady increase from 5.46% ± 0.99 at 18 hours, 7.73% ± 1.84 at 24 hours to 16.44% ± 3.14 at 48 hours. With the higher concentration of 0.739 µM MM6 had an even greater effect. Viability at 18 hours was only 52.13% ± 6.47, which further decreased to 34.97% ± 8.12 at 24 hours and 11.05% ± 2.34 at 48 hours. No increase was found in the percentage early apoptosis between the set times , but late apoptosis increased from 16.72% ± 3.94 at 18 hours to 23.98% ± 4.84 at 24 hours and 24.36% ± 3.85 at 48 hours. Necrosis increased accordingly from 21 79% ± 3.48 at 18 hours to 36.41% ± 9.30 at 24 hours and 63.83% ± 5.42 at 48 hours. The results obtained in this study show that MM6 did induce apoptosis in Jurkat cells at both the concentrations that were tested.

Table 6.1: The mean percentage of Jurkat cells still viable, in early apoptosis, late apoptosis and necrosis ± SEM, treated with different concentrations of $[Au(dppe)_2]Cl$ and cisplatin for 18, 24 and 48 hours.

Mean percentage(1) of Jurkat cells still viable, in early apoptosis, late apoptosis and necrosis ± SEM, treated with different concentrations of $[Au(dppe)_2]Cl$ and cisplatin for 18, 24 and 48 hours.

	Control	$[Au(dppe)_2]Cl$ 0.157 (µM)	$[Au(dppe)_2]Cl$ 0.314 (µM)	Cisplatin 0.707 (µM)	Cisplatin 1.414 (µM)
% Viable cells 18 hours	93.18 ± 1.06	91.78 ± 1.01	91.14 ± 1.18	93.57 ± 0.073	90.62 *(2) ± 1.5
% Early apoptosis	1.91 ± 0.43	2.05 ± 0.42	1.74 ± 0.25	1.99 ± 0.45	3.26 ± 1.00
% Late apoptosis	2.05 ± 0.27	3.85 * ± 0.97	4.23 ± 1.25	2.12 ± 0.23	2.75 ± 0.57
% Necrosis	1.22 ± 0.36	1.45 * ± 0.34	1.70 * ± 0.31	1.27 ± 0.24	1.57 ± 0.31
% Viable cells 24 hours	93.18 ± 1.13	90.90 * ± 1.36	90.52 ** ± 1.52	90.70 * ± 0.97	88.72 *** ± 1.62
% Early apoptosis	2.25 ± 0.55	2.48 ± 0.56	2.33 ± 0.59	2.72 ± 0.48	3.84 ± 0.79
% Late apoptosis	2.33 ± 0.23	3.80 * ± 0.68	4.37 ± 0.75	3.54 ± 0.66	3.69 ± 0.51
% Necrosis	1.29 ± 0.33	1.91 ± 0.43	2.01 * ± 0.45	1.70 * ± 0.38	1.94 ** ± 0.48
% Viable cells 48 hours	93.81 ± 0.45	69.38 ± 11.95	34.49 * ± 16.43	86.24 * ± 2.77	70.99 *** ± 3.1
% Early apoptosis	2.69 ± 0.48	4.30 * ± 1.10	2.24 ± 0.46	6.63 * ± 2.23	7.39 ± 2.65
% Late apoptosis	1.48 ± 0.08	12.7 ± 4.91	15.61 * ± 4.16	3.52 ** ± 0.47	12.88 ** ± 2.76
% Necrosis	0.99 ± 0.11	12.53 ± 6.38	68.06 * ± 2.51	1.74 * ± 0.23	4.69 * ± 1.21

(1) Mean of 7 independent experiments.

(2) Significance was determined by the Student's t-test for paired values. * $p < 0.01$; ** $p < 0.001$ and *** $p < 0.0001$ compared to the untreated control.

Table 6.2: The mean percentage of Jurkat cells still viable, in early apoptosis, late apoptosis and necrosis ± SEM, treated with different concentrations of MM4, MM5 and MM6 for 18, 24 and 48 hours.

Mean percentage[1] of Jurkat cells still viable, in early apoptosis, late apoptosis and necrosis ± SEM, treated with different concentrations of MM4, MM5 and MM6 for 18, 24 and 48 hours.

	MM4 0.337 (µM)	MM4 0.674 (µM)	MM5 0.261 (µM)	MM5 0.522 (µM)	MM6 0.369 (µM)	MM6 0.738 (µM)
% Viable cells 18 hours	90.69 *[2] ± 1.32	77.67 ± 3.72	91.88 * ± 1.38	87.52 ± 3.28	79.53 * ± 2.86	52.13** ± 6.47
% Early apoptosis	2.99 ± 0.74	2.89 ± 0.90	2.04 ± 0.40	4.05 ± 1.30	4.65 ± 1.35	3.85 ± 0.71
% Late Apoptosis	3.02 ± 0.54	10.72 ** ± 2.03	3.23 * ± 0.51	3.93 ± 0.97	7.52 ** ± 1.03	16.72** ± 3.94
% Necrosis	1.94 ** ± 0.32	7.22 ** ± 1.57	2.17 ± 0.76	2.38 * ± 0.59	5.46 ** ± 0.99	21.79** ± 3.48
% Viable cells 24 hours	90.09 ** ± 1.10	69.65 ** ± 5.67	90.46 * ± 2.16	80.64 ± 8.83	77.17 ** ± 3.37	34.97*** ± 8.12
% Early Apoptosis	2.58 ± 0.51	2.43 ± 0.46	3.03 ± 0.51	2.60 ± 0.23	2.28 ± 0.21	3.80 ± 1.24
% Late Apoptosis	4.08 ** ± 0.55	15.96 ± 2.33	3.17 * ± 0.87	7.49 ± 3.27	11.82 ** ± 1.77	23.98** ± 4.84
% Necrosis	2.49 ** ± 0.55	11.15 * ± 3.13	2.33 ± 0.93	8.04 ± 5.46	7.73 ** ± 1.84	36.41** ± 9.30
% Viable cells 48 hours	90.45 * ± 1.58	47.58 ** ± 10.87	90.20 ** ± 1.52	75.28 ± 13.74	70.69 ** ± 2.24	11.05*** ± 2.34
% Early Apoptosis	3.11 ** ± 0.69	1.99 ± 0.18	3.81 ± 0.77	3.20 * ± 0.88	3.15 ± 0.62	1.10 ** ± 0.29
% Late Apoptosis	4.09 ± 1.41	19.88 ** ± 3.41	2.37 * ± 0.19	5.95 ± 2.02	14.92 * ± 4.12	24.36*** ± 3.85
% Necrosis	3.20 * ± 0.71	36.08 * ± 9.80	2.47 ± 1.01	15.37 ± 12.5	16.44 ** ± 3.14	63.83*** ± 5.42

(1) Mean of 7 independent experiments.

(2) Significance was determined by the Student's t-test for paired values. * $p < 0.01$; ** $p < 0.001$ and *** $p < 0.0001$ compared to the untreated control.

Discussion

Jurkat T leukemia cells are a well known model system for apoptosis, since they are vulnerable to diverse stimuli, such as death ligands and conventional chemotherapeutic drugs like cisplatin and camptothecin (Wang *et al*., 2006). Jurkat T leukemia cells were selected for this study on these grounds.

$[Au(dppe)_2]Cl$ induced apoptosis in Jurkat cells at both the concentrations that were used, with more effect at the higher concentration of 0.314 µM. Cisplatin's effects were limited, but the indication is that apoptosis was induced. MM4 had very little effect at the lower concentration, but at the higher concentration indications are that apoptosis was induced. MM5 at the concentration of 0.261 µM had no effect on the Jurkat cells during the 48 hour incubation period. The higher concentration did have an effect on the cells, but it seems that necrosis was more indicative than apoptosis. MM6 had very clear apoptotic effects at both the concentrations tested, more so with the higher concentration.

A critical point for the quantization of apoptosis is that, irrespective of the initiating insult, the time course of apoptosis is very fast. The clearance of the resultant debris (either by 'professional' phagocytes or bystander (amateur) phagocytes) is rapid. Reports of clearance times of 1 hour and less are considered typical (Hall, 1999). This might explain the lack of great differences in early and late apoptosis observed in this study.

Because of the rapid nature of apoptosis it means that in any static analysis, a very small number of apoptotic cells observed at any given instant might in fact, reflect a very considerable contribution to cell turnover (Hall, 1999).

Stage 2

Chapter 7: Cell cycle

7.1 Introduction

The cell cycle is the most fundamental process that occurs in the eukariotic cells and is quite literally a matter of life and death. The cell cycle is an ordered set of events culminating in cell division into two daughter cells. Non-dividing cells exists outside the cell cycle in G_0. The phases of the cell cycle are designated G_1, S, G_2 and M. In G_1 (gap 1) cells increase in size, produce RNA and synthesize protein. In S (synthesis) DNA replication occurs to produce DNA ready for cell division. In G_2 (gap 2) cells continue to grow and produce new proteins. In M (mitosis) cell growth and protein production stop, and each cell undergoes a complex and orderly division into two daughter cells (Thomas and Goodyer, 2003).

Figure 7.1: Cell cycle and its phases (Golias *et al*., 2004).

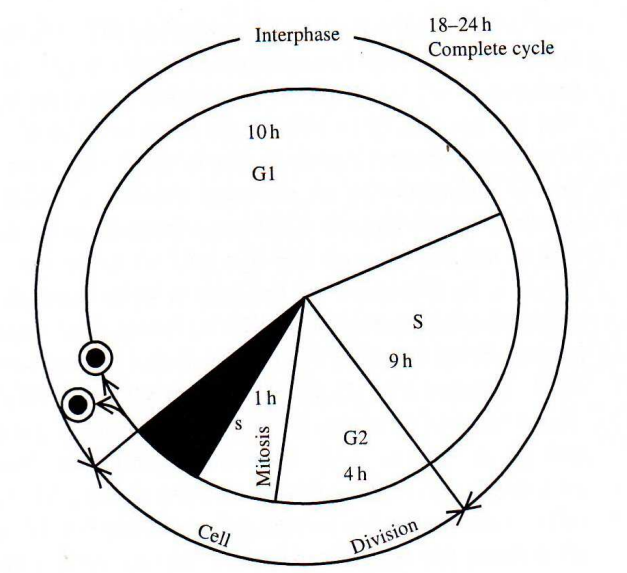

Different cells have various methods of regulating the cell cycle. Modulating the expression of growth-related and cycle-regulating genes is one such method. In different cells, the same gene could be regulated at different levels. Another important regulatory system is the control of critical steps in the cell cycle, which are called checkpoints. Before passing through these checkpoints, the integrity of the genome and the proper operation of the cell cycle regulatory component must be controlled. At these steps, a cell determines whether to progress into the next step and to divide, to leave the cell cycle and become quiescent, or to undergo apoptosis (Tonini *et al*., 2002). There is a lot of experimental and clinical evidence supporting the notion that the cell cycle machinery is commonly targeted on oncogenesis. While numerous cell cycle regulators qualify as proto-oncogenes or tumour suppressors and their aberrations may provide direct proliferative advantage to cancer cells, defects in checkpoint mechanisms act more indirectly yet affect both tumour progression and response to anticancer therapy (Bartek *et al*., 1999).

The cell cycle in eukaryotes is regulated by cyclin-dependant kinases. T cyclins, members of the cell regulator family, bind to and activate cyclin-dependant kinases. Sequential formation, activation and subsequent inactivation of cyclins and cyclin-dependant kinases are critical for the control of the cell cycle (Park *et al*., 2002). Cell cycle is inhibited by brake molecules termed cyclin-dependant kinase inhibitors. Successful transformation and unchecked cell proliferation appears to require the co-ordinated up-regulation of cyclin-dependant kinases and/or the suppression of cyclin-dependant kinase inhibitors (Dobashi, 2005).

Uncontrolled proliferation is a hallmark of cancer cells. Molecular analysis of human tumours and animal models has provided a clear basis for the understanding of the cellular processes that govern cell cycle progression, in normal and tumour cells. Many cell cycle regulators controlling the correct entry and progression through the cell cycle are altered in tumours. Most, if not all, human cancers show a deregulated control of G_1 phase progression. Human neoplasms develop following the progressive accumulation of genetic and epigenetic alterations to oncogenes and tumour-suppressor genes. Such

genes positively controlling cell cycle checkpoints can be targets for oncogenic activation in cancer, whereas negative regulators such as tumour-suppressor genes are targeted for inactivation (Golias *et al*., 2004).

Oncogenes and tumour suppressor genes are involved with some aspect of mitogenic signal transduction or checkpoint control. Mitogenic signal transduction involves numerous recognized oncoproteins, including the extracellularly secreted growth factors, growth factor receptors, cytoplasmic signal transduction cascades and transcription factors. These oncoproteins, in a normal cell, carry a signal from the cell surface to the nucleus with the end result being transcription and initiation of the cell cycle. In transformed cells, these signal transduction pathways are always "turned on" or their inhibitory mechanisms are "turned off" (Schafer, 1998). Transformed cell lines often carry defects in one or more proteins that regulate cell cycle, and therefore can be used as a model to study how cell cycle controls cell death (Zhu and Anasetti, 1995).

Chromosomal DNA replication occurs during S phase. Although the length of the S phase can vary significantly between different cell types, several absolute controls exist that dictate when and how many times in a cell cycle DNA replication can occur. Chromosomes must be duplicated only once in each cell cycle. This implies that once chromosomes have replicated, the cell must first pass through mitosis before it can re-replicate its DNA again. The emerging picture is one of tight interdependency between the S phase and M phase. S-M control ensures that the general cell cycle events are maintained in the correct order and that genome transmission occurs faithfully from generation to generation (Dalton, 1998).

7.2 Aim

The aim of this study was to determine whether $[Au(dppe)_2]Cl$, cisplatin, MM4, MM5 and MM6 have an effect on the cell cycle of Jurkat cells.

7.3 Materials and methods

7.3.1 Reagents

i. Ribonuclease A (from bovine pancreas)

Ribonuclease A, cat no R 4875, was supplied by Sigma (St Louis, USA). 2 mg was dissolved in 1 ml 1.12% w/v sodium citrate. Solution was made up immediately prior to use.

ii. . Propidium iodide

Propidium iodide, cat no P-4170, was supplied by Sigma (St Louis, USA). 5 mg was dissolved in 100 ml 1.12% w/v sodium citrate. Solution was stored at 4ºC and care was taken to keep it in the dark.

iii. PBS

Phosphate buffered saline, cat no 211248, was supplied by The Scientific Group (Johannesburg, RSA). 9.23 g was dissolved in 1 liter de-ionized water and stored at 4 ºC.

iv. Ethanol

99.9% pure ethanol was supplied by Radchem (Brackendowns, RSA) and used undiluted.

v. Sodium citrate

Sodium citrate, cat no 6435, was supplied by Merck (Darmstadt, Germany). A 1.12% w/v solution was made up and stored at 4ºC.

7.3.2 Method

A standard flow cytometric method with propidium iodide (PI) was used. Cell cycle analysis was performed using flow cytometric evaluation of DNA content. PI fluorescence as an indicator of relative DNA content per cell was measured by flow

cytometry. The percentages of cells in G_1, S and G_2/M phases were estimated from the DNA content histogram obtained from each cell sample using a computer software program (Scott *et al*., 2004).

$[Au(dppe)_2]Cl$, cisplatin, MM4, MM5 and MM6 were tested to determine whether they induce cell cycle changes in Jurkat cells.

Concentrations equal to the IC_{50} value and double the IC_{50} value of the experimental compounds were used.

Cell concentration that was used: 3×10^5 cells per ml.

Cells were counted and made up to 3×10^5 cells per ml in RPMI supplemented with 10% FCS as described in **Chapter 3**.

Experiments were set up in 75 cm^3 tissue culture flasks.

i. Untreated cell suspensions (untreated control)

45 ml cell suspension

5 ml tissue culture medium supplemented with 10% bovine FCS.

ii. Cell suspensions treated with experimental compounds

45 ml cell suspension

5 ml of the experimental compounds diluted to the concentrations described in **Table 7.1** and **Table 7.2** in RPMI supplemented with 10% bovine FCS.

Cell suspensions were incubated at least 1 hour at 37°C and in an atmosphere of 5% CO_2 before the experimental compounds were added.

Cell suspensions were incubated with the experimental compounds for 18, 24 and 48 hours at 37°C and in an atmosphere of 5% CO_2 in tissue culture flasks.

15 ml of the cell suspension was decanted from culture flasks at the set times and centrifuged for 5 minutes at 200G. Cells were re-suspended in 500 µl PBS and chilled well on ice. Flow cytometer tubes were prepared, each tube containing 500 µl of ice-cold 100% ethanol. The cold cell suspension was pipetted rapidly into the cold ethanol and mixed by forcing air bubbles through the suspension with a pipette. The cell suspension was kept on ice for 15 minutes and stored sealed in this state in the fridge until analyzed. The cell suspension was centrifuged for 3 minutes at 300G and the supernatant removed carefully with a Pasteur pipette. 125 µl RNAse (2mg/ml 1.12% w/v sodium citrate) was added to each tube and mixed well. The cell suspension with RNAse was incubated at 37°C for 15 minutes in a water bath. 125 µl PI was added to each tube and mixed well. Samples were allowed to stand at room temperature in the dark for at least 30 minutes before analyzing.

A Cytomics FC 500 series Beckman Coulter flow cytometer was used. The Multi-cycle for Windows program was used to calculate the results from the raw data obtained on the flow cytometer.

7.4 Results

Results are expressed as the mean percentage of cells in the different phases of the cell cycle ± SEM. Each value represents the mean of 8 independent experiments. The Student's t-test for paired values was used for the statistical analysis of the data.

Table 7.1 represents the mean percentages of cells in G_1, S and G_2/M phases of the cell cycle ± SEM of Jurkat cells treated with different concentrations of $[Au(dppe)_2]Cl$ and cisplatin for 18, 24 and 48 hours.

This table shows that the untreated control did not show major differences over 18, 24 and 48 hours in the different phases of the cell cycle. G_1 phase fluctuated from 60.55% ± 1.04 at 18 hours to 54.48% ± 2.05 at 24 hours and 52.32% ± 1.42 at 48 hours.

$[Au(dppe)_2]Cl$ showed a significant increase in the percentage of cells arrested in G_1 phase at 18 and 24 hours at both the concentrations tested. This effect was totally lost at 48 hours where the percentage cells in G_1 phase are equal to those of the control. The percentage of cells in the S phase decreased significantly at both the lower and the higher concentrations of $[Au(dppe)_2]Cl$ compared to the control at time 18 hours. The same was found at time 24 hours. At time 48 hours an increase was found in the percentage of cells in the S phase but only significantly so at the higher concentration of 0.314 µM. The percentage of cells in G_2/M phase showed no change compared to the control at time 18 hours, but at 24 hours there was a significant decrease in the percentage of cells at both the concentrations in this phase. The same trend was found for both concentrations at time 48 hours with a decrease in the percentage of cells in G_2/M phase. From these results it seems as if $[Au(dppe)_2]Cl$ arrests the cell cycle in the G_1 phase.

Cisplatin decreased the percentage of cells in the G_1 phase significantly at both the concentrations tested and at all three the time intervals used. The percentage cells in the S phase increased significantly at time 18 and 24 hours but decreased at time 48 hours. The decrease at 48 hours was only significant at the lower concentration of 0.707 µM. The percentage cells in G_2/M phase did not show significant changes at time 18 and 24 hours, but doubled at 48 hours for the lower concentration of 0.707 µM and quadrupled for the higher concentration of 1.414 µM when compared to the control. These results indicate that cisplatin arrests the cell cycle of Jurkat cells in the S phase of their cell cycle.

Table 7.2 represents the mean percentages of cells in G_1, S and G_2/M phases of the cell cycle ± SEM of Jurkat cells treated with different concentrations of MM4, MM5 and MM6 for 18, 24 and 48 hours.

This table shows that the percentage of cells in G_1 phase in the Jurkat cells treated with MM4 showed no change (both concentrations) at time 18 hours compared to the control. At time 24 hours, however, a significant increase is seen for both the concentrations tested. The percentage cells in G_1 phase at 48 hours also show an increase but only

significantly at the higher concentration of 0.674 µM. The S phase at time 18 hours indicates a significant decrease in the percentage of cells at the higher concentration, while there is a significant decrease at time 24 hours for both the concentrations tested. At time 48 hours only the higher concentration shows a significant decrease in the percentage of cells in the S phase. No significant effect was observed in the percentage of cells in the G_2/M phase at the concentration of 0.337 µM at time 18 hours, while the higher concentration showed a significant increase. At time 24 and 48 hours no significant effect was recorded in the percentage cells in G_2/M phase for either the concentrations of MM4 that were tested. These results indicate a G_1 arrest at 24 hours, but overall this compound does not induce major changes in the cell cycle of Jurkat cells.

MM5 induced an increase in the percentage of cells in G_1 phase significantly at both concentrations tested and at time 18, 24 and 48 hours. The percentage of Jurkat cells in the S phase of their cell cycle decreased significantly at the higher and the lower concentrations tested and also at all the time intervals tested. At time 18 hours a significant increase is seen in the percentage cells in G_2/M phase at the lower concentration of 0.261 µM. The percentage of Jurkat cells in G_2/M phase at 24 hours decreased significantly at both the concentrations tested. No significant changes were observed in G_2/M phase for either the concentrations at time 48 hours. The results obtained for MM5 strongly indicates that this compound also arrests the cell cycle of Jurkat cells in the G_1 phase as did $[Au(dppe)_2]Cl$.

MM6 showed contrasting effects on the cell cycle of Jurkat cells at the two concentrations that were tested. The higher concentration of 0.739 µM had opposite effects than those observed at the lower concentration of 0.369 µM. At 18 hours the lower concentration the percentage of cells in G_1 phase increased significantly, while the percentage cells in S phase decreased significantly. No significant increase of percentage G_2/M cells was observed. At the higher concentration the percentage of cells in G_1 phase decreased significantly, while the percentage cells in S phase increased significantly. No significant increase of percentage G_2/M cells was observed for either the concentrations that were tested. At 24 hours the lower concentration followed the same trend as at 18

hours, a significant increase in the percentage G_1 cells with an accompanying decrease in the percentage S phase cells. The higher concentration of 0.739 µM showed a decrease in both the percentage G_1 and S phase cells. No significant increase of percentage G_2/M cells was observed for the lower concentration, but a significant increase was found at the higher concentration. At 48 hours 0.369 µM showed a significant increase in the percentage G_1 cells with a significant decrease in the percentage S phase cells. No significant decrease of percentage cells in G_2/M phase was found. At 48 hours 0.739 µM showed a significant decrease in the percentage G_1 cells and an increase in the percentage cells in the S phase. A significant increase in the percentage of cells in the G_2/M phase was observed. From these results it would seem that MM6 arrests the cell cycle of Jurkat cells in the G_1 phase at the lower concentration and in the S phase at the higher concentration.

Table 7.1: The mean percentages of cells in G_1, S and G_2/M phases of the cell cycle ± SEM of Jurkat cells treated with different concentrations of $[Au(dppe)_2]Cl$ and cisplatin for 18, 24 and 48 hours.

Mean percentages[1] of cells in G_1, S and G_2/M phases of the cell cycle ± SEM of Jurkat cells treated with different concentrations of $[Au(dppe)_2]Cl$ and cisplatin for 18, 24 and 48 hours.

	Control	$[Au(dppe)_2]Cl$ 0.157 (µM)	$[Au(dppe)_2]Cl$ 0.314 (µM)	Cisplatin 0.707 (µM)	Cisplatin 1.414 (µM)
% cells in G_1 18 hours	60.55 ± 1.19	66.05 ***[2] ± 1.04	69.03 *** ± 0.61	53.705 *** ± 1.99	51.89 *** ± 1.90
% cells in S	28.20 ± 1.24	22.74 *** ± 1.13	19.98 *** ± 0.66	33.54 *** ± 1.83	34.56 *** ± 1.85
% cells in G_2/M	11.25 ± 0.31	11.21 ± 0.62	10.99 ± 0.54	12.76 ± 0.72	13.55 ± 0.77
% cells in G_1 24 hours	54.48 ± 2.05	63.052 *** ± 1.59	67.31 *** ± 0.82	47.29 *** ± 2.25	46.04 *** ± 2.55
% cells in S	36.27 ± 1.59	28.93 *** ± 1.30	25.34 *** ± 0.89	41.86 *** ± 1.95	42.786 *** ± 2.30
% cells in G_2/M	11.26 ± 0.70	8.021 *** ± 0.46	7.35 *** ± 0.151	10.849 *** ± 0.63	11.637 *** ± 0.85
% cells in G_1 48 hours	52.32 ± 1.42	52.81 ± 1.52	51.36 ± 1.29	38.95 ± 2.85	24.06 ± 4.34
% cells in S	31.58 ± 1.46	34.53 ± 2.43	36.52 * ± 1.44	26.95 * ± 0.74	30.19 ± 1.75
% cells in G_2/M	15.43 ± 0.95	11.68 * ± 1.55	11.36 ** ± 0.900	31.37 * ± 3.84	45.65 ** ± 3.40

(1) Mean of 8 independent experiments.

(2) Significance was determined by the Student's t-test for paired values. * $p < 0.01$; ** $p < 0.001$ and *** $p < 0.0001$ compared to the untreated control.

Table 7.2: The mean percentages of cells in G_1, S and G_2/M phases of the cell cycle ± SEM of Jurkat cells treated with different concentrations of MM4, MM5 and MM6 for 18, 24 and 48 hours.

Mean percentages(1) of cells in G_1, S and G_2/M phases of the cell cycle ± SEM of Jurkat cells treated with different concentrations of MM4, MM5 and MM6 for 18, 24 and 48 hours.

	MM4 0.337 (µM)	**MM4 0.674 (µM)**	**MM5 0.261 (µM)**	**MM5 0.522 (µM)**	**MM6 0.369 (µM)**	**MM6 0.739 (µM)**
% cells in G_1 18 hours	61.60 ± 0.70	62.28 ± 1.51	63.76 **(2) ± 0.85	65.46 ** ± 1.53	63.11* ± 1.26	54.30 * ± 1.92
% cells in S	25.48 ± 1.02	24.30 ** ± 1.40	24.161 *** ± 0.86	22.28 *** ± 0.84	23.90 ** ± 1.27	32.15 * ± 1.21
% cells in G_2/M	12.92 ± 0.86	13.42 * ± 1.11	12.083 * ± 0.28	12.27 ± 1.19	12.99 ± 1.11	13.55 ± 1.3
% cells in G_1 24 hours	63.31 ** ± 0.81	64.031 ** ± 1.69	61.80 ** ± 1.13	66.51 *** ± 1.17	65.99 *** ± 1.41	52.90 ± 2.17
% cells in S	26.47 *** ± 0.77	23.86 *** ± 0.72	28.26 ** ± 0.90	23.05 *** ± 0.97	23.69 *** ± 0.71	30.87 ± 1.55
% cells in G_2/M	10.22 ± 0.71	11.64 ± 1.80	9.94 * ± 0.31	10.44 ± 0.50	11.48 ± 1.04	16.19 * ± 1.37
% cells in G_1 48 hours	56.71 ± 1.74	56.87 * ± 2.07	56.16 * ± 0.94	59.97 ** ± 1.66	60.81 * ± 2.64	45.17 * ± 3.52
% cells in S	28.33 ± 1.38	25.80 ** ± 0.74	27.95 * ± 0.48	26.17 ** ± 0.73	24.57 * ± 1.53	31.22 ± 5.99
% cells in G_2/M	14.612 ± 0.82	14.91 ± 2.06	15.15 ± 1.21	13.62 ± 1.15	14.66 ± 1.97	22.32 * ± 2.71

(1) Mean of 8 independent experiments.

(2) Significance was determined by the Student's t-test for paired values. * $p < 0.01$; ** $p < 0.001$ and *** $p < 0.0001$ compared to the untreated control.

7.5 **Discussion**

The cell cycle is of key importance to many areas of drug discovery. On the one hand this fundamental process provides the opportunity to discover new targets for anti-cancer agents and improved chemotherapeutics, but on the other hand drugs and targets in other therapeutic areas must be tested for undesirable effects on the cell cycle (Thomas and Goodyer, 2003).

As already mentioned in **Chapter** 6 Jurkat T leukemia cells are a well known model system for apoptosis, since they are vulnerable to diverse stimuli, such as death ligands and conventional chemotherapeutic drugs like cisplatin and camptothecin (Wang *et al.*, 2006). It was therefore decided to use Jurkat cells for this part of the study as well to determine whether MM4, MM5 and MM6 had any effect on the cell cycle of these cells compared to $[Au(dppe)_2]Cl$ and cisplatin.

$[Au(dppe)_2]Cl$, cisplatin, MM4, MM5 and MM6 (0.369µM) arrested the cell cycle in the G_1 phase. MM6 at the higher concentration of 0.739 µM arrested the cell cycle in the S phase. The difference between the percentages of the different phases and their controls are not very significant. A possible reason for this might be because the cells used in this study were not synchronized and this can explain why there were still a lot of cells in the other phases of the cell cycle. Another possible reason can be that the incubation time for these experiments was only one cell cycle (48 hours) and a more profound result might have been obtained with a longer incubation period. A longer incubation time was not tried because of the toxicity of these compounds.

Cisplatin increases the ratio between the sensitivity of tumour cells versus normal cells to ionizing radiation which greatly improve cancer treatment. One of the methods of radio sensitization of tumour cells is the concomitant application of chemotherapeutic agents that alter DNA sensitivity to irradiation. Cisplatin appears (like other platinum – based anti-cancer drugs) to be an excellent radio-sensitizer (Garmuszek *et al.*, 2002).

Stage 3

Chapter 8: *In vitro* radioactive labeled drug uptake

8.1 Introduction

The field of oncology has undergone a revolution in drug discovery and therapeutic approaches led primarily through an increased understanding of genetic and molecular mechanisms in cancer evolution. Correspondingly, the previously held empirical random screening method in oncological drug development is being gradually replaced with the concept of rational drug design. This process identifies specific targets responsible for malignant cellular transformation and more importantly, drugs that can overcome them, rather than to simply using the anti-proliferative activity of a drug as an endpoint. New agents discovered for possible use as anti-cancer therapy include genes, proteins, growth factors and receptors, and those involved in specific pathways, for example, angiogenesis, signal transduction, cell cycle, cell apoptosis, invasion, metastasis, drug resistance and blood flow. There is a need for an additional method of evaluating potential new drugs and to optimize existing treatment strategies (Gupta *et al*., 2002).

Radioisotopes have proven to be an indispensable tool in biomedical research and have played a pivotal role in the investigation of absorption, distribution, metabolism and excretion properties of new chemical entities over the past several decades. The main advantage of using radioisotopes in studying the disposition of new drug candidates is the ease of detection and the achievement of high sensitivity, especially when compounds with high specific activity are used (Dalvie, 2000).

Kinetic studies using radio labeled drug are extremely sensitive for detecting alterations in drug efflux and accumulation but does not provide information on the intracellular distribution of drug (Breuninger *et al*., 1995).

Previous studies have indicated that $[Au(dppe)_2]Cl$ exhibits anti-tumour activity in a wide range of tumour models in mice. The lipophilic cationic properties of this compound promoted its non-selective uptake into the mitochondria of cells. Hence, strategies were adopted to synthesize more hydrophilic analogues that would retain their anti-tumour activity, while being less toxic to the mitochondria of normal cells (Berners-Price *et al*., 1986).

The effect of some anti-tumour agents is related to the extent of their penetration into and their accumulation and retention within tumour cells. The acquired resistance of tumour cells to some agents, a crucial problem in cancer chemotherapy, is also related to intra-cellular drug accumulation and retention (Tsuruo *et al*., 1982). Resistance in cells was associated with decreased drug accumulation and enhanced drug efflux and/or reduced intracellular drug binding (Nakagawa *et al*., 1992). Drug accumulation in cells can be easily determined with radio labeled compounds.

8.2 Aim

To compare drug uptake of MM5 and MM6 labeled with ^{198}Au *in vitro* with $[^{198}Au(dppe)_2]Cl$, using a cisplatin sensitive ovarian cancer cell line (A2780) and its cisplatin resistant subline (A2780 Cis).

8.3 Materials and methods

8.3.1 Reagents

i. PBS

Phosphate buffered saline, cat no 211248, was supplied by The Scientific Group (Johannesburg, RSA). 9.23 g was dissolved in 1 liter de-ionized water and stored at 4 ºC.

ii. Preparation of ^{198}Au labeled [Au(dppe)$_2$]Cl, MM5 and MM6 (This procedure was done at NECSA).

[Au(dppe)$_2$]Cl, and the selected compounds were labeled with ^{198}Au by NECSA (Nuclear Energy Corporation of South Africa).

Irradiation of Au-metal

The radioactive experiment was done using 41.9 mg activated Au and 30.5 mg cold Au for the synthesis ClAuTHT. ClAuTHT will be precursor for the three Au-complexes. The Au was activated for 10 minutes in the hydraulic B-position.

Experimental procedure

1a) Au(s) + HCl + HNO_3 → $HAuCl_4.4H_2O$ (Day 1)

41.9 mg activated Au and 30.5 mg cold Au (0.368 mmol) was added to a 10 ml vial (V1) followed by 680 µl HCl/HNO_3 (3:1; bubbled with Ar). 18.15 mCi was read on the Capintec (Au-198 calibration factor = 149). It was placed inside a lead pot on the hotplate at 45°C while it was stirred and covered with a test tube (serving as a watch glass) to minimize evaporation of the acid. This step took approximately 2 hours. The aqueous part was evaporated by increasing the temperature to 50°C while blowing argon (Ar) into the vial. The yellow residue was washed with 650 µl HCl followed by 650 µl H_2O and dried at 50°C after each addition (each drying process took 45-60 minutes). The product activity was 19.2 mCi and a 100% yield was assumed.

1b) $HAuCl_4.4H_2O$ + 2 THT → ClAuTHT (Day 1 and 2)

The product in vial 1 was dissolved in 900 µl EtOH/H_2O (5:1). The solution was filtered through a Millex GP 0.22 µm filter into vial 2 to ensure that all un-dissolved particles were removed. The filter was rinsed three times with additional EtOH/H_2O which was also collected in vial 2. The solution was evaporated under Ar to ± 1000 µl (60 minutes).

The vial was sealed and an Ar needle inserted which was followed by the vent-needle. A 1 ml syringe was rinsed three times with Ar from the vial before taking 600 µl THT (10 times excess). Ar was blown over THT before extracting the solution. This was added drop wise to vial 2. The solution was stirred 15 minutes, before the vial was opened and the white precipitate filtrated. The fluid was removed with a syringe (long needle) while under Ar. The precipitate was washed twice with 500 µl EtOH (bubbled with Ar) and filtrated. The same procedure was followed as described earlier; with a syringe (some activity is lost because of the syringe). The precipitate was dried with water vacuum for 60 minutes and dissolved in a minimum volume of ± 7.4 ml chloroform (calculated as 12.3 mg/ml $CHCl_3$). This solution was divided into three different vials designated for $ClAu(dppe)_2$, $Au(dpmaa)_2Cl.2SnBu2$ (MM5) and $Au(dpmaa)_2Cl.SnBu2$ (MM6).

2a) Cl AuTHT + 2 dppe → $ClAu(dppe)_2$– Day 2

2.93 µl Cl AuTHT (= 3.6 mg; 0.0111 mmol) was evaporated (10 minutes). 1.0 ml THF (bubbled with Ar) was added to 0.0222 mmol dppe (8.84 mg) in a separate vial (under Ar). This solution was added to vial 2.1 containing the dried $AuTHTCl_2$ (under Ar) and stirred. A precipitate was formed at 7 minutes and the reaction continued for 15 minutes. The white precipitate was dried in a vacuum for 30 minutes.

2b) 2 x Bu2Sn (O,O-dpmaa) + Cl AuTHT → $Au(dpmaa)_2Cl.2SnBu2$ (MM5)

179 µl Cl AuTHT (= 2.2 mg, 0.007 mmol) was evaporated (10 minutes). 0.5 ml THF (bubbled with Ar) was added to 9.83 mg Bu2Sn (O,O-dpmaa) (0.014 mmol) in a separate vial (under Ar). This solution was added to vial 2.2 containing the dried $AuTHTCl_2$

(under Ar) and stirred. A deep yellow-orange precipitate was formed and the reaction took 15 minutes. The yellow-orange precipitate was dried in a vacuum for 30 minutes.

2c) dpmaa + Bu2Sn (O,O-dpmaa) + Cl AuTHT → $Au(dpmaa)_2Cl.SnBu2$ (MM6)

131 µl Cl AuTHT (=1.61 mg; 0.005 mmol) was evaporated (10 minutes). 0.5 ml THF (bubbled with Ar) was added to 0.005 mmol Bu2Sn (O,O-dpmaa) (3.6 mg) and 0.005 mmol dpmaa (3.13mg) in a separate vial (under Ar). This solution was added to vial 2.3 with dried $AuTHTCl_2$ (under Ar) and stirred. A light cream yellow precipitate was formed and the reaction took 15 minutes. The precipitate was dried in a vacuum for 30 minutes.

Preparation of ^{198}Au labeled experimental compounds (the day of experiment).

i. $[Au(dppe)_2]Cl$

Molecular weight: 1028 g/mol

A 10 mM stock solution was prepared by dissolving 10.28 mg of the compound in 1 ml DMSO. Dilutions (1, 5 and 10 µM) were done in RPMI medium supplemented with 10 % bovine FCS just prior to the experiment.

ii. $(Bu_2Sn)_2Audpmaa$ (MM5)

Molecular weight: 1661.85 g/mol

A 10 mM stock solution was prepared by dissolving 16.62 mg of the compound in 1 ml DMSO. Dilutions (1, 5 and 10 µM) were done in RPMI medium supplemented with 10 % bovine FCS just prior to the experiment.

iii. $Bu_2SnAudpmaa$ (MM6)

Molecular weight: 1432.2 g/mol

A 10 mM stock solution was prepared by dissolving 14.32 mg of the compound in 1 ml DMSO. Dilutions (1, 5 and 10 µM) were done in RPMI medium supplemented with 10 % bovine FCS just prior to the experiment.

8.3.1 Method

A standard method to measure drug uptake in cancer cells was used. Cellular uptake of the drugs was measured in RPMI supplemented with 10 % bovine FCS (Tsuruo *et al*., 1982).

A2780 and A2780 cis cell cultures were used. Two sets of gloves were used and gold jewelry was removed as a safety measure. Experiments were carried out in a registered radioactive laboratory and applicable safety measures were adhered to.

Cells were trypsinized, counted and made up to a final concentration of $5x10^6$ cells/ml. RPMI supplemented with 10 % FCS was used to make the dilutions. Concentrations of 1, 5 and 10 µM were used for each of the experimental compounds.

5 ml polypropylene tubes with screw tops were used for these experiments.

900 µl of cell suspension (both cell lines) and 100 µl of each of the concentrations of the experimental compounds were incubated for 1 hour at 37°C and in an atmosphere with 5% CO_2. Cell suspensions were centrifuged at 800G for 5 minutes; supernatant removed and transferred to clean labeled tubes. Cells were washed with PBS and centrifuged at 800G for 5 minutes. PBS was removed and transferred to clean labeled tubes. Cells, supernatant and PBS were counted separately on a gamma counter. Each sample was counted for 1 minute. A Packard Cobra II Auto Gamma counter was used.

8.4 Results

The results are expressed as mean Becquerel (Bq)/total ± SEM. 1 Becquerel = amount of material which will produce 1 nuclear decay per second. Each value represents the mean of 6 independent experiments.

Table 8.1 represents the mean percentage of uptake of ^{198}Au-labeled $[Au(dppe)_2]Cl$, MM5 and MM6 ± SEM in A2780 and A2780 cis cells after treatment with different concentrations for 1 hour.

This table shows that $[Au(dppe)_2]Cl$ had the best uptake by the A2780 (cisplatin sensitive) cells at the lowest concentration of 1 mM. 45.74% ± 4.4 $[Au(dppe)_2]Cl$ was taken up. 32.59% ± 3.44 and 33.95% ± 2.64 was taken up by the A2780 cells at the concentrations of 5 and 10 mM respectively. Drug uptake of $[Au(dppe)_2]Cl$ by the A2780 cis (cisplatin resistant) cells was considerably lower. Only 13.92% ± 0.93 was taken up by these cells at the concentration of 1 mM and at 5 and 10 mM, 23.66% ± 2.55 and 26.25% ± 1.97 was taken up respectively. $[Au(dppe)_2]Cl$ was taken up the best at the lowest concentration of 1mM by both the cell lines tested. On average 32.43% $[Au(dppe)_2]Cl$ was taken up by the A2780 cells and an average of only 21.28 % by the A2780 cis cells.

MM5 was not taken up well by either of the 2 cell lines tested. 5.04% ± 0.73 was taken up by the A2780 cells at the concentration of 1mM. The percentage uptake was even lower at 5 and 10 mM with 4.14% ± 0.38 and 3.77% ± 0.26 respectively. MM5 showed only 2.99% ± 0.38 uptake by the A2780 cis cells at the lowest concentration of 1 mM. At 5 mM only 1.4% ± 0.11 was taken up and at 10 mM, 1.50% ± 0.14. An average of 4.32% of MM5 was taken up by the A2780 cells and an average of 1.96% was taken up by the A2780 cis cells. The uptake of MM5 was considerably less than what was found for $[Au(dppe)_2]Cl$ on the 2 cell lines tested.

MM6 was also not taken up well by the 2 cell lines tested. 3.01% ± 0.33 was taken up at concentration 1mM by A2780 cells and 2.12% ± 0.23 at concentration 5mM. At concentration 10 mM only 1.66 % ± 0.27 of MM6 was taken up by the A2780 cells. 2.76% ± 0.45 of MM6 was taken up by the A2780 cis cells at the lowest concentration of 1mM. At 5 and 10 mM, 0.80% ± 0.13 and 0.94% ± 0.03 was taken up respectively. An average of 2.26% of MM6 was taken up by the A2780 cells and an average of only 1.5% was taken up by the A2780 cis cells.

Figure 8.1 and 8.2 represents the mean Bq/total ± SEM ^{198}Au labeled $[Au(dppe)_2]Cl$ taken up by A2780 and A2780 cis cells respectively. Cells were incubated for 1 hour with 1, 5 and 10 µM of the experimental compounds. Each Value represents the mean of 6 independent experiments.

Figure 8.3 and 8.4 represents the mean Bq/total ± SEM ^{198}Au labeled MM5 taken up by A2780 and A2780 cis cells respectively. Cells were incubated for 1 hour with 1, 5 and 10 µM of the experimental compounds. Each Value represents the mean of 6 independent experiments.

Figure 8.5 and 8.6 represents the mean Bq/total ± SEM ^{198}Au labeled MM6 taken up by A2780 and A2780 cis cells respectively. Cells were incubated for 1 hour with 1, 5 and 10 µM of the experimental compounds. Each Value represents the mean of 6 independent experiments.

Table 8.1: The mean percentage of uptake of ^{198}Au-labeled [Au(dppe)$_2$]Cl, MM5 and MM6 ± SEM in A2780 and A2780 cis cells after treatment with different concentrations for 1 hour.

Mean percentage(1) of uptake of ^{198}Au-labeled [Au(dppe)$_2$]Cl, MM5 and MM6 ± SEM in A2780 and A2780 cis cells after treatment with different concentrations for 1 hour.

Drug	Concentration	% Uptake A2780 ± SEM	% Uptake A2780 cis ± SEM
[Au(dppe)$_2$]Cl	1 mM	45.74 ± 4.4	13.92 ± 0.93
[Au(dppe)$_2$]Cl	5 mM	32.59 ± 3.44	23.66 ± 2.55
[Au(dppe)$_2$]Cl	10 mM	33.95 ± 2.64	26.25 ± 1.97
MM5	1 mM	5.04 ± 0.73	2.99 ± 0.38
MM5	5 mM	4.14 ± 0.38	1.40 ± 0.11
MM5	10 mM	3.77 ± 0.26	1.50 ± 0.14
MM6	1 mM	3.01 ± 0.33	2.76 ± 0.45
MM6	5 mM	2.12 ± 0.23	0.80 ± 0.13
MM6	10 mM	1.66 ± 0.27	0.94 ± 0.03

(1) Each value represents the mean of 6 independent experiments

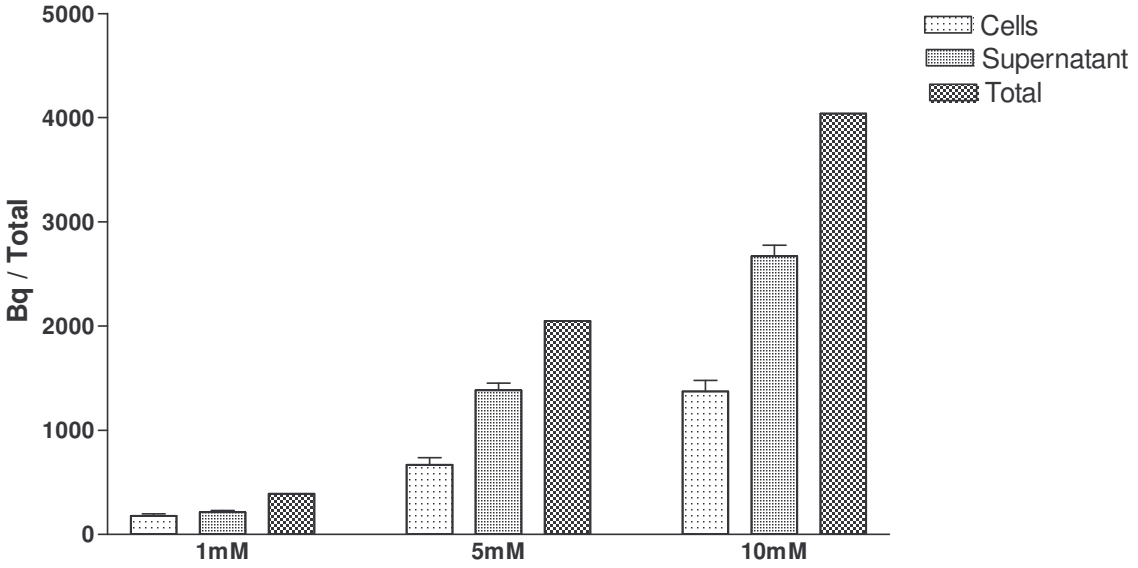

Figure 8.1: Mean percentage [^{198}Au(dppe)$_2$]Cl uptake by A2780 cells ± SEM. Each value represents the mean of 6 independent experiments.

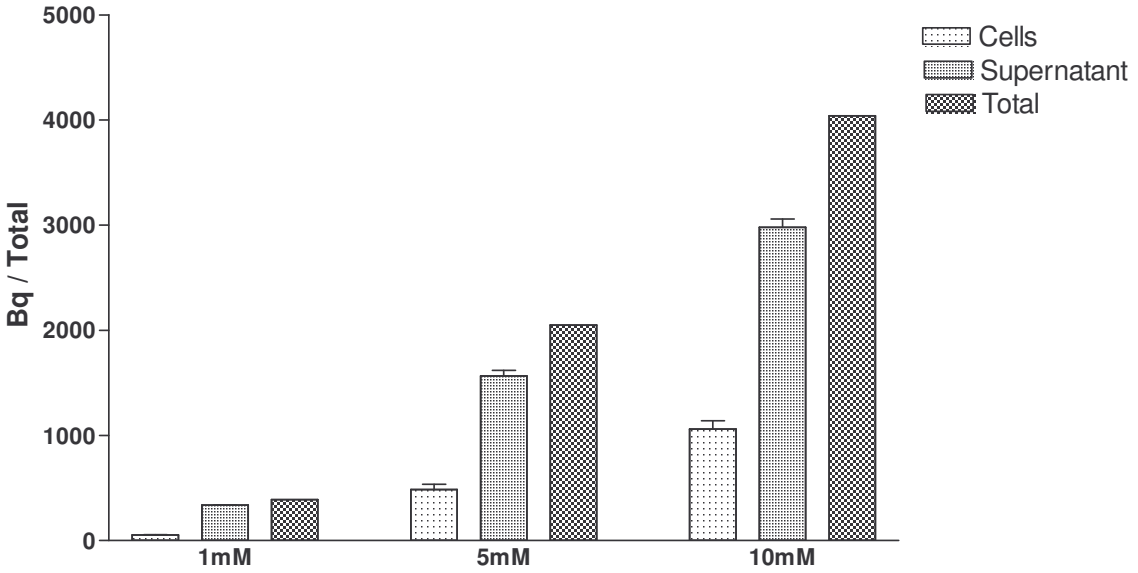

Figure 8.2: Mean percentage [^{198}Au(dppe)$_2$]Cl uptake by A2780 cis cells ± SEM. Each value represents the mean of 6 independent experiments.

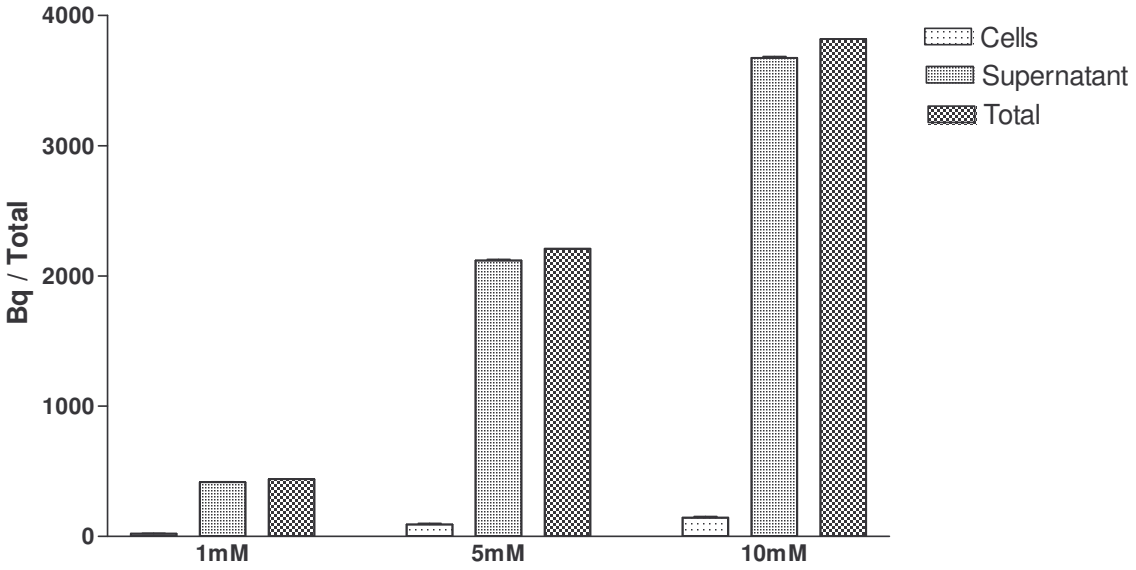

Figure 8.3: Mean percentage ^{198}Au labeled MM5 uptake by A2780 cells ± SEM. Each value represents the mean of 6 independent experiments.

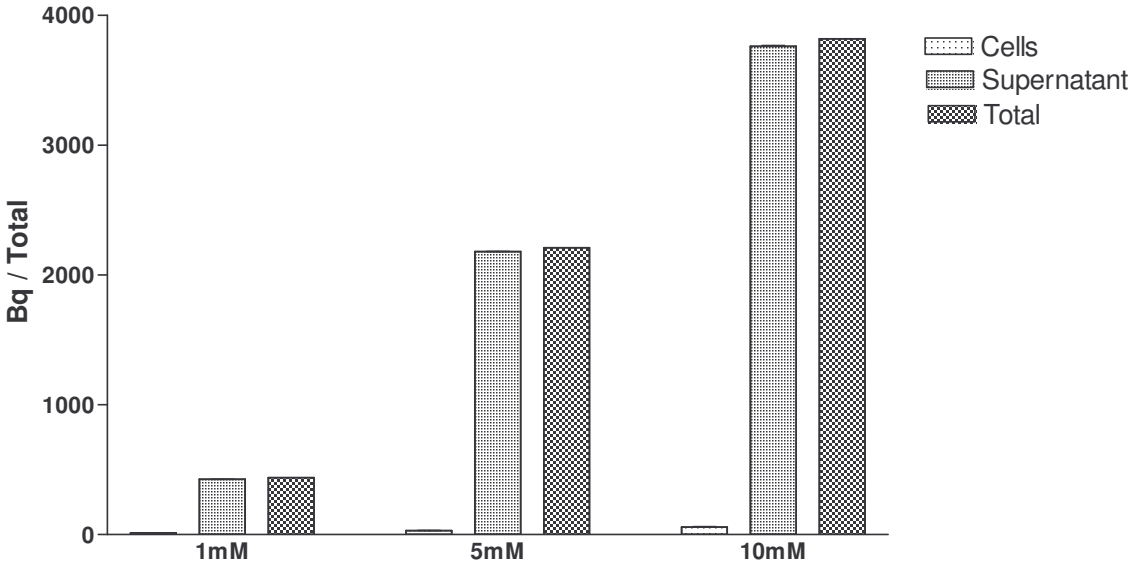

Figure 8.4: Mean percentage ^{198}Au labeled MM5 uptake by A2780 cis cells ± SEM. Each value represents the mean of 6 independent experiments.

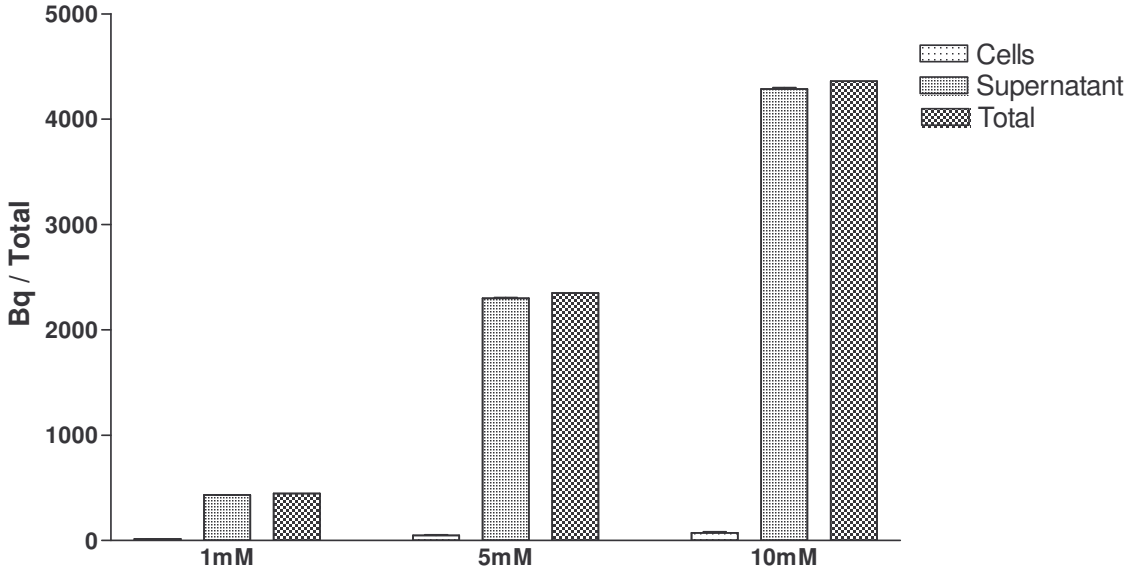

Figure 8.5: Mean percentage ^{198}Au labeled MM6 uptake by A2780 cells ± SEM. Each value represents the mean of 6 independent experiments.

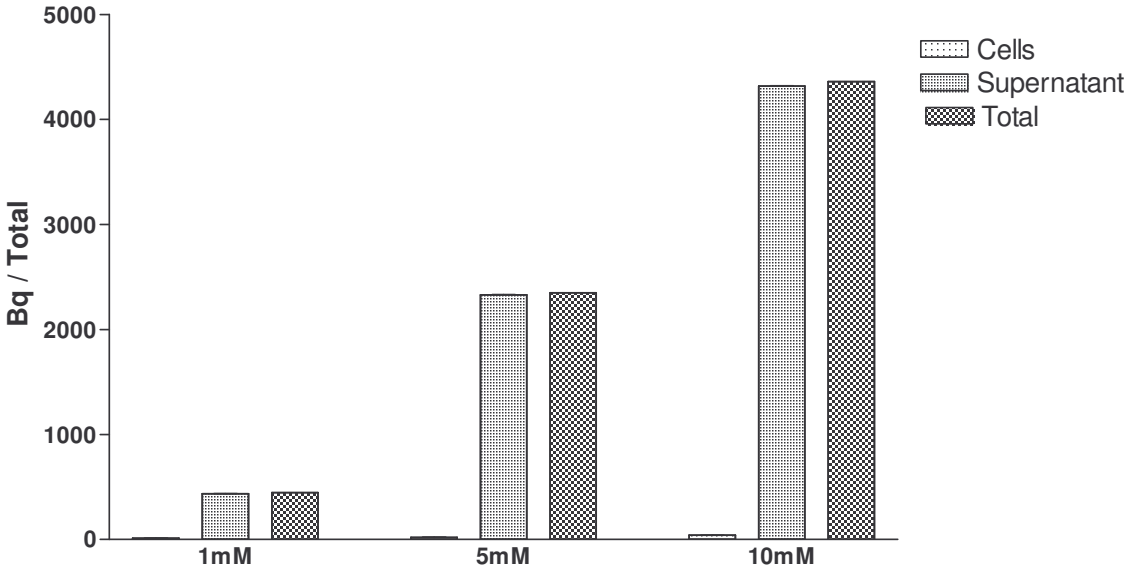

Figure 8.6: Mean percentage ^{198}Au labeled MM6 uptake by A2780 cis cells ± SEM. Each value represents the mean of 6 independent experiments.

Discussion

The results obtained in the octanol/water partition coefficient (**Chapter 2**) determinations showed $[Au(dppe)_2]Cl$ to be strongly lipophilic with a log P value of 1.136. MM5 and MM6 on the other hand had log P values of -1.045 and -1.209 respectively which suggests that they have strong hydrophilic characteristics. These differences can explain the better cellular uptake of $[Au(dppe)_2]Cl$. $[Au(dppe)_2]Cl$ is more lipophilic which makes it easier to cross membranes and enter the cells. MM5 and MM6 are more hydrophilic and are not able to cross membranes that easily, and can therefore not enter the cells. MM6 is more hydrophilic than MM5 and is therefore taken up even less than MM5.

The results obtained in the radio labeled drug uptake experiment confirm the results that were obtained in the octanol/water partition determinations in **Chapter 2**.

Stage 3

Chapter 9: *In vivo* radioactive drug distribution

9.1 Introduction

This study was carried out in close collaboration with NECSA.

Adult rats were used to determine the bio-distribution of ^{198}Au labeled [Au(dppe)$_2$]Cl, MM4 and MM6.

Six rats per compound (total of 18 rats) were used. The animals were kept in separate cages at UPBRC (University of Pretoria Biomedical Research Centre) and provided with husbandry and management practices with emphasis on environmental enrichment to optimize the health and mental status of the animals. The animals were fed a balanced diet and water was available *ad libitum*.

9.2 Aim

To determine drug distribution *in vivo* using ^{198}Au labeled [Au(dppe)$_2$]Cl, MM4 and MM6 in rats.

9.3 Materials and methods

9.2.1 Experimental compounds

Preparation of ^{198}Au labeled [Au(dppe)$_2$]Cl, MM5 and MM6

Preparation of ^{198}Au labeled [Au(dppe)$_2$]Cl, MM5 and MM6 was done at NECSA as described in **Chapter 8**.

Preparation of ^{198}Au labeled experimental compounds (the day of experiment).

i. Audppe

1200 µl EtOH (ethanol) and 7200 µl H_2O was added to 11.43 mg Audppe. A 3 ml fraction was filtered (Millex GP 0.22 µm). An injection volume of 500 µl and an activity of 25 µCi were used ($5.0X10^{-2}$ µCi/µl).

ii. MM5

400 µl DMSO, 1600 µl EtOH and 7200 µl H_2O were added to 11.43 mg MM5. The filtered 4000 µl fraction had an activity of 11 µCi. An injection volume of 500 µl and an activity of 1.375 µCi were used ($2.75X10^{-3}$ µCi/µl).

iii. MM6

280 µl DMSO was added to 7.16 mg MM6. 700 µl EtOH and 2400 µl H_2O was added to 100 µl of the MM6 suspension. The filtered solution had an activity of 13 µCi. An injection volume of 450 µl and an activity of 1.83 µCi were used ($4.06X10^{-3}$ µCi/µl).

9.2.2 Method

The method for this study was adapted from a study done by Zeevaart *et al*., (2004).

The tests were carried out over two consecutive days, one day for $[Au(dppe)_2]Cl$ and one day for MM5 and MM6. A total of 18 rats were used (6 per compound).

Six rats were each injected IV with an extremely low, non-toxic dosage of ^{198}Au labelled $[Au(dppe)_2]Cl$, MM5 and MM6 in the tail vein. Dosages were determined using the results obtained in the cytotoxicity assays done on primary cell cultures.

After 6 hours the animals were sacrificed using an isofluoraan overdose. Several selected organ samples (heart, lung, spleen, liver, kidney, bladder, muscle, small intestine, stomach and blood) were collected from each rat. Each organ sample was weighed and counted 1 minute in a well type counter. A Canberra Model uniSPEC Universal MCA (Multi Channel Analyzer) system with Canberra 3" x 3" Nal(TL) Well detector was used to count the organ samples.

9.3 Results

Results are expressed as the mean percentage injected dose per gram of organ ± SEM. Each value represents the mean of 6 independent experiments.

Table 9.1 represents he mean bio distribution of ^{198}Au labeled $[Au(dppe)_2]Cl$, MM5 and MM6 in selected organs of the rat ± SEM after 6 hours of treatment.

This figure shows that the heart had higher levels of $[Au(dppe)_2]Cl$ than MM5 and MM6. The lungs showed very high levels of $[Au(dppe)_2]Cl$ compared to MM5 and MM6. MM5 had the highest level in the liver; while MM6 had the lowest. The spleen showed fairly high levels of $[Au(dppe)_2]Cl$ and MM5, but MM6 is very low. In the kidneys $[Au(dppe)_2]Cl$ had the highest levels followed by MM6. The bladder had very low levels

of MM5 and MM6 with $[Au(dppe)_2]Cl$ slightly higher. MM5 is almost not detectable in the stomach; with MM6 slightly higher. $[Au(dppe)_2]Cl$ had the highest levels in the stomach, but these were also very low. $[Au(dppe)_2]Cl$ had the highest level in the small intestine followed by MM6 and lastly MM5. MM5 and MM6 had equally low levels in the muscle. $[Au(dppe)_2]Cl$ had the highest levels in the blood of the 3 compounds tested. MM5 had a slightly higher level than MM6 in the blood.

Table 9.1: The mean bio distribution of ^{198}Au labeled [Au(dppe)$_2$]Cl, MM5 and MM6 in selected organs of the rat ± SEM after 6 hours of treatment.

Mean bio distribution(1) of ^{198}Au labeled [Au(dppe)$_2$]Cl, MM5 and MM6 in selected organs of the rat ± SEM after 6 hours of treatment.

Organ	[Au(dppe)$_2$]Cl % injected dose/g	MM5 % injected dose/g	MM6 % injected dose/g
Heart	0.0151 ± 0.0046	0.0017 ± 0.0001	0.0008 ± 0.0001
Lungs	0.4358 ± 0.2188	0.0063 ± 0.0004	0.0014 ± 0.0001
Liver	0.0212 ±0.0062	0.0376 ± 0.0032	0.0041 ± 0.0002
Spleen	0.1080 ± 0.0438	0.0927 ± 0.0101	0.0045 ± 0.0002
Kidney	0.0358 ± 0.0104	0.0122 ± 0.0006	0.0157 ± 0.0004
Bladder	0.0052 ± 0.0016	0.0018 ± 0.0004	0.0018 ± 0.0003
Stomach	0.0024 ± 0.0007	0.0002 ± 0.0000	0.0010 ± 0.0004
Muscle	not done	0.0006 ± 0.0001	0.0005 ± 0.0001
Blood	0.0166 ± 0.0049	0.0038 ± 0.0002	0.0019 ± 0.0001
Small intestine	0.0420 ± 0.0161	0.0045 ± 0.0012	0.0074 ± 0.0019

(1) Mean of 6 independent experiments.

.

9.4 Discussion

The bio distribution showed predominantly high reticulo-endothelial uptake for all the compounds. The solubility of these compounds was very low. The high lung uptake of $[Au(dppe)_2]Cl$ can be the result of colloid forming because of the low solubility.

Higher levels of distribution were found for $[Au(dppe)_2]Cl$ than for MM5 and MM6. These results confirm those obtained with the octanol/water partition coefficient (**Chapter 2**) and the radio labeled drug uptake experiments (**Chapter 8**). MM5 and MM6 are more hydrophilic and according to the results obtained in these experiments, they have limited bio-distribution in comparison to the more lipophilic $[Au(dppe)_2]Cl$ (Wunderlich *et al*., 2004).

Radio labeled compounds were used successfully and confirmed the predictions of lower uptake with higher hydrophilicity.

Chapter 10: Discussion and conclusions

The aim of this study was to determine whether the three novel gold compounds (MM4, MM5 and MM6), selected for this study, have higher selectivity for cancer cells with less toxicity towards normal cells than $[Au(dppe)_2]Cl$, and also to determine whether they have improved bio distribution compared to $[Au(dppe)_2]Cl$. The aim was also to compare the anti-mitochondrial characteristics of $[Au(dppe)_2]Cl$ with the novel compounds to see whether they have the same mechanism of action. The experiments that were selected for this study, to achieve the aim and objectives, have been described.

Results obtained in this study have indicated that $[Au(dppe)_2]Cl$ is a strong lipophilic compound, while MM4 only had limited lipophilic characteristics. MM5 and MM6 on the other hand were strong hydrophilic compounds, and exhibited more selectivity towards the tumour cells and were consequently less toxic to the normal cells. MM4 showed very little specificity towards cancer cells, while MM5 and MM6 were ± 2.5 times more selective towards cancer cells than normal cells.

Berners-Price *et al*., (1999), established a significant correlation between drug uptake and the octanol/water partition coefficient of a compound. $[Au(dppe)_2]Cl$ had strongly lipophilic characteristics and cells had a much higher uptake of this compound compared to MM5 and MM6 which were strong hydrophilic. ^{198}Au labeled $[Au(dppe)_2]Cl$, MM5 and MM6 were used to determine drug uptake. These experiments indicated that very little MM5 and MM6 were taken up by the cells. It is interesting to note that these compounds had very low IC_{50} values which indicate strong inhibition of growth. This suggests that growth inhibition is not related to drug uptake in these compounds. Drug uptake was dependant on the octanol/water partition coefficient.

$[Au(dppe)_2]Cl$ depolarized the mitochondrial membranes of both Jurkat cells and PHA stimulated human lymphocytes very significantly. The three novel compounds depolarized the mitochondrial membranes of Jurkat cells but to a lesser extent than

$[Au(dppe)_2]Cl$. MM4, MM5 and MM6 had a more pronounced effect on the mitochondrial membranes of the PHA stimulated lymphocytes but it was still to a lesser extent than $[Au(dppe)_2]Cl$. The same trend was seen in the plasma membrane potential determinations. $[Au(dppe)_2]Cl$ depolarized the plasma membranes of both Jurkat cells and PHA stimulated lymphocytes very significantly. MM4, MM5 and MM6 depolarized the plasma membranes of Jurkat cells, but only MM6 did so significantly. MM4 and MM5 depolarized the plasma membranes of the PHA stimulated lymphocytes to a lesser extent than MM6. These results suggest that MM6 had a more pronounced effect on the mitochondrial and plasma membranes of the cells tested than the other two novel compounds.

$[Au(dppe)_2]Cl$ induced apoptosis in the Jurkat cells at both the concentrations tested. The effect was more pronounced at the higher concentration which was to be expected. MM4 induced apoptosis only at the higher concentration. The results obtained from these experiments suggest that MM5 did not induce apoptosis but that the necrosis cell death pathway is more indicative for this compound. MM6 had very clear apoptotic effects at both the concentrations tested, more so with the higher concentration.

Cell cycle experiments were carried out to determine whether these experimental compounds have an effect on this crucial process of cell life. Results from these experiments indicated that $[Au(dppe)_2]Cl$, MM4 and MM5 arrested the cell cycle in the G_1 phase. MM6 at the lower concentration arrested the cell cycle in the G_1 phase and at the higher concentration in the S-phase. The difference between the percentages of the different phases and their controls were not very significant, which indicates that these compounds do not have a great effect on the cell cycle of Jurkat cells.

Based on the *in vitro* results of MM5 and MM6 it was decided to do an animal study to determine the bio distribution of these compounds. ^{198}Au labeled $[Au(dppe)_2]Cl$, MM5 and MM6 was used in rats. The bio distribution showed predominantly high reticulo-endothelial uptake for all the experimental compounds. The solubility of these compounds was very low. The lungs showed high uptake of $[Au(dppe)_2]Cl$ which could

be the result of colloid forming which is a result of the low solubility. Higher levels of distribution was found for $[Au(dppe)_2]Cl$ than for MM5 and MM6. These results confirm those obtained in the octanol/water partition coefficient experiments and the radio labeled drug uptake experiments. MM5 and MM6 are more hydrophilic and according to the results obtained in these experiments, they have limited bio distribution in comparison to the more lipophilic $[Au(dppe)_2]Cl$.

Future work

The results obtained in this study do not give a clear indication of the precise mode of action that is apparent for MM4, MM5 and MM6. There are indications that a similar mode of action to that of $[Au(dppe)_2]Cl$ might be applicable. MM5 and MM6 are more selective towards cancer cells than normal cells and this is an important characteristic which cannot be ignored. Future studies must include experiments to try and pinpoint the mechanism of action of these compounds. Solubility is a problem which should be addressed before any further animal studies could be done. MM5 and MM6 show promise to be developed further as anti-cancer agents.

References

1. Anderson R, Smit M J and van Rensburg C E J. Lysophospholipid- mediated inhibition of Na, K – adenosine triphosphatase is a possible mechanism of immunorepressive activity of cyclosporin A. Mol. Pharmacol, 1993; **44**: 605-619.

2. Alberts B, Bray D, Lewis J, Raff M, Roberts K and Watson JD. Molecular Biology of The Cell, Third edition; 1994. Garland Publishing Inc. New York and London.

3. Asche P C and Berry M D. Apoptotic signaling cascades. Progress in Neuro-Psycopharmacology & Biological Psychiatry, 2003; **27**: 199-214.

4. Baguley B C and Marshall E S. *In vitro* modeling of human tumour behavior in drug discovery programmes. European Journal of Cancer, 2004; **40**: 794-801.

5. Barnard P J, Ho A Y , Baker M V, Day D A, and Berners-Price S J. Gold – Phosphine and Gold-carbene Complexes as Potential Mitochondrial Targeting Agents. Gold 2003, **Conference on the Science, Technology and Industrial Applications of Gold,** Vancouver, September, 2003, pp. 883-887, Paper s36a1258p883; available on the web at: http://www.gold.org/discover/sciindu/gold2003/pdf/s36a1258p883.pdf.

6. Barnard P J, Baker M V, Berners-Price S J and Day D A. Mitochondrial permeability transition induced by di-nuclear gold(I)-carbene complexes: potential new anti-mitochondrial anti-tumour agents. Journal of Inorganic Biochemistry, 2004; **98**: 1642-1647.

7. Bartek J, Lukas J and Bartkova J. Perspective: Defects in cell cycle and cancer. Journal of Pathology, 1999; **187**: 95-99.

8. Basso E, Fante L, Fowlkes J, Petronilli V, Forte M A and Bernardi P. Properties of the permeability transition pore in mitochondria devoid of cyclophilin D. The Journal of Biological Chemistry, 2005; **19**: 18558-18561.

9. Bernardi P, Petronilli V, Di Lisa F and Forte M. A mitochondrial perspective on cell death. Trends in Biochemical Sciences, 2001; **26** (2): 112-117.

10. Berners-Price S J, Bowen R J, Galettis P, Healy P C and McKeage M J. Structural and solution of gold(I) and silver(I) complexes of bidentate pyridyl phosphines: selective anti-tumor agents. Coordination Chemistry reviews, 1999; **186**: 823-836.

11. Berners-Price S J, Mirabelli C K, Johnson R K, Mattern M R, McCabe F L, Faucette L F, Sung C-M, Mong S-M, Sadler P J and Crooke S T. *In vivo* anti-tumor activity and *in vitro* cytotoxic properties of Bis [1, 2-bis(diphenyl phosphino)ethane]gold(I)chloride. Cancer Res., 1986; **46**: 5486-5493.

12. Bertram R, Pedeson M G, Luciani D S and Sherman A. A simplified model for mitochondrial ATP production. Journal of Theoretical Biology, 2006; **243**: 575-586.

13. Bonire J J and Fricker S P. The anti-tumour profile of some 1,2-diaminocyclohexane organotin complexes. Journal of Inorganic Biochemistry, 2001; **83**: 217-221.

14. Bortner C D and Cidlowski J A. Caspase independent / dependent regulation of K^+, cell shrinkage, and mitochondrial membrane potential during lymphocyte apoptosis. J Biol Chem, 1999; **31**: 21953-21962.

15. Bowen R J. PhD Thesis. Hydrophilic bidentate phosphines and their group 11 complexes: potential anti-tumour agents. Griffith University, Australia, 1999; 112.

16. Braun A, Hämmerle S, Suda K, Rothen-Rutishauser B, Günthert M, Krämer S and Wunderli-Allenspach H. Cell cultures as tools in bio pharmacy. European Journal of Pharmaceutical Sciences, 2000; **11**: S51- S60.

17. Breuninger L M, Paul S, Gaughan K, Miki T, Chan A and Aaronson S A. Expression of multi drug resistance-associated protein in NIH/3T3 cells confers multi drug resistance associated with increased drug efflux and altered intracellular drug distribution. Cancer Reaearch, 1995; **55**: 5342-5347.

18. Caldwell G, Neuse E W, and van Rensburg C E J. Cytotoxic activity of two polyaspartamide-based monoamineplatinum(II) conjugates against the HeLa cell line. Appl. Organometallic Chemistry, 1999; **13**: 189-194.

19. Carlson K and Ehrich M. Organophosphorous compound-induced modification of SH-SY5Y human neuroblastoma mitochondrial trans membrane potential. Toxicology and Applied Pharmacology, 1999; **160**: 33-42.

20. Caruso F, Villa R V, Rossi M, Pettinari C, Paduano F, Pennati M, Daidone M G and Zaffaroni N. Mitochondria are primary targets in apoptosis induced by the mixed phosphine gold species chlorotriphenylphosphine-1,3-bis(diphenylphosphino)propanegold(I) in melanoma cell lines. Biochemical Pharmacology, 2007; **73**: 773-781.

21. Chen, L B. Mitochondrial membrane potential in living cells. Annu. Rev. Cell Biol., 1988; **4**:155-188.

22. Clifton GC, Li X, Reutter W, Hixson DC and Josic D. Comparative proteomics of rat liver and Morris hepatoma 7777 plasma membranes. Journal of Chromatography B, 2006; doi:10.1016/jchromb.2006.08.047.

23. Cossarizza A, Baccarani-Contri M, Kalashnikova G and Franceschi C. A new method for the cytofluorimetric analysis of mitochondrial membrane potential using the J-aggregate forming lipophilic cation 5,5',6,6'tetrachloro-1,1',3,3'-tetraethylbenzimidazolcarbocyanine iodide (JC-1). Biochemical and Biophysical Research Communications, 1993; **197** (1): 40-45.

24. Cree I A and Andreotti PE. Measurement of Cytotoxicity by ATP-based luminescence assay in primary cell cultures and cell lines. Toxicology *in vitro*, 1997; **11**: 553-556.

25. Dalton S. Cell cycle control of chromosomal DNA replication. Immunology and Cell Biology, 1998; **76**: 467-472.

26. Dalvie D. Recent advances in the applications of radioisotopes in drug metabolism, toxicology and pharmacokinetics. Current Pharmaceutical Design, 2000; **6** (10): 1009-1028.

27. Darrouzain F, Dallet P, Dubost J, Ismaili L, Pehercqe F, Bannwarth B, Matoga M and Guillaume Y C. Molecular lipophilicity determination of a huperzine series by HPLC: Comparison of C18 and IAM stationary phases. Journal of Pharmaceutical and Biomedical Analysis, 2006; **41**: 228-232.

28. Davis S, Weiss M J, Wong J R, Lampidis T J and Chen L B. Mitochondrial and plasma membrane potentials cause unusual accumulation and retention of Rhodamine 123 by human breast adenocarcinoma-derived MCF 7 cells. The Journal of Biological Chemistry, 1985; **260** (25): 13844-13850.

29. Debatin K M, Poncet D and Kroemer G. Chemotherapy: targeting the mitochondrial cell death pathway. Oncogene, 2002; **12** (57): 8786-803. Review.

30. Dobashi Y. Cell cycle regulation and its aberrations in human lung carcinoma. Pathology International, 2005; **55**: 95-105.

31. Don A S and Hogg P J. Mitochondria as cancer drug targets. Trends in Molecular Medicine, 2004; **10** (8): 372-378.

32. Eisler R. Chrysotherapy: a synoptic review. Inflammation Research, 2003; **52**: 487-501.

33. Freshney R I. Culture of Animal Cells: A manual of basic technique. 4th Ed. Wiley-Liss Publishers, New York, 2000.

34. Frühauf N R, Oldhafer K J, Höltje M, Kaiser G M, Frühauf J H, Stavrou G A, Bader A and Broelsch C E. A bio artificial liver support system using primary hepatocytes: A preclinical study in a new porcine hepatectomy model. Surgery, 2004; **136**: 47-56.

35. Garmuszek P, Licińska I, Skierski J S, Koronkiewicz M, Mirowski M, Wierccioch R and Mazurek A P. Biological investigation of the platinum (II)-[*I] iodohistamine complexes of potential synergistic anti-cancer activity. Nuclear Medicine and Biology, 2002; **29**: 169-175.

36. Giovannini C, Matarrese P,Scazzocchio B, Sanchez M, Masella R and Malorni W. Mitochondria hyper polarization is an early event in oxidized low-density lipoprotein-induced apoptosis in Caco-2 intestinal cells. FEBS Letters, 2002; **523**: 200-206.

37. Golias C H, Charalabopoulos A and Charalabopoulos K. Cell proliferation and cell cycle control: a mini review. Int J Clin Pract, 2004; **58**: 1134-1141.

38. Gupta N, Price P M and Aboagye E O. PET for *in vivo* pharmacokinetic and pharmacodynamic measurements. European Journal of Cancer, 2002; **38**: 2094-2107.

39. Hall P A. Assessing apoptosis: a critical survey. Endocrine-Related Cancer, 1999; **6**: 3-8

40. Hallgas B, Dobos Z, Ösz E, Hollósy F, Schwab R E, Szabó E Z, Erös D, Idei M, Kéri G and Lóránd T. Characterization of lipophilicity and anti-proliferative activity of *E*-2-arylmethylene-1-tetralones and their hetero analogues. Journal of Chromatography B, 2005; **819**: 283-291.

41. Hoke G D, Rush G F, Bossard G E, McArdle J V, Jensen B D and Mirabelli C K. Mechanism of alterations in isolated rat liver mitochondrial function induced by gold complexes of bidentate phosphines. The Journal of Biological Chemistry, 1988; **263** (23): 11203-11210.

42. Hoke G D, McCabe F L, Faucette L F, O'Leary Bartus J, Sung C-M, Jensen B D, Heys R, Rush G F, Alberts D W, Johnson R K, and Mirabelli C K. *In vivo* development and *in vitro* characterization of a subclone of Murine P388 Leukemia resistant to Bis(diphenylphosphine)ethane. Molecular Pharmacol., 1991; **39** (1): 90-97.

43. [1]Hollósy F, Lóránd T, Örfi L, Erös D, Kéri G and Idei M. Relationship between lipophilicity and anti-tumour activity of library of Mannich ketones determined by high-performance liquid chromatography, log P calculation and cytotoxicity test. Journal of Chromatography B, 2002; **768** (2): 361-368.

44. [2]Hollósy F, Seprödi J, Örfi L, Erös D, Kéri G and Idei M. Evaluation of lipophilicity and anti-tumour activity of parallel carboxamide libraries. Journal of Chromatography B, 2002; **780** (2): 355-363.

45. Jayaraman S. Flow cytometric determination of mitochondrial membrane potential during apoptosis of T lymphocytic and pancreatic beta cell lines: Comparison of tetramethylrhodamineethylester (TRME), chloromethyl-X-rosamine (H_2-CMX-Ros) and Mito Tracker Red 580 (MTR580). Journal of Immunological Methods, 2005; **306**: 68-79.

46. Kainthla R P, Kashyap R S, Prasad S, Purohit H J, Taori G M and Daginwala H F. Evaluation of adenosine de-aminase assay for analyzing T-lymphocyte density *in vitro*. *In Vitro* Cell. Dev. Biol. – Animal, 2006; **42**: 287- 289.

47. Kawai H, Suzuki T, Kobayashi T, Mizuguchi H, Hayakawa T and Kawanishi T. Simultaneous imaging of initiator/effector caspase activity and mitochondrial membrane potential during cell death in living HeLa cells. Biochimica et Biophysica Acta, 2004; **1693**: 101-110.

48. Keen H G, Dekker B A, Disley L, Hastings D, Lyons S, Reader A J, Ottewell P, Watson A and Zweit J. Imaging apoptosis in vivo using ^{124}I-annexin V and PET. Nuclear Medicine and Biology, 2005; **32**: 395-402.

49. Kőpf-Maier P. Complexes of metals other than platinum as anti-tumor agents. European Journal of Clinical Pharmacology, 1994; **47** (1):1-16.

50. Koya K, Li Y, Wang H, Ukai T, Tatsuta N, Kawakami M, Shishido T and Chen L B. MKT-077, a novel Rhodacyanine dye in clinical trials, exhibits anti-carcinoma activity in preclinical studies based on selective mitochondrial accumulation. Cancer Research, 1996; **56**: 538-543.

51. Kuan N K and Passaro E. Apoptosis: Programmed Cell Death. Arch. Surg., 1998; **133**: 773-775.

52. [1]Liu M, Yue P Y, Wang Z and Wong R N. Methyl protodioscin induces G_2/M arrest and apoptosis in K562 cells with the hyper polarization of mitochondria. Cancer Letters, 2005; **224**: 229-241.

53. [2]Liu X, Tanaka H, Yamauchi A, Testa B and Chuman H. Determination of lipophilicity by reversed phase high performance liquid chromatography influence of 1-octanol in the mobile phase. Journal of Chromatography A, 2005; **1091**: 51-59.

54. Ludovico L, Rodrigues F, Almeida A, Silva T S, Barrientos A and Côrte-Real M. Cytochrome release and mitochondria involvement in programmed cell death induced by acetic acid in *Sacchromyces cerevisiae.* Molecular biology of the cell, 2002; **13**: 2598-2606.

55. Mann Cynthia L and Cidlowski John A. Glucocorticoids regulate plasma membrane potential during rat thymocyte apoptosis *in vitro* and *in vivo*. Endocrinology, 2001; **142**: 421-429.

56. Mckeage M J, Berners-Price S J, Galettis P, Bowen R J, Brouwer W, Ding L, Zhuang L and Baguley B C. Role of lipophilicity in determining cellular uptake and anti tumour activity of gold phosphine complexes. Cancer Chemother Pharmacol, 2000; **46**: 343-350.

57. McKeage M J, Maharaj L and Berners-Price S J. Mechanisms of cytotoxicity and anti-tumour activity of gold (I) phosphine complexes: the possible role of mitochondria. Coordination Chemistry Reviews 2002; **232**: 127-135.

58. Michie J, Akudugu J, Binder A, Van Rensburg C E J and Böhm L. Flow cytometric evaluation of apoptosis and cell viability as a criterion of anti-tumour drug toxicity. Cancer Research, 2003; **56**: 544-550.

59. Mitochondrion. http://en.wikipedia.org/wiki/mitochondria.

60. Modica-Napolitano J S and Aprille J R. Delocalized lipophilic cations selectively target the mitochondria of carcinoma cells. Advanced Drug Delivery Reviews, 2001; **49**, Issues 1-2: 63-70.

61. Mosmann T. Rapid colorimetric assay for cellular growth and survival: application to proliferation and cytotoxicity assays. Journal of Immunological Methods, 1983; **65**: 55-63.

62. Nakagawa M, Schneider E, Dixon K H, Horton J, Kelly K, Morrow C and Cowan K H. Reduced intracellular drug accumulation in the absence of P-glycoprotein (mdr1) over expression in mitoxantrone-resistant human MCF 7 breast cancer cells. Cancer Research, 1992; **52**: 6175-6181.

63. Nieuwoudt M J, Kreft E, Olivier B, Malfeld S, Vosloo J, Stegman F, Kunneke R, Van Wyk A J and Van der Merwe S W. A large-scale automated method for Hepatocyte isolation: Effects on proliferation in culture. Cell Transplantation, 2005; **14** (5): 291-299.

64. Nolte F, Friedrich O, Rojewski M, Fink R H A, Schrezenmeier H and Körper S. Depolarization of the plasma membrane in the arsenic trioxide (As_2O_3) - and anti-CD95- induced apoptosis in myeloid cells. FEBS Letters, 2004; **578**: 85-89.

65. Nuutinen U, Postilla V, Mättö M, Eeva J, Ropponen A, Eray M, Riikonen P and Pelkonen J. Inhibition of PI3-kinase-Akt pathway enhances dexamethasone-induced apoptosis in a human follicular lymphoma cell line. Experimental Cell Research, 2006; **312**: 322-330.

66. Paillard F, Finot F, Mouche I, Prenez A and Vericat J A. Use of primary cultures of rat hepatocytes to predict toxicity in the early development of new chemical entities. Toxicology *in vitro*, 1999; **13**: 693-700.

67. Park W H, Seol J G, Kim E S, Kang W K, Im Y H, Jung C W, Kim B K and Lee Y Y. Monensin-mediated growth inhibition in human lymphoma cells through cell cycle arrest and apoptosis. British Journal of Haematology, 2002; **119**: 400-407.

68. PHA 5110 Partitioning and Complexation. http://www.cop.ufl.edu.safezone/prokai/pha5100/partitn.htm

69. Plášek J, Vojtšková A and Houštěk J. Flow-cytometric monitoring of mitochondrial depolarization: from fluorescence intensities to milli volts. Journal of Photochemistry and Photobiology B: Biology, 2005; **78**: 99-108.

70. Plasma membrane. http://en.wikipedia.org/wiki/Plasma_membrane.

71. Preston T J, Abadi A, Wilson L and Singh G. Mitochondrial contributions to cancer cell physiology: potential for drug development. Advanced Drug Delivery Reviews, 2001; **49** (1-2): 45-61.

72. Radošević K, Bakker Schut T C, van Graft M, de Grooth B G and Greve J. A flow cytometric study of the membrane potential of natural killer and K562 cells during the cytotoxic process. Journal of Immunological Methods, 1993; **161**: 119-128.

73. Renehan A G, Booth C and Potten C S. What is apoptosis and why is it important? BMJ, 2001; **322**: 1536-1538.

74. Rodriguez-Enriquez S, He L and Lemasters J L. Role of mitochondrial permeability transition pores in mitochondrial autophagy. The International Journal of Biochemistry & Cell Biology, 2004; **36** (12): 2463-2472.

75. Rottenberg H and Wu S. Quantitative assay by flow cytometry of the mitochondrial membrane potential in intact cells. Biochimica et Biophysica Acta (BBA) – Molecular Cell Research, 1998; **1404** (3): 393-404.

76. Rüdel H. Case study: bioavailability of tin and tin compounds. Ecotoxicology and Environmental Safety, 2003; **56**: 180-189.

77. Salvioli S, Ardizzini A, Franceschi C and Cossarizza A. JC-1, but not DiOC6(3) or rhodamine 123, is a reliable fluorescent probe to assess mitochondrial membrane potential changes in intact cells: implications for studies on mitochondrial functionality during apoptosis. FEBS Letters, 1997; **411**: 77-82.

78. Saraste A and Pulkki K. Morphologic and biochemical hallmarks of apoptosis. Cardiovascular Research, 2000; **45**: 528-537.

79. Schafer K A. The cell cycle: a review. Vet. Pathol., 1998; **35**: 461-478.

80. Scott S L, Gumerlock P H, Beckett L, Li Y and Goldberg Z. Survival and cell cycle kinetics of human prostate cancer cell lines after single- and multi-fraction exposures to ionizing radiation. Int. J. Radiation Oncology Biol. Phys., 2004; **1**: 219-227.

81. Scholz F, Gulaboski R and Caban K. The determination of standard Gibbs energies of transfer of cations across the nitrobenzene/water interface using a three-phase electrode. Electrochemistry Communications, 2003; **5**: 929-934.

82. Schoonen W G E J, de Roos J A D M and Westerink E D. Cytotoxic effects of 110 reference compounds on HepG2 cells and for 60 compounds on HeLa, ECC-1 and CHO cells. IIMechanistic assays on NAD(P)H, ATP and DNA contents. Toxicology *in vitro*, 2005; **19**: 491-503.

83. Shapiro, H M. Membrane potential estimation by flow cytometry. Methods, 2000; **21**: 271-279.

84. Smiley S T, Reers M, Mottola-Hartshorn C, Chen A, Smith T W, Steele G D and Chen L B. Intracellular heterogeneity in mitochondrial membrane potentials revealed by a J-aggregate forming lipophilic cation JC-1. Proc. Natl. Acad. Sci. USA, 1991; **88**: 3671-3675.

85. Smith P F, Hoke G D, Alberts D W, Bugelski P J, Lupo S, Mirabelli C K and Rush G F. Mechanism of toxicity of an experimental bidentate phosphine gold complexed anti-neoplastic agent in isolated rat hepatocytes. Pharmacology and Experimental Therapeutics, 1989; **249** (3), 944-950.

86. Somosy Z. Radiation response of cell organelles. Micron, 2000; **31**: 165-181.

87. Susin S A, Zamzami N and Kroemer G. Mitochondria as regulators of apoptosis: doubt no more. Biochimica et Biophysica Acta, 1998; **1366**: 151-165.

88. Tabassum S and Pettinari C. Chemical and biotechnological developments in organotin cancer chemotherapy. Journal of Organometallic Chemistry, 2006; **691**: 1761-1766.

89. Thomas N and Goodyer I D. Stealth sensors: real-time monitoring of the cell cycle. TARGETS, 2003; **2** (1), 26-33.

90. Tiekink Edward R T. Gold derivatives for the treatment of cancer. Critical reviews in Oncology/Hematology, 2002; **42**: 225-248.

91. Tonini T, Hillson C and Claudio P P. Interview with the retinoblastoma family members: do they help each other? Journal of Cellular Physiology, 2002; **192**: 138-150.

92. Tsuruo T, Iida H, Tsukagoshi S and Sakurai Y. Increased accumulation of Vincristine and Adriamycin in drug-resistant P388 tumor cells following incubation with calcium antagonists and calmodulin inhibitors. Cancer Research, 1982; **42**: 4730-4733.

93. Tuschl H and Schwab C E. Flow cytometric methods used as screening tests for basal toxicity of chemicals. Toxicology *in vitro*, 2004, **18**: 483-491.

94. Vámosi G, Bodnár A, Damjanovich S, Nagy P, Varga Z and Damjanovich L. The role of supramolecular protein complexes and membrane potential in transmembrane signaling processes of lymphocytes. Immunology Letters, 2006; **104**: 53-58.

95. Van Rensburg C E J, Anderson R, Joone G, Myer M S and O'Sullivan J F. Novel tetramethylpiperidine-sustituted phenazines are potent inhibitors of P-Glycoprotein activity in a multi drug resistant cancer cell line. Anti-Cancer Drugs, 1997; **8**: 708-713.

96. Wang P, Song J H, Song D K, Zhang J and Hao C. Role of death receptor and mitochondrial pathways in conventional chemotherapy drug induction of apoptosis. Cell Signaling, 2006; **18**: 1528-35.

97. Waterhouse N J, Ricci J E and Green D R. And all of a sudden it's over: mitochondrial outer-membrane permeabilization in apoptosis. Biochimie, 2002; **84**: 113-121.

98. Winship K A. Toxicity of tin and its compounds. Adverse Drug React Acute Poisoning Rev, 1988; **7**(1): 19-38.

99. Woodle E S and Kulkarni S. Programmed cell death. Transplantation, 1998; **6**: 681-691.

100. Wunderlich G, Grüning T, Paulke B R, LieskeA and Kotzerke J. Nuclear Medicine and Biology, 2004; **31**: 87-92.

101. Zeevaart J R, Jansen D R, Botelho M F, Abrunhosa A, Gomes C, Metello L, Kolar Z I, Krijger G C, Louw W K A and Dormehl I C. Comparison of the predicted *in vivo* behaviour of the SN(II)-mAPDDMP complex and the results as studied in a rodent model. Journal of Inorganic Biochemistry, 2004; **98**(9): 1521-1530.

102. Zhu L and Anasetti C. Cell cycle control of apoptosis in human leukemic T cells. The Journal of Immunology, 1995; **154**: 192-200.